



**Universität für Bodenkultur Wien**  
University of Natural Resources  
and Life Sciences, Vienna

Department of Applied Genetics and Cell Biology



Head: Univ. Prof. Mag. Dr. Joseph Strauss

Supervisor: Univ. Prof. Dipl. Ing. Dr.rer.nat. Eva Stöger

Co-supervisor: Mag. Dr. Barbara Korbei

**FUNCTIONAL ANALYSIS OF TOL PROTEINS-GATEKEEPERS  
FOR VACUOLAR SORTING OF PLASMA MEMBRANE  
PROTEIN IN PLANTS**

Dissertation  
for obtaining a doctorate degree  
at the University of Natural Resources and Life Sciences, Vienna

Submitted by:

Lucinda De-Araujo

Vienna, 06.05.2019

## ACKNOWLEDGEMENTS

Undertaking this PhD has been a truly life-changing experience for me and it would not have been possible to do without the support and guidance that I received from many people.

Firstly, I would like to express my sincere gratitude to my advisor supervisor Mag. Dr. Barbara Korbei, for giving me the opportunity to work on her team, for continuous support on my PhD study, for her patient, motivation and immense knowledge. Her guidance helped me in all the time of research and writing this thesis. I would like to thank you for encouraging and helping me to complete my PhD and at the same time allowing me to understand that, there are difficulties in science but we need to keep positive. Your positive nature and advices during all this years have been invaluable.

I would like to thank Univ. Prof. Mag. Dr. rer. nat. Eva Stöger for supporting my PhD thesis at the DAGZ as a supervisor and for being supportive when it was necessary.

I would like to thank my committee member's professor Assoc. Prof Dr Christian Luschnig and Dr. Andrea Pitzschke, for serving as my committee members and for your comments and suggestions, thanks to you.

I want to thank all my former and current lab team for constant support in scientific and non-scientific topics, Christina, Jeanette, Julia, Lisa, and Max.

I would like to thank Assoc. Prof Dr. Christian Luschnig; Mag. Dr. Doris Lucyshyn and Assoc. Prof. Dr. Kleine-Vehn, together with their group members for scientific and fruitful discussions that contributed significantly to my work.

I would like to thank my office team with whom I shared the last months of writing my thesis for providing good environment and productive conversations. To Birgit for our discussions and jokes during break time.

## ACKNOWLEDGEMENTS

Finally yet importantly, I want to thank my family that supported me unconditionally at all times and kept my motivation up even in difficult moments. To my beloved children's Evelyn and Lucio, I express my deepest appreciation for being such a good kids always cheering me up.

This work has been supported by a grant from Doctorate fellowship from the Austrian Academy of Sciences (26 project "DOC ÖAW") To Lucinda De-Araujo and by the grant from Austrian Science Fund (FWF P30850, V 382 Richter-Program to Barbara Korbei).

This thesis work was carried out at Department of Applied Genetics and Cell Biology (DAGZ), BOKU

## ABSTRACT

Plants have developed many different mechanisms to promptly respond to their changing and often times stressful environment. For this, plasma membrane (PM) protein abundance and localization are under tight regulation. PM proteins destined for degradation are ubiquitinated and sorted by the ESCRT (Endosomal Sorting Complex Required for Transport) machinery via endosomal vesicles to the vacuole for degradation. In higher plants, the TOL (TOM1-like) proteins work as a molecular player in the first steps in the protein degradation of ubiquitinated PM proteins, functioning as alternate to the ESCRT-0 complex. The detailed mechanism for this starting point is however still unclear. In this study I could demonstrate that different members of the TOL proteins have different localization, playing a role between the PM and the cytoplasm, which points toward different functions of the TOLs. Additionally, I could show that the TOLs interact with phospholipids, most strongly with phosphatidic acid known as important lipid in stress responses, as well as ubiquitin via their conserved ubiquitin binding domains. I generated a ubiquitin binding deficient TOL6 allele by mutagenizing essential amino acids, which was unable to rescue the pleiotrophic phenotype of a higher order TOL mutant (*tolQ*) and showed pronounced differences in its subcellular localization to the wild type allele. Ubiquitin receptors, containing ubiquitin binding domains, are frequently subjected to a regulatory mechanism termed coupled monoubiquitination, whereby their own ubiquitination affects their ability to bind ubiquitin. I found various TOLs to be ubiquitinated *in vivo*. Moreover, for TOL6 I could show that only the cytosolic pool of TOL6 is ubiquitinated, while the PM associated one is not. A constitutively ubiquitinated TOL6 localized more to the cytoplasm and partially lost its ability to rescue the *tolQ* phenotype. Thus, TOLs function upstream in the ESCRT pathway, where they bind to ubiquitinated cargo via their conserved ubiquitin binding domains and their localization and function is potentially regulated by a mechanism termed coupled monoubiquitination. This study, which focused on the localization, regulation and interactions of TOLs thus closed a gap in the knowledge about the degradation of ubiquitinated PM and thus the fine-tuning of the response to the environment and adaptation of higher plants.

## ZUSAMMENFASSUNG

Pflanzen haben unterschiedliche Mechanismen entwickelt, um schnell auf ihre sich ändernde Umgebung zu reagieren und dafür wird die Anzahl und Lokalisierung von Plasmamembran (PM)-Proteinen exakt reguliert. Die zum Abbau bestimmten PM-Proteine werden ubiquitiniert und mittels der ESCRT-Maschinerie (Endosomal Sorting Complex Required for Transport) über endosomale Vesikel zur Vakuole zum Abbau sortiert. In höheren Pflanzen sind die TOL (TOM1-like)-Proteine verantwortlich für die ersten Schritten beim Abbau von ubiquitinierten PM-Proteinen und können somit als Alternative zum ESCRT-0-Komplex betrachtet werden. Der detaillierte Mechanismus ist jedoch noch unklar. In dieser Studie konnte ich zeigen, dass verschiedene Mitglieder der TOL-Proteine eine unterschiedliche Lokalisierung haben und eine Rolle zwischen dem PM und dem Zytoplasma spielen, was auf unterschiedliche Funktionen der TOLs hinweist. Außerdem interagieren die TOLs mit Phospholipiden, am stärksten mit PA (Phosphatidsäure), ein wichtiges Lipid bei Stressreaktionen, sowie mit Ubiquitin, über ihre konservierten Ubiquitin-Bindungsdomänen. Ein ubiquitinbindungs-defizientes TOL6-Allel, welches durch Mutagenisierung essentieller Aminosäuren erzeugt wurde, konnte den pleiotrophen Phänotyp einer TOL-Mutante höherer Ordnung (*tol/Q*) nicht retten konnte und zeigte deutliche Unterschiede in seiner subzellulären Lokalisation im Vergleich zum Wildtyp-Allel. Ubiquitin-Rezeptoren, die Ubiquitin-Bindungsdomänen enthalten, unterliegen häufig einem Regulationsmechanismus, der als gekoppelte Monoubiquitinierung bezeichnet wird, wobei ihre eigene Ubiquitinierung ihre Fähigkeit beeinflusst Ubiquitin zu binden. Darüber hinaus werden verschiedenen TOLs *in vivo* ubiquitiniert und im spezifischen wird TOL6 nur in der zytosolischen Fraktion ubiquitiniert, während dies bei den PM lokalisierten TOL6 Proteinen nicht der Fall ist. Ein konstitutiv ubiquitiniertes TOL6 war stärker im Zytoplasma lokalisiert und verlor teilweise seine Fähigkeit, den *tol/Q*-Phänotyp rückgängig zu machen. Daher funktionieren TOLs in den Anfangsschritten des ESCRT-Pathways, wo sie über ihre konservierten Ubiquitin-Bindungsdomänen an ubiquitinierte Proteine binden, und ihre Lokalisierung und Funktion wird möglicherweise durch einen Mechanismus reguliert, der als gekoppelte Monoubiquitinierung bezeichnet wird. Diese Studie, die sich auf Lokalisierung, Regulierung und Wechselwirkungen von TOLs konzentrierte, schloss somit eine

Wissenslücke über den Abbau ubiquitinerter PM und damit die Feinabstimmung der Reaktion auf die Umwelt und die Anpassung höherer Pflanzen.

## TABLE OF CONTENTS

1	INTRODUCTION .....	1
1.1.	The endosomal system .....	2
1.2.	Clathrin mediated endocytosis.....	6
1.3.	The role of ubiquitin in the endocytic system .....	8
1.4.	Importance of ESCRT machinery in plants.....	11
1.5.	Ubiquitin Binding Domains (UBD).....	14
	The VHS Domain.....	16
	The GAT domain .....	17
1.6.	Coupled Monoubiquitination .....	18
1.7.	Protein-lipid interactions in the endocytic system of plants.....	19
2	AIM OF THIS THESIS WORK.....	22
3	MATERIALS AND METHODS.....	24
3.1.	Chemicals, reagents and enzymes.....	24
3.2.	Oligonucleotides and primers combinations .....	24
3.3.	Bacterial strains .....	27
3.3.1.	<i>Escherichia coli</i> (E. coli) strains .....	27
3.3.2.	<i>Agrobacterium tumefaciens</i> strains.....	28
3.4.	Descriptions of Genetic Modified Organisms (GMOs) used .....	28
3.5.	<i>Arabidopsis thaliana</i> mutants and reporter lines.....	28
3.6.	Cloning Strategies .....	29
3.7.	Antibodies.....	35
3.8.	General molecular biological methods.....	36
3.8.1	Plant genomic DNA isolation by CTAB method .....	36

## TABLE OF CONTENTS

3.8.2	Plasmid DNA isolation with kit.....	37
3.8.3	Spectrophotometric quantification of DNA .....	37
3.8.4	Mini-Preparation of <i>E. coli</i> plasmid DNA by the “boiling method” .....	38
3.8.5	Polymerase Chain Reaction (PCR).....	38
3.8.6	Site-directed Mutagenesis by Polymerase Chain Reaction (PCR) with proof-reading Kappa Hifi Kit.....	41
3.8.7	Polymerase chain reaction (PCR) to get DNA with T/A overhang.....	42
3.8.8	DNA gel-electrophoresis .....	43
3.8.9	DNA digestion with restriction endonucleases .....	44
3.8.10	Purification of DNA fragments from agarose gels .....	44
3.8.11	Dephosphorylation of enzyme-digested DNA ends.....	44
3.8.12	Cloning of PCR fragments .....	44
3.8.13	T4 DNA Ligation.....	45
3.8.14	Blue-White Selection of positive clones .....	45
3.8.15	Media and growth conditions for bacteria .....	45
3.8.16	Preparation of electrocompetent <i>E.coli</i> .....	47
3.8.17	Preparation of electrocompetent <i>A. tumefaciens</i> .....	47
3.8.18	Electroporation of <i>E. coli</i> and <i>A. tumefaciens</i> .....	48
3.8.19	Preparation of bacterial -80 °C glycerol stocks .....	48
3.9.	Plant Methods.....	48
3.9.1.	Seed harvesting and storage .....	48
3.9.2.	Seed sterilization.....	48
3.9.3.	Cultivation on solid media .....	49
3.9.4.	Plant cultivation on soil .....	51
3.9.5.	<i>A. tumefaciens</i> mediated plant transformation by Floral Dip Method .....	51
3.9.6.	GUS staining and microscopic preparations .....	52



## TABLE OF CONTENTS

3.9.7.	Confocal Laser Scanning Microscopy (CLSM).....	53
3.9.8.	Analysis of plant development .....	54
3.9.9.	Computer software.....	55
3.10.	Biochemical Methods .....	55
3.10.1	Induction of Protein expression in BL21 (DE3) .....	55
3.10.2	Extraction of recombinant proteins from BL21 .....	56
3.10.3	Binding Assay with glutathione-magnetic beads.....	57
3.10.4	Discontinuous SDS-Polyacrylamide Gel Electrophoresis (SDS-PAGE).....	59
3.10.5	Coomassie blue staining .....	63
3.10.6	Western Blot and detection .....	64
3.10.7	Extraction and purification of HIS-tag recombinant protein from BL21 (DE) 65	
3.10.8	Protein purification .....	66
3.10.9	Affinity purification of rabbit serum containing $\alpha$ -TOL6 antibody .....	67
3.10.10	PIP strip .....	68
3.10.11	Small scale protein extraction for Western blot.....	69
3.10.12	General plant protein extraction.....	69
3.10.13	Total membrane protein extraction from <i>Arabidopsis thaliana</i> .....	70
3.10.14	Immunoprecipitation of whole TOL protein .....	74
3.10.15	Immunoprecipitation of the protein by Crosslink method .....	76
3.10.16	Immunoprecipitation out of total soluble and membrane fraction protein using crosslinking method .....	78
3.10.17	Protein extraction from plants and immunoprecipitation of TOLs using anti-GFP microbeads.....	78
4	RESULTS.....	80

4.1. Affinity purified anti-TOL6 antibody recognizes endogenous and transgenic TOL6 .....	80
4.2. Expression of TOL protein in planta .....	82
4.3. TOL proteins have different subcellular localization in plant.....	84
4.4. TOL interaction with phospholipids.....	86
4.5. TOL Interaction with Ubiquitin .....	88
4.5.1 TOL6 interacts with ubiquitin and alteration of its UBDs interferes with its ability to bind to ubiquitin .....	92
4.5.2 Mutations of the UBDs of TOL6 alter the <i>in planta</i> localization of TOL6 ....	93
4.5.3 TOL6 with deficient UBDs is not functional in planta.....	95
4.5.4 Mutation of TOL6 UBD affects plant development.....	97
4.6. TOL Proteins are ubiquitinated in planta .....	99
4.6.1 TOL6 is ubiquitinated <i>in planta</i> , specifically in its cytoplasmic fraction.....	99
4.6.2 Ubiquitination of other TOL family members.....	104
4.7. Constitutively ubiquitinated TOL proteins affects the plant regulatory mechanism	105
4.7.1 Constitutively ubiquitinated TOL6 affects its distribution and function in plant	107
4.7.2 Constitutively ubiquitinated TOL6 has a diminished functionality in planta	109
4.7.3 Monoubiquitination of TOL6 affects plant development .....	111
4.7.4 Constitutively ubiquitinated TOL1 alters its distribution and function in plant	113
4.7.5 Constitutively ubiquitinated TOL5 alter the distribution and function in plant	117
5 DISCUSSION .....	119

## TABLE OF CONTENTS

5.1.	The TOL protein family play a role in the degradation of PM proteins between the PM and the cytoplasm.....	119
5.2.	TOLs bind to phospholipids .....	120
5.3.	Mutation of the UBD of TOL6 alter the localization and functionality .....	122
5.4.	TOL proteins are ubiquitinated and potentially regulated by a mechanism termed coupled monoubiquitination .....	124
6	REFERENCES:.....	135
7	INDEX OF FIGURES.....	147
8	INDEX OF TABLES.....	149
9	ABREVIATIONS .....	150
10	APENDIX.....	152

# 1 INTRODUCTION

In multicellular organisms the plasma membrane (PM) functions as a boundary between the extracellular and intracellular space. At the PM, external and internal stimuli are continuously transmitted via receptors, channels, lipids or other proteins localized at the PM. Thus, the protein composition and abundance at the PM, which is extremely important for development, cell survival and physiological responses, is highly regulated. One important mechanism involved in regulating protein composition is a process termed endocytosis. Endocytosis is responsible for the internalization of cellular components localized or synthesized at the PM (Paez Valencia et al., 2016).

Endocytosis internalizes PM proteins and extracellular substances via endocytic vesicles, which are released from the PM, transported through the cytoplasm and fuse to endosomes (Paez Valencia et al., 2016). In mammals and yeast, early endosomes (EE) are the first organelle reached by the PM cargo, while in plants, the Trans Golgi-Network (TGN) is the same compartment as the EE, forming the Trans Golgi-Network/Early endosome (TGN/EE) (Dettmer et al., 2006; Lam et al., 2007). The PM proteins destined for degradation are frequently ubiquitinated and sorted into endosomal vesicles by the ESCRT (Endosomal Sorting Complex Required for Transport) machinery (Dettmer et al., 2006; Paez Valencia et al., 2016). In higher plants, the TOL (TOM1-like) proteins seems to be responsible for initiating and guiding the ubiquitinated PM protein for degradation to the vacuole (Korbei et al., 2013). The detailed mechanism for this starting point is still unclear.

### **1.1. The endosomal system**

In eukaryotic cells, membrane trafficking is essential for various cellular processes including the communication between cells and their surrounded environment as well as nutrient exchanges (Geldner and Jurgens, 2006; Paez Valencia et al., 2016). Proteins like transporters and receptors, which are synthesized in the Endoplasmic Reticulum (ER), are transported to the PM via intermediated endomembrane compartments by the secretory pathway (Dettmer et al., 2006; Otegui and Spitzer, 2008). The secretory pathway is also responsible for secreting enzymes and peptide ligands from ER to the extracellular environment (Otegui and Spitzer, 2008). When new protein are synthesized, they are first sorted to the TGN before being transported to the vacuole (Dettmer et al., 2006; Paez Valencia et al., 2016) or to the PM. Reciprocally, substances like transporters and receptors are internalized from PM via the endocytic pathway and transported to the vacuole/lysosome for degradation or recycled back to the PM (Dettmer et al., 2006; Paczkowski et al., 2015). Thus these two pathways intersect in post-Golgi compartments of the endomembrane system where secretion and endocytosis meet (Richter et al., 2009).

Another important trafficking route in the post-Golgi endomembrane system is endocytosis. Endocytosis is a process where cells internalizes parts of their PM components and other substances by forming endocytic vesicles (Otegui et al., 2001). Many PM proteins are cycling between the endosomal compartments and PM (Geldner, 2004; Geldner and Jurgens, 2006). When endocytosed PM proteins are not recycled back to the PM (recycling pathway), they passes on to the vacuoles/lysosomes for degradation (Richter et al., 2009). Figure 1 shows clearly the specific routes of proteins trafficking in mammals.

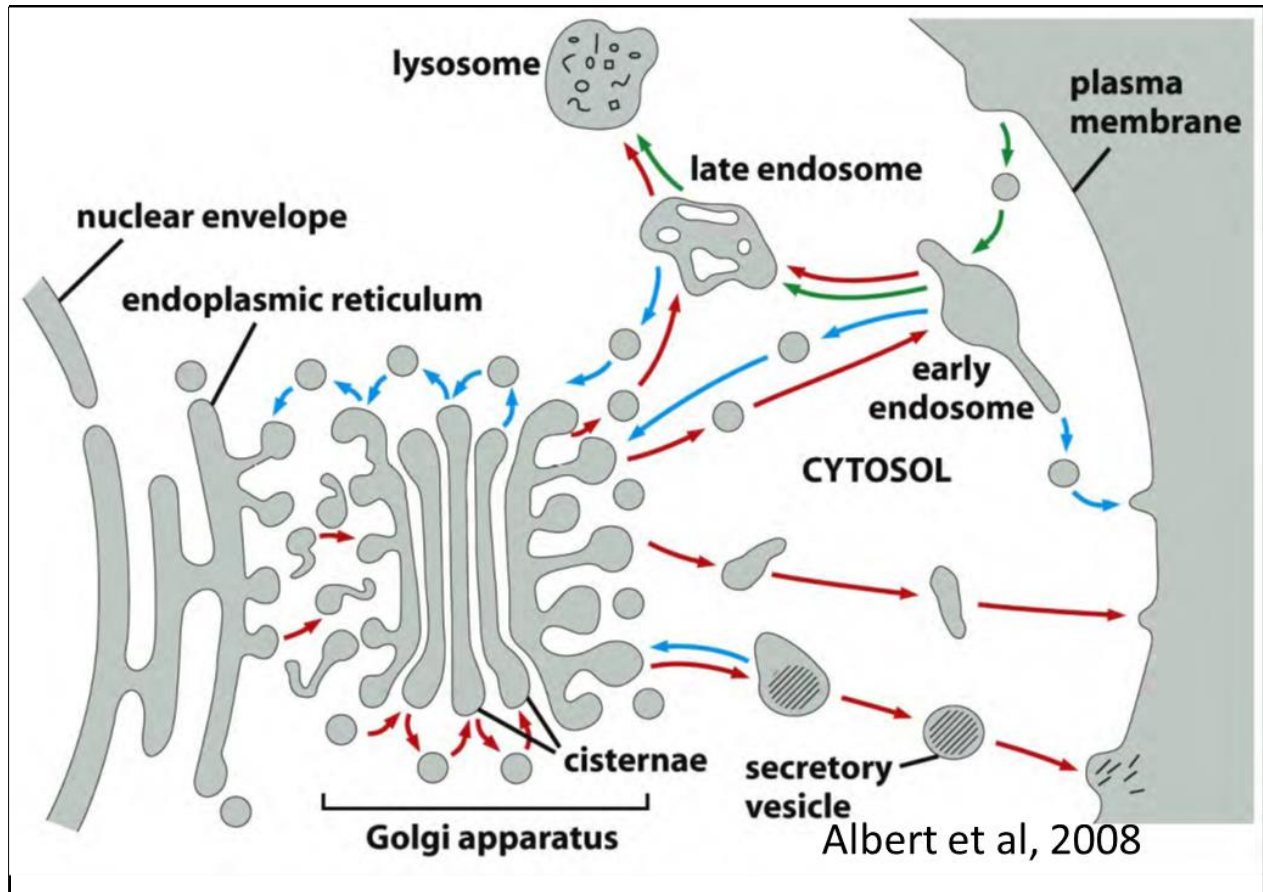


**Figure 1 Secretory and endocytic pathway:** (adapted from Albert et al, 2008). Proteins are transported from ER to the PM or to the lysosome (via endosome) by Secretory pathway (red arrow). In endocytic pathway (green arrows), proteins are internalized in vesicles from the PM and delivered to the early endosome and then to the lysosome (via late endosome). Many endocytosed proteins are retrieved from early endosome to the PM for reuse, some from early and late endosome to the Golgi apparatus (blue arrows).

In animal and yeast, the endosomes are classified in four classes: early, recycling, intermediate and late endosome based on their biochemical function and composition (Henne et al., 2011). The early endosome is the first compartment to receive endocytosed cargo. From there recycled endosome, endocytosed cargos are recycled back to the PM (Otegui and Spitzer, 2008; Paez Valencia et al., 2016). The early and recycled endosome mature to form the late endosome or multivesicular bodies (MVB) (Huotari and Helenius, 2011). The MVB has a sorting function in recycling of vacuolar cargo receptor back to the TGN and sorting of PM proteins for degradation (Otegui and Spitzer, 2008). The endocytosed membrane proteins are sorted into domains of the endosomal membranes, which invaginates and pinches off to form ILVs (Raiborg et al., 2003).

The MVB fuse with the vacuole/lysosome, releasing the ILVs into the vacuolar lumen for degradation by hydrolases (Huotari and Helenius, 2011). Eventually, proteases and lipases in the lysosomes digest all of the internal membranes produced by the invaginations within the MVBs (Huotari et al., 2012; Raiborg et al., 2003). The invagination processes are essential to achieve complete digestion of endocytosed membrane proteins, because the outer membrane of the MVB becomes continuous with the lysosomal membrane, and for example lysosomal hydrolases inside the lysosomes could not digest the cytosolic domains of endocytosed transmembrane proteins, if the protein were not localized in internal vesicles (Fig. 2) (Huotari et al., 2012; Raiborg et al., 2003). Thus, the endosomes and the endomembrane system are important players in regulation of protein composition of PM, TGN and vacuoles/lysosomes (Fig. 2) (Huotari and Helenius, 2011; Otegui and Spitzer, 2008).

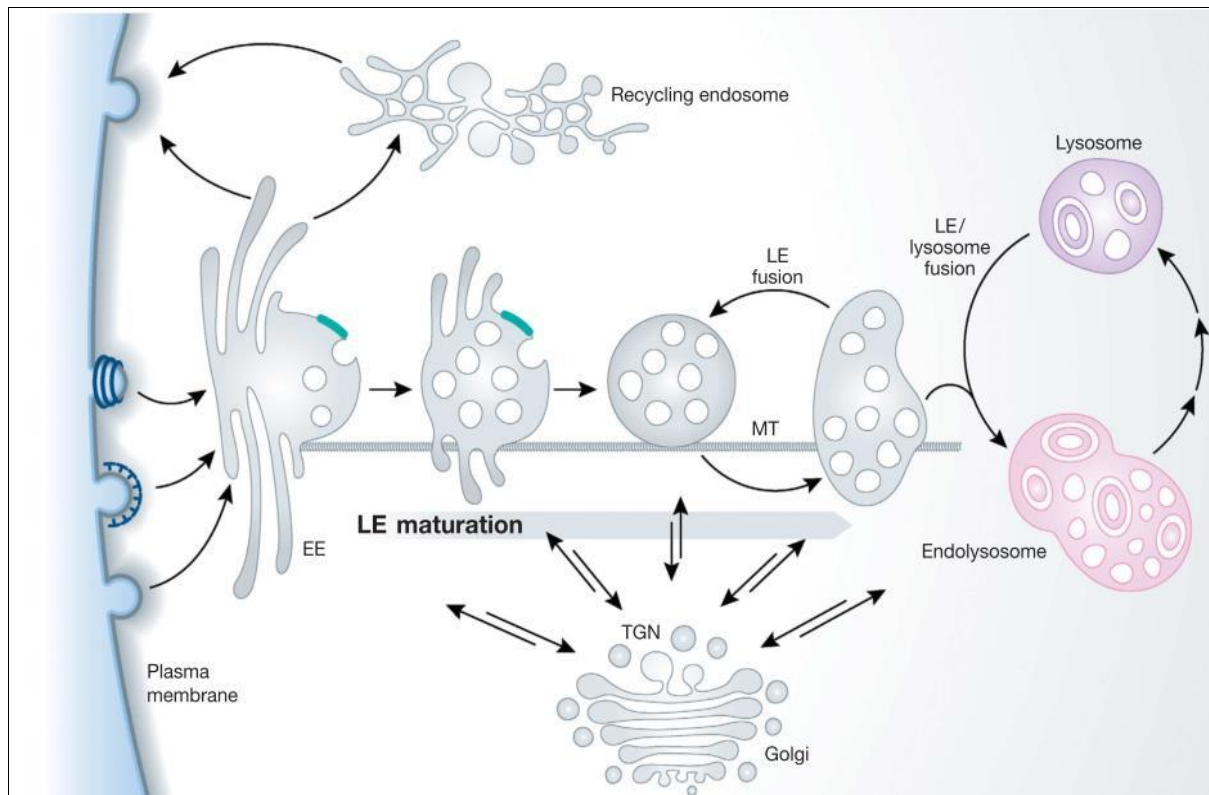


**Figure 2 Endocytic pathway** : (adapted from (Huotari and Helenius, 2011)). Maturation of early endosome to late endosome occurs through the formation of MVB, which contain large amounts of invaginated membrane and internal vesicles. MVB moves inward along microtubules (MT), continually shedding transport vesicles that recycle components to the PM. They gradually convert to the late

endosome either by fusion with each other or by fusion with pre-existing late endosome. The late endosomes (LE) no longer send vesicles to the PM.

In plants, differently to animal cells, the TGN acts as an EE, receiving the endocytosed cargoes from the PM (Dettmer et al., 2006; Lam et al., 2007). At the TGN/EE, the endocytic and secretory pathway meets and many events like sorting and recycling take place (Dettmer et al., 2006; Viotti et al., 2010). The TGN/EE is important sorting point where many transport routes can start leading the cargoes for example back to PM or to vacuole for degradation (Gendre et al., 2011; Scheuring et al., 2011). A group of vesicles that bud from TGN/EE sorting specific cargoes could potentially be seen as recycling endosomes and regulate the distribution and abundance of proteins they are carrying (Kleine-Vehn and Friml, 2008), but the presence of such specialized compartments is still not well defined (Paez Valencia et al., 2016; Robinson and Pimpl, 2013). The TGN is associated with the RAB GTPases RABA4b, RabA1, RABA2 and RABA3, vacuolar H<sup>+</sup> ATPase subunit VHA-a1 and the SYP41/SYP61/VTI12 SNARE (soluble NSF attachment protein receptor) complex in plants and is derived from the trans-most Golgi cisternae by cisternae maturation (Chow et al., 2008; Kang et al., 2011). The endosomes derived from TGN are able to internalize the limiting membrane and form ILVs thereby maturing into late multivesicular endosomes or MVBs and later fuse with the vacuoles (Isono and Kalinowska, 2017). The composition of multivesicular endosomes are based on three Rab5-type GTPases (RABF2a/RHA1, RABF2b/ARA7, and RABF1/ARA6) and the Rab7-type GTPase RABG3f (Heard et al., 2015). In the endosomal pathway of plants, many different mechanisms occur to recycle protein cargo or to sort them to the vacuole for degradation (Fig. 3) (Paez Valencia et al., 2016).



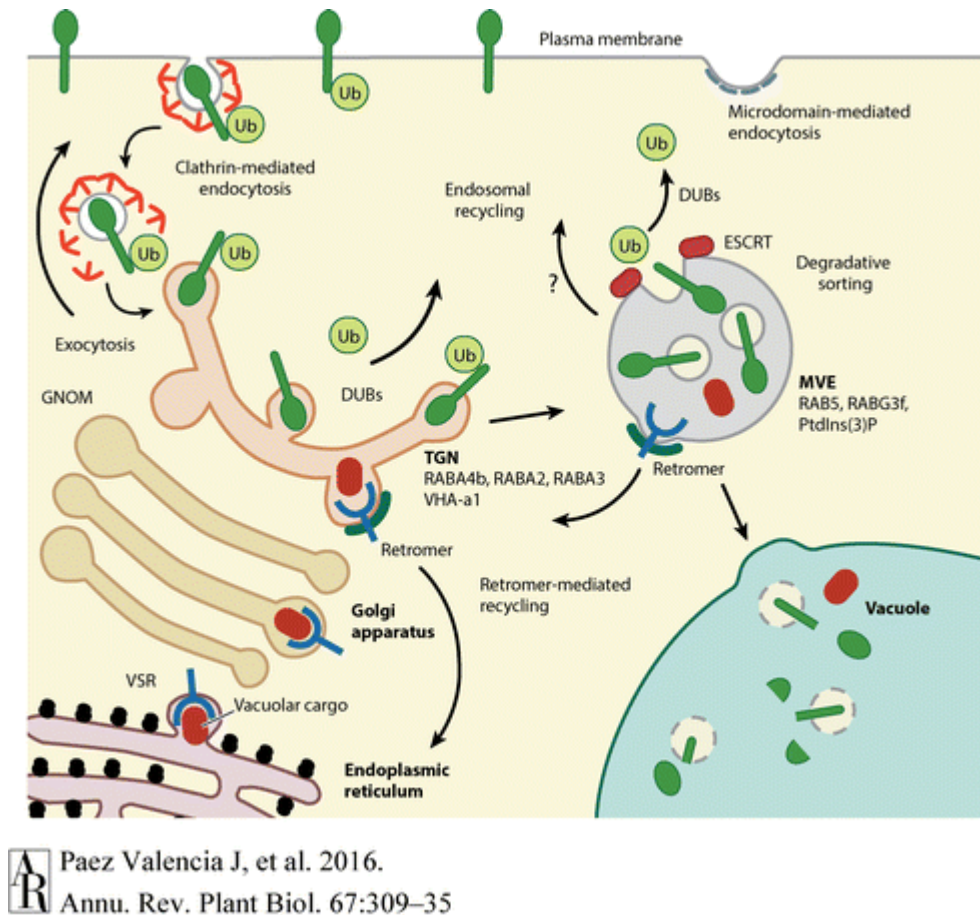


**Figure 3 General overview of endocytic and endosomal trafficking** : (adapted from (Paetz Valencia et al., 2016)).

## 1.2. Clathrin mediated endocytosis

One of the most important endocytic mechanisms in plants and animals is clathrin-mediated endocytosis (CME) (Paetz Valencia et al., 2016). The clathrin coat assembles into triskelia composed of three clathrin heavy chains (CHCs) and three clathrin light chains (CLCs) (McMahon and Boucrot, 2011). CME is well-established mechanism where PM bends into the cytoplasm to form a clathrin-coated pit (McMahon and Boucrot, 2011). The trafficking pathway involves transport vesicles coated with clathrin and adaptor protein (AP) complexes. The expression of dominant negative variants of clathrin heavy chain interfere with endocytosis of the auxin efflux carriers PIN1 and PIN2 (Dhonukshe et al., 2007). Clathrin adaptors are important for forming a connection between the clathrin coat and specific membrane phospholipids and cargo proteins thereby providing specificity to the cargo to be selected and captured within the clathrin coated pit and later

the clathrin coated vesicle (Paez Valencia et al., 2016). Clathrin interacts with cargo via adaptor proteins and the AP-2, which is the most important adaptor for endocytosis initiation (Di Rubbo et al., 2013). AP-2 interacts with specific phospholipids and cargo proteins at the membranes and additionally with specific monomeric adaptors, which together help form the clathrin-coated-vesicles (Di Rubbo et al., 2013; Gadeyne et al., 2014). The TGN and some endosomes also have the same budding mechanism whereby clathrin-coated vesicles are formed (Paez Valencia et al., 2016). CME is divided in five steps: nucleation, clathrin coat assembly, membrane scission, and uncoating (McMahon and Boucrot, 2011). In mammals, CME is initiated by adaptor proteins complex AP-2, which can be activated by binding cargo-sorting motifs and PtdIns(4,5)P<sub>2</sub> (Honing et al., 2005; Peters and de Groot, 2012) and by binding clathrin and PtdIns3P (Fingerhut et al., 2001; Rapoport et al., 1997) as well as by phosphorylation (Fingerhut et al., 2001). In addition, the AP-2 is also activated by interacting with other accessory adaptor proteins such as EGFR-phosphorylated substrate protein 15 (Eps15), intersectin, and muniscin proteins such as FCHO (Fer/CIP4 homology domain only), which could potentially be recruited to the initiation sites before the AP-2 (Henne et al., 2011; Henry et al., 2012). The AP-2 complex has a crucial role in CME in animals but in plants, on the contrary plants without AP-2 can still be viable (Fan et al., 2013; Kim et al., 2013). The main reason is that in plants there are two adaptor complexes: the AP-2 complex was demonstrated to be involved in CME of *Arabidopsis thaliana*, which binds at the same time to clathrin, cargo protein and (PtdIns(4,5)P<sub>2</sub>) at PM (Paez Valencia et al., 2016) and plants have additionally kept an ancestral adaptor complex called TPLATE, that plays a role in the CME nucleation complex (Gadeyne et al., 2014). It consists in eight core subunits (TPLATE, TASH3, LOLITA, TWD40-1, TWD40-2, TML, AtEH1, and AtEH2), which assemble at distant sites of CME initiation, proceeding the recruitment of AP-2 (Gadeyne et al., 2014). Differently to AP-2, the TPLATE plays important role in plant development (Gadeyne et al., 2014). The TPLATE in plants can interact with clathrin (both CHCs and CLCs), AP-2, proteins containing the ANTH domain, and dynamin-related proteins (DRPs) (Fig 4) (Gadeyne et al., 2014). Some of the TPLATE subunits TASH3, TML, AtEH1, and AtEH2 contain conserved domains that are present in Eps15, intersectin, and muniscins which are involved in membrane interactions, cargo recognition, and binding and recruitment of accessory proteins (Zhang et al., 2015).

Besides that, there is also a family of genes encoding monomeric adaptors of the AP180 N-Terminal Homology (ANTH) and EPSIN N-Terminal Homology (ENTH) domain families (Holstein and Oliviussen, 2005; Zouhar and Sauer, 2014).

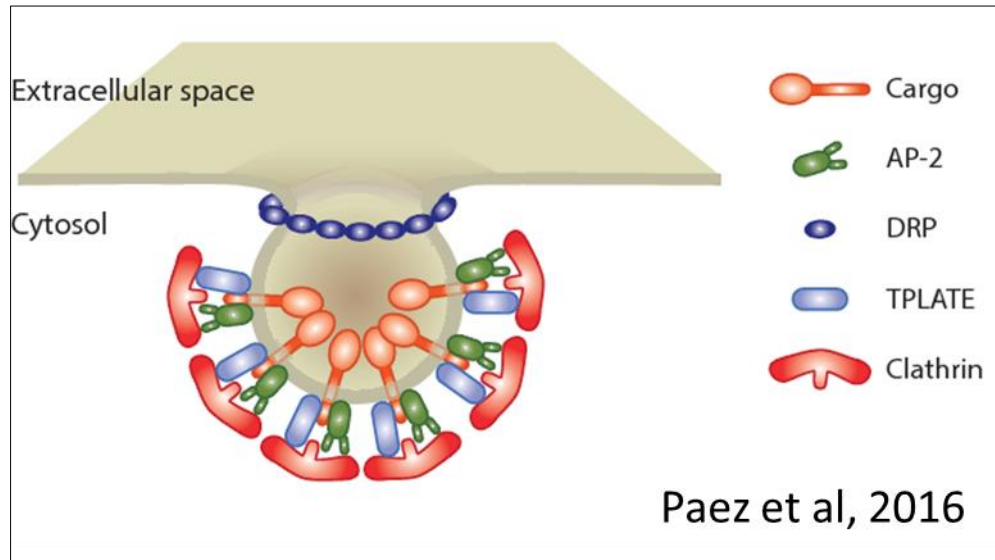


**Figure 4 Clathrin mediated endocytosis :** (Adapted from (Paez Valencia et al., 2016))

### 1.3. The role of ubiquitin in the endocytic system

The sorting mechanism of endocytosed PM protein destined for degradation depends on the post-translational modification of the cargo proteins by ubiquitin or ubiquitination (Komander and Rape, 2012). Ubiquitination acts as a principal signal for endocytosis of PM proteins and acts as a key regulator in sorting process of endocytosed membrane proteins destined for degradation (Leitner et al., 2012; Scheuring et al., 2011). Ubiquitination plays an important role in the regulation of endocytic and vesicular trafficking pathway, by regulating many different processes like endocytosis, vesicular trafficking, cell-cycle control, stress response, DNA repair, signaling, transcription and gene silencing (Dubeaux and Vert, 2017; Piper et al., 2014). Ubiquitinated proteins are sorted via recognition of their ubiquitin moieties by different ubiquitin binding proteins termed ubiquitin receptors (Prag et al., 2007).

During ubiquitination, an ubiquitin protein is added via an isopeptide bond between the carboxyl terminus of ubiquitin with the amino-group of a lysine residue in the target protein. Three important enzymes are involved in ubiquitination: ubiquitin-activating enzymes (E1), ubiquitin conjugating enzyme (E2) and a ubiquitin ligase (E3) (d'Azzo et al., 2005; Fujita et al., 2002). Ubiquitin ligases, works as a platform that coordinate substrate recognition with ubiquitin transfer (Fujita et al., 2002). The E3 ligase and adaptor proteins bind directly to the substrates and the selection of substrate residue destined for ubiquitination is realized by a particular architecture of the substrate/ligase complex which determines the orientation to the thioester-linked ubiquitin (Piper et al., 2014). The addition of ubiquitin can follow different patterns according to the E2 and E3 enzymes involved, whereby a single ubiquitin can be added to the target protein, resulting in monoubiquitination, or several ubiquitins can be added to different lysine residues on the target protein resulting in poly-monoubiquitination (d'Azzo et al., 2005; Sigismund et al., 2004). Furthermore, an ubiquitin can be added to an already covalently attached ubiquitin via one of the seven internal lysines (K6, K11, K27, K29, K33, K48, and K63) of ubiquitin, resulting in polyubiquitin chains (Varadan et al., 2004). The resulting linkage types are structurally different, depending on the lysines used. While the K48-linked di-ubiquitin is relatively compact, the K63-linked di-ubiquitin adopts an open conformation (Tenno et al., 2004; Varadan et al., 2004). These differences are important for ubiquitin binding proteins, which bind to different ubiquitination patterns with different affinities (Galan and Haguenauer-Tsapis, 1997; Terrell et al., 1998). The number and spatial orientation of added ubiquitin entities are crucial for protein's destiny (Hicke and Dunn, 2003; Ikeda and Dikic, 2008; Kim et al., 2007). In this context, K48-poly-ubiquitination of soluble proteins results in their cytosolic degradation by the 26S proteasome (Finley et al., 1994).

In order to remove damaged proteins from the cell surface or simple for programmed biological response, ubiquitination can be used as a quality control mechanism and PM proteins are sorted to the vacuole for degradation by ubiquitination process (Piper et al., 2014). Ubiquitin can also work in the context of other weaker internalization signals like the aggregate effect of multiple ubiquitin and non-ubiquitin signals become sufficient for incorporation into clathrin-coated vesicles (Boname and Lehner, 2011). Monoubiquitination and K63-ubiquitination are signals that control endocytosis and

vacuolar sorting of PM proteins and K63-ubiquitination is the major poly-ubiquitin chain that operates in the internalization steps leading to lysosomal/vacuolar degradation (Boname and Lehner, 2011). The attachment of single ubiquitin to a membrane bound protein facilitates sorting ILV of late endosome/multivesicular bodies followed by lysosomal degradation, which potentially requires K63-polyubiquitination (Piper et al., 2014; Raiborg and Stenmark, 2009). For some PM proteins, ubiquitination is not essential for their internalization, but it still plays a role later in the endocytic pathway for other trafficking steps (Huang et al., 2007; Huang et al., 2006).

Some ubiquitin binding domains (UBD) containing proteins are localized at CME sites and can function as adaptors for different subsets of ubiquitinated proteins (Mayers et al., 2013; Sato et al., 2009). The ubiquitin moiety of ubiquitinated cargoes helps sequestration of the cargo into the forming clathrin-coated vesicle as well as potentially their proper assembly, through the interaction with UBD of the associated nucleation machinery (Henry et al., 2012; Kang et al., 2013). In mammals and yeast epsin and epsin15 adaptor protein are important to link the ubiquitinated cargoes to the clathrin-mediated endocytic machinery that contains ubiquitin interacting motif (UIM) domain and interact with each other (Klapisz et al., 2002). Epsin contains an ENTH domain, which is structurally similar to the VHS domain, and which binds to PtdIns(4,5)P<sub>2</sub> as well as an UIM that interact with ubiquitinated cargo (Sen et al., 2012). Epsin helps binding to K63-poly-ubiquitin, which correlates well with the requirement of multiple ubiquitin as an internalization signal (Chen and De Camilli, 2005; d'Azzo et al., 2005). In plants a large number of A/ENTH-domain proteins are predicted in the *Arabidopsis* genome, which potentially function to sort cargo at the early endosomes for degradation, but their physiological roles are not well understood and they have not been found to contain UBDs (Zouhar and Sauer, 2014).

When membrane proteins are delivered to early endosome, they can be sorted into intraluminal vesicles (ILVs) or can stay at the surface membrane of endosome, which can be recycled back to the PM (Huotari et al., 2012). Proteins are definitively degraded when they reach the ILV, as this sorting step is irreversible (Piper et al., 2014). Some proteins function as deubiquitinating enzymes (DUBs), which removes and remodel the ubiquitin chains in the endosomal pathway (Nagel et al., 2017; Urbe, 2005). DUBs ubiquitin peptidases, which removes ubiquitin from substrate have a critical importance in

controlling the levels of substrate for protein ubiquitination as well as the recycling of the ubiquitin molecules (Clague et al., 2012). Furthermore, DUBs contribute to the modulation of the ubiquitin signal by removing or trimming it, therefore reversing or reinforcing pathways, whereby some proteins are deubiquitinated and recycled back to the PM (Hicke and Dunn, 2003; Urbe, 2005).

#### **1.4. Importance of ESCRT machinery in plants**

Ubiquitination is the major sorting signal for endosomal-mediated degradation. Proteins that are ubiquitinated are endocytosed and if they are not deubiquitinated and recycled to the plasma membrane, they are sorted into ILV of MVB by Endosomal Sorting Complex Required for Transport (ESCRT) machinery, which conducts the ubiquitinated cargo proteins to the vacuole for degradation (Gao et al., 2017; Isono and Kalinowska, 2017; Paez Valencia et al., 2016). The ESCRT machinery is evolutionarily conserved machinery responsible not only for the sorting of the ubiquitinated cargo, but also for membrane deformation and scission from the inner face of a membrane away from cytoplasm (Gao et al., 2017; Katzmann et al., 2003; Raiborg and Stenmark, 2009). Multiple subunits of the ESCRT machinery contain ubiquitin binding domains and in mammalian and fungi, four ESCRT complexes are described (ESCRT-0, I, II and III), which are important for recognition, concentration and sequestering of ubiquitinated cargo (Clague et al., 2012). The ESCRT-0 is the initial point for recognition of ubiquitinated cargo at early endosomes and is followed by recruitment of ESCRT-I (Clague et al., 2012). In mammals/yeast the ESCRT-0 consists of two subunits, the STAM (Signal-transducing adapter molecule) proteins in mammals or Hse1 (Hbp, STAM; EAST1) in yeast, which form a multifunctional complex with Hrs (hepatocyte growth factor-regulate substrate) in mammals and Vps27 (Vacuolar Protein Sorting 27) protein in yeast (Bilodeau et al., 2003; Katzmann et al., 2003). The mammalian complex (STAM/Hrs) contains ubiquitin-binding domains like the Vps27/Hrs/STAM (VHS) domain, a ubiquitin interacting motif (UIM), and a GAT (GGA (Golgi-localized, Y-ear-containing ARF-binding protein) /TOM (Target of Myb 1)) domains (Mizuno et al., 2003).

After the ubiquitinated cargo is sequestered by the ESCRT-0, which recruits the ESCRT-I, it is passed on to the ESCRT-II complex, which also contains ubiquitin-binding subunits.

The ESCRT-II in turn induces deformation of the membrane and finally passes the ubiquitinated cargo to the ESCRT-III, which does not contain any UBDs anymore, and mediates further membrane deformation and scission and subunit recycling (Henne et al., 2011; Richter et al., 2009). The affinity of ESCRT complex to the ubiquitinated cargo is important to keep the cargo on ESCRT – positive endosome and subsequent degradation (Henne et al., 2011).

Members of two other protein families, GGA3 (Golgi-localized, Y-ear-containing, ARF-binding protein 3) and TOM1 (target of Myb1), also contain VHS domains and bind to ubiquitinated cargo at endosomal membranes (Puertollano, 2005; Puertollano and Bonifacino, 2004). ESCRT-0 subunits and GGA proteins were not identified in plants (Winter and Hauser, 2006), but the highly conserved TOM1 like proteins, which work as a functional equivalent to the ancestral ESCRT-0 (Blanc et al., 2009), were identified. Our recent studies described this family of nine proteins termed TOL (TOM1-like) proteins in *Arabidopsis thaliana* (Korbei et al., 2013) which are necessary for the endocytic downregulation of PM localized proteins like of PIN2 and KNOLLE (Korbei et al., 2013) and BOR1 (Yoshinari et al., 2018) and they bind ubiquitinated cargo presumably via their predicted UBDs, the N-terminal VHS and Gat domains (Korbei et al., 2013).

The first contact between the ubiquitinated cargo and ESCRT-0, which in plants is replaced by TOL proteins, occurs in earlier stages in plants endosomal system (Gao et al., 2017; Isono and Kalinowska, 2017; Korbei et al., 2013). The recruitment of the ubiquitinated cargo to other ESCRT subunits occurs along the endosomal compartments, showing a difference distribution of ESCRT subunits along the endosomal sorting route (Scheuring et al., 2011) with *Arabidopsis thaliana*, TOL6 localized at the PM and TGN/EE (Gao et al., 2017; Isono and Kalinowska, 2017; Korbei et al., 2013). Another plant proteins, SH3P2 localized in close proximity to PM has a role on recognition of ubiquitinated cargo that are to be sorted into ESCRT pathway by interacting with ESCRT-I subunit VPS23 (Nagel et al., 2017). It was also shown that, the ESCRT-I is localized at Golgi apparatus and TGN but not at MVB (Scheuring et al., 2011), the ESCRT-II localized at the TGN while the ESCRT-III localized at MVBs (Cai et al., 2014; Scheuring et al., 2011). The differential ESCRT complexes localizations indicate their sequential recruitment and release from membranes (Fig. 4).

In membrane trafficking of plants there are some unique proteins that participate in the ESCRT pathway (Gao et al., 2017; Isono and Kalinowska, 2017; Korbei et al., 2013). The SH3P2 that localizes at PM is involved in vesicle trafficking where it binds to K-63 linked ubiquitin chains of membrane proteins in close proximity to PM (Nagel et al., 2017). Upon binding to ubiquitinated cargo at PM, SH3P2 could enrich ubiquitinated cargo at the endosomal membrane and, by interacting with VPS23, could pass them to the ESCRT machinery (Nagel et al., 2017). The SH3P2 on CCVs could function together with ESCRT-I subunit VPS-23 and DUB AMSH3. Since SH3P2 localizes at PM, whereas VPS23 and AMSH3 do not, SH3P2 could also have an ESCRT-I- and DUB independent function at the PM (Nagel et al., 2017). ESCRT subunits involved in membrane trafficking of plants like FYVE/FREE1, ALG-2-interacting protein X (Alix), TOLs, VPS23.1 and the ESCRT-II subunit VPS36 were described to interact with ubiquitin or ubiquitin chain (Gao et al., 2014; Kalinowska et al., 2015; Korbei et al., 2013). SH3P2 was also shown to interact with FYVE/FREE1 (Gao et al., 2014; Kolb et al., 2015). Thus, the ubiquitin-binding proteins interact and function together increasing their affinity to ubiquitin chain therefore enhancing the efficiency of sorting the cargos into ESCRT-dependent endocytosis degradation pathway (Nagel et al., 2017).



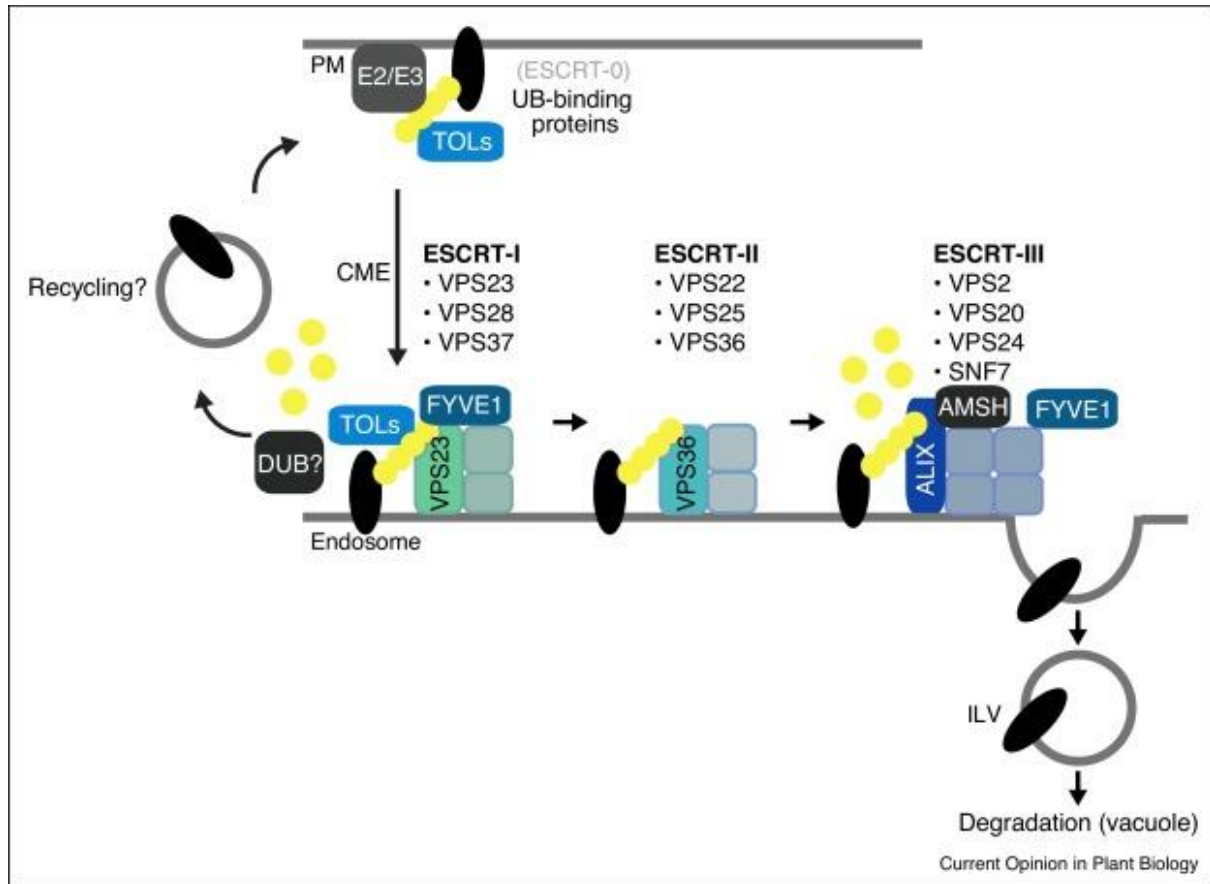


**Figure 5 Recognition and degradation of ubiquitinated PM-proteins by ESCRT and ESCRT-interacting proteins :** (Adapted from (Isono and Kalinowska, 2017)).

### 1.5. Ubiquitin Binding Domains (UBD)

The ubiquitin signal is recognized and decoded by UBD. UBD are specialized domains that bind ubiquitin with a low affinity, allowing the proteins they contain to thus act as ubiquitin receptors (Dikic et al., 2009). UBDs bind to the exposed hydrophobic patch of ubiquitin molecule surrounding isoleucine at position 44 (I44) with weak micromolar affinity (Dikic et al., 2009). Allowing the ubiquitin to adopt several conformations that can be captured via UBD by a variable combination of conformational selection (Long and Bruschweiler, 2011; Peters and de Groot, 2012; Wlodarski and Zagrovic, 2009). These domains are found in large variety of cellular proteins and link the ubiquitin signals to specific cellular response like endocytosis, degradation, or translocation of modified

protein (Dikic et al., 2009; Piper et al., 2014). In the endocytic pathway, ubiquitin acts in two different ways: as a sorting signal on cargo being recognized by UBD-containing sorting receptors, or by modifying the endocytic machinery (Piper et al., 2014), where ubiquitination of subunits of the endocytic machinery has a regulatory function (Dikic et al., 2009).

In the endocytic pathway, ubiquitin recognition occurs at membranes where proteins diffuse only in two dimensions rather than in three (Husnjak and Dikic, 2012). Furthermore, the ubiquitin receptors have additional motifs that bind weakly to their ubiquitinated partner proteins. This increases the avidity and enhance the specificity to the selected target (Husnjak and Dikic, 2012). Most of UBD interacts with mono-ubiquitin but shows a binding preference towards a specific chain type (Husnjak and Dikic, 2012). When an ubiquitin is permanently attached to the cargo, a single ubiquitin is enough to sort the cargo for degradation (Raiborg et al., 2002; Stringer and Piper, 2011), but this single ubiquitin is exceptionally weak as an internalization signal and therefore ubiquitin operates better in chains (Bertelsen et al., 2011). Differently, to the endocytic internalization, for the MVB sorting K63-linked-ubiquitin chain are the key signal, rather than a mono-ubiquitin (Huang et al., 2013). Furthermore, the formation of the chains and their disassembly by DUBs occurs continuously during the transport of ubiquitinated cargo in the endocytic pathway, resulting in a very specific binding to the UBD-containing sorting receptors and therefore allowing for fine-tuning between the endocytosis, recycling or degradation pathways (Clague et al., 2012). Mono-ubiquitination of ubiquitin receptors can change the conformation of UBD containing proteins, altering their capacity to recognize and sort the ubiquitinated cargo (Hoeller et al., 2006).

The TOL proteins have a crucial function in vacuolar targeting and subsequent degradation of ubiquitinated membrane proteins. TOL proteins contain two well-conserved UBDs, namely the VHS domain at the N-terminus followed by a GAT domain (Fig. 6) (Korbei et al., 2013; Sauer and Friml, 2014). Presumably, the TOL proteins binds to ubiquitin via these two well conserved ubiquitin binding domains (VHS and GAT) similar to the non-plant organisms.

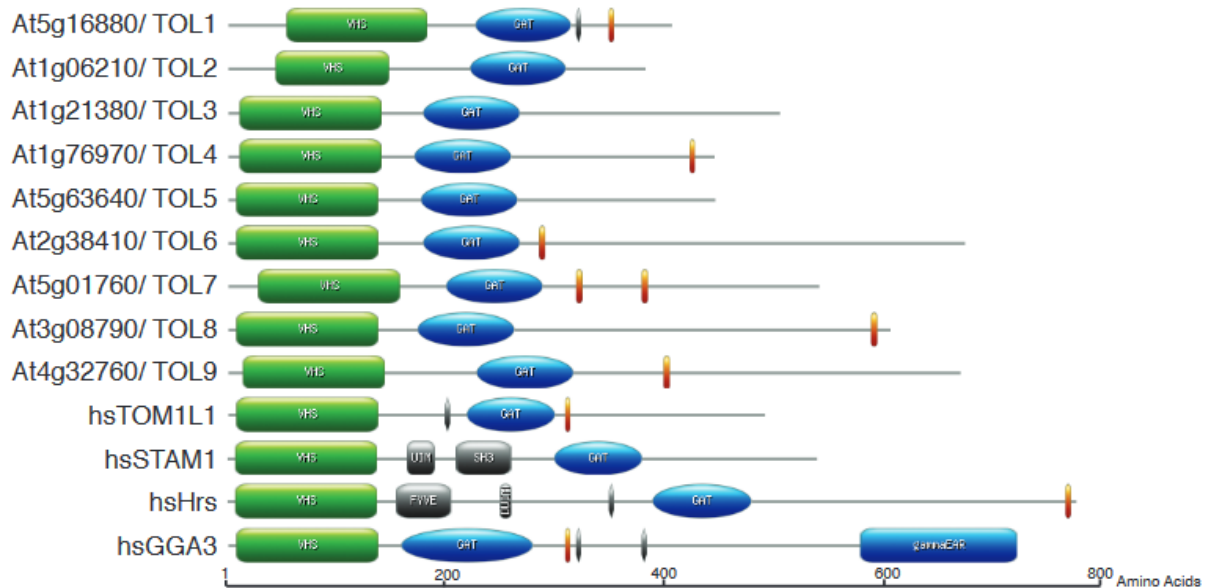


**Figure 6** In silico analysis of the domains of proteins with VHS and GAT domains in *Arabidopsis thaliana* and *Homo sapiens* : (adapted from Korbei et al., 2013). Abbreviations: VHS (Vps27/Hrs/STAM domain, in green), GAT (GGA and TOM domain, in blue), FYVE (Fab1/YOTP/Vac1/EEA1 domain), UIM (ubiquitin-interacting motif), DUIM (double UIM) and SH3 (Src homology-3) (Korbei et al., 2013).

## The VHS Domain

Initially the VHS (Vps27-Hrs-STAM) domain (Fig. 7, left side ) was described based on the sequence homology by yeast Vps27p and mammalian Hr and STAM (Lohi et al., 2002). The VHS domain is a common UBD with octa-helical structure, which is predominantly present at the N-terminus of proteins involved in vesicular trafficking in eukaryotes (Wang et al., 2010). In mammals, there are 9 proteins containing the VHS domain: Hrs, STAM1, STAM2, GGA1, GGA2, GGA3, Tom1, Tom1L1, Tom1L2 (Wang et al., 2010). Due to its super-helical structure it was suggested to provide a common protein-protein interaction surface (Mao et al., 2000; Mizuno et al., 2003). The importance of the VHS domain as UBD was elucidated by *in vitro* assays analyzing the N-terminal part of the STAM protein including UIM and VHS domain (Mizuno et al., 2003). Although analysis of the individual domains revealed similar ubiquitin binding affinities, deletion of the VHS impaired ubiquitin binding activity more severely than deletion of UIM in the mammalian ESCRT-0 subunit STAM (Mizuno et al., 2003). The tandem location of VHS and UIM in Hse1 and STAM might have a synergistic effect in their ubiquitin binding affinity, whereas

in Vps27 and Hrs the FYVE domain located in between may disturb (Mizuno et al., 2003). Nevertheless these domains can interact with ubiquitin independently, although it's still not clear whether VHS and UIM bind to different sites of ubiquitin or if they bind different ubiquitin molecules simultaneously (Mizuno et al., 2003).

The most conserved amino acids liable for ubiquitin binding are located in the  $\alpha$ 2- and  $\alpha$ 4-helix of VHS (Wang et al., 2010), oriented towards the surface of the protein to promote ubiquitin interaction (Lange et al., 2011). The binding affinity for VHS to ubiquitin is relatively low, reflecting the fast dissociation rate and the rapid assembly and disassembly of the protein complex for ubiquitinated cargo sorting (Lange et al., 2011).

### **The GAT domain**

The GAT (GGA and Tom) domain (Fig. 7 – right side), was initially discovered in GGA (Golgi-localized, gamma-ear containing, ADP-ribosylation factor binding) proteins as a family of monomeric clathrin adaptor proteins regulating vesicular transport between the Trans Golgi network (TGN) and the endosomal system (Collins et al., 2003; Dell'Angelica et al., 2000). The structural organization of the GGA GAT domain includes two independent subdomains: the C-terminal and the N-terminal GAT domain (Collins et al., 2003). Whereas the N-terminal hook (171-210 residues) interact with the ARF1-GTP targeting the GGA to the Golgi (Bonifacino, 2004), the C-terminal helical bundle (211-299 residues) is responsible for ubiquitin binding (Bilodeau et al., 2004). Within the C-terminal  $\alpha$ 3-helix of the GGA GAT domain, one uncharged and two hydrophobic amino acids are well conserved residues involved in ubiquitin binding (Puertollano and Bonifacino, 2004; Shiba et al., 2004). The second ubiquitin interaction region was discovered in the  $\alpha$ 1-helix including an acidic, hydrophobic and another acidic amino acid pointing to the same surface of the helix more or less well conserved in Tom and GGA proteins (Bilodeau et al., 2004; Prag et al., 2005).

Two intertwined GAT domains each consisting of 3  $\alpha$ -helices, built up the core complex of Vps27/Hse1 and Hrs/STAM with a barbell-like structure (Prag et al., 2007). One bundle of the barbell is composed of  $\alpha$ 1 and  $\alpha$ 3-N-terminus of Hse1 and  $\alpha$ 3-C-terminus of Vps27, whereas the other one is patterned mirror-inverted (Prag et al., 2007). The central part of

each  $\alpha 3$ -helix together forms the two-stranded coiled coil of the barbell. The GAT domains 20 therefore are essential domains in assembling the multivalent ubiquitin binding machinery of the ESCRT-0 (Prag et al., 2007).

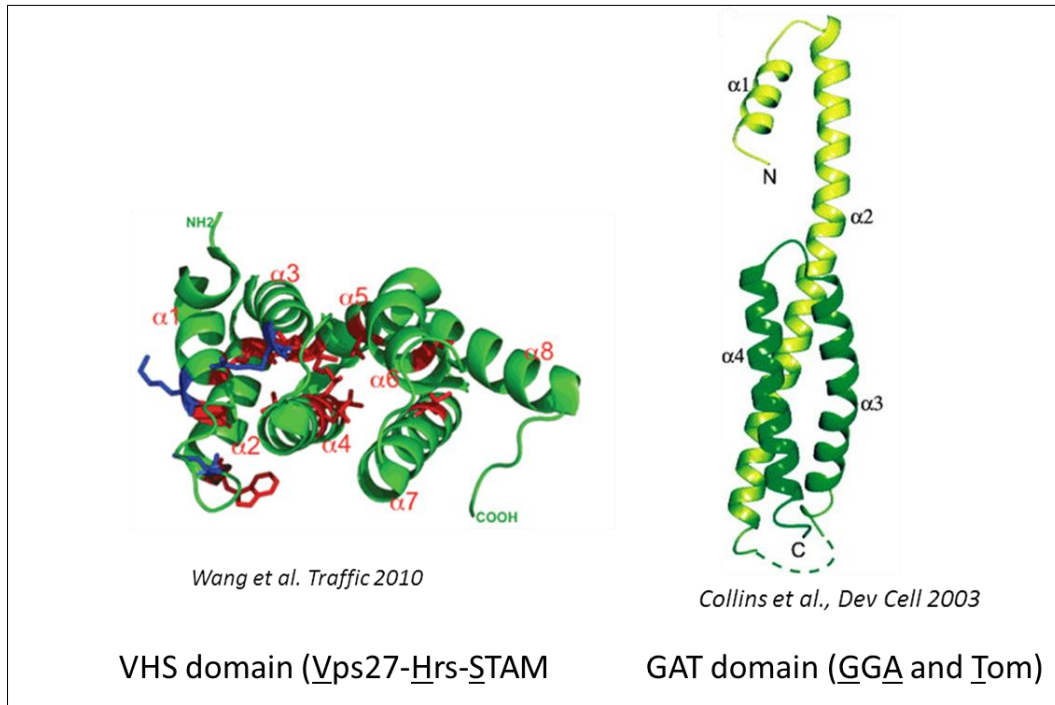


**Figure 7 Protein structure of VHS and GAT domain :** (Adapted from (Collins et al., 2003); (Wang et al., 2010) respectively).

## 1.6. Coupled Monoubiquitination

Ubiquitination participates in the regulation of the endocytic pathway but also affects the abundance of endocytic sorting machinery components by inducing its proteasomal degradation (Husnjak and Dikic, 2012). Furthermore, ubiquitin also generates interaction network by regulating the interactions between proteins that are important for endocytic machinery organization (Hoeller et al., 2006; Hoeller and Dikic, 2010). Many cellular processes like protein degradation, DNA repair, peroxisome biogenesis, viral budding, signal transduction and membrane trafficking are regulated by ubiquitination (Haglund and Dikic, 2005; Haglund and Stenmark, 2006). Furthermore, many different biochemical processes are regulated by ubiquitination, which recognize ubiquitinated proteins by their ubiquitin receptors (Haglund and Dikic, 2005; Haglund and Stenmark, 2006). Ubiquitin

adaptors contain one or more UBD which recognizes ubiquitin but also allows them to be monoubiquitinated themselves in a process called “coupled monoubiquitination” (Pickart, 2001). It was demonstrated that, monoubiquitination of endocytic proteins like Eps15 and others, results in intramolecular interaction between UBDs, therefore avoiding them to bind in trans to ubiquitinated targets. Thus, monoubiquitination controls the fate of ubiquitinated targets by regulating the function of ubiquitin receptors (Hoeller et al., 2006). In monoubiquitinated ubiquitin receptors, an intramolecular interaction between the monoubiquitin and their own UBDs occurs, leading to the auto-inhibition of the endocytic adaptor (Hoeller et al., 2006). Coupled monoubiquitination works as a negative-feedback control in molecular machineries which requires transient and consecutive interactions between ubiquitin receptors and their ligands (Haglund and Stenmark, 2006). Furthermore, coupled monoubiquitination prevents binding to the ubiquitinated cargo, as the UBD is already occupied either by intra- or by intermolecular ubiquitin binding (Blanc et al., 2009).

### **1.7. Protein-lipid interactions in the endocytic system of plants**

The acquirement of the membrane identities are promoted by combinations between the presence of specific lipids and proteins on each membrane (Jean and Kiger, 2012). Peripheral membrane proteins can be anchored to membranes by different mechanisms like protein-protein and protein-lipid interactions (Cho and Stahelin, 2005). Phosphoinositides (PIs) are considered as the major determinants of membrane identities on the cytosolic side of eukaryotic cell membranes (Balla, 2013; Heilmann, 2016). Even though they occur in very low abundance, PIs are important players for the recruitment of peripheral proteins to membranes (Balla, 2013; Heilmann, 2016). They are composed of a glycerol backbone, two non-polar fatty acid tails and a phosphate group substituted with an inositol polar head group, which can be phosphorylated at various positions on their polar head (Platre and Jaillais, 2016). PIs are mono-, bis- and tris-phosphorylated

derivatives of phosphatidylinositol and PI compositions differ between the PM and different organelle membranes (Balla, 2013).

Membrane identity in the endocytic pathway is also defined by a PI cascade in animal as well as in plants, although their PI composition in the different organelle membranes differ markedly (Noack and Jaillais, 2017; Posor et al., 2015). In animals, this PI cascade starts from PI(4,5)P<sub>2</sub> at the PM, uses transient accumulation of PI(4)P and PI(3,4)P<sub>2</sub> during endocytosis, and leads to accumulation PI3P in early endosomes and then PI(3,5)P<sub>2</sub> in late endosomes (Jean and Kiger, 2012). Plants have two shorter, largely independent phosphoinositide cascades centered on TGN/EE and LE/MVB endosomes. Those cascades are important for the membrane trafficking allowing the membrane identity to evolve dynamically during the course of trafficking (Jean and Kiger, 2012). The PI abundance in specific membranes is determined by PI-kinases and phosphatases (Barbosa et al., 2016). In plants, the PI(4)P and PI(4,5)P<sub>2</sub> are found at the PM, while PI 3P resides in the late endosomes and the tonoplast (Barbosa et al., 2016). The organelle functions are determined by the distribution of the membrane-specific PI which regulate the specific PI kinase or phosphatases allowing therefore the recruitment of specific related binding proteins (Behnia and Munro, 2005).

In many biological processes and organisms, the organization of polar domains is controlled by the asymmetric PI distribution (Shewan et al., 2011). Some cellular compartments are marked by the presence of specific lipids, and recognition of these lipids is required for intracellular trafficking machinery to discern one intracellular organelle from another (Behnia and Munro, 2005). The acidic phospholipids are exclusively used as a binding target and the domains and proteins that binds membrane surfaces vary widely in their binding mechanisms (Testerink and Munnik, 2005). In plants phosphatidic acid (PA) represent a minor membrane phospholipid formed in several stress conditions (Testerink and Munnik, 2005). PA is one of the lipid signaling, which accumulates rapidly in response to different environmental signals, like in response to a wide array of abiotic stress stimuli (McLoughlin and Testerink, 2013). PA formation provides the cell with spatial and transient information about the external environment by acting as a protein-docking site in cellular membranes (McLoughlin and Testerink, 2013).

The plant PM has a specific electrostatic signature that is driven by PI(4)P and recruits proteins with polybasic sequence (Platre and Jaillais, 2016). PI also recruit coat proteins, such as the Adaptor Proteins (AP) complex involved in Clathrin-coated vesicle formation (Posor et al., 2015). There is a direct relation between PIs and the recognition of ubiquitin sorting signal during membrane trafficking. Moreover, the trafficking of ubiquitinated cargo may be directly regulated by the same phosphoinositide's that recruits their associated adaptors to the appropriate organelle membrane. The PI leads an ubiquitin ligase to internal organelle membrane (Dunn et al., 2004). Since The ESCRT-0 in yeast and mammals recognizes ubiquitinated cargo on early endosomes by their unique enrichment for certain PIs (Demmel et al., 2008). It becomes interesting to investigate if the plants substitute of ESCRT-0, the TOL proteins also binds to PIs. The FYVE domain which interact with PIPs in yeast and mammals is not present in TOL proteins (Demmel et al., 2008) thus, presumably the VHS domain works as a functional substitute for PI binding to the TOL proteins.



## 2 AIM OF THIS THESIS WORK

In higher plants, a protein family, the TOL (TOM1-like) proteins, function as principal gating factors for recognition of ubiquitinated cargo at the PM destined for degradation (Isono and Kalinowska, 2017; Korbei et al., 2013; Sauer and Friml, 2014). TOL proteins are characterized by two  $\alpha$ -helical UBDs, the N-terminal VHS domain, followed by a GAT domain. Both VHS and GAT domains potentially interact with ubiquitin as well as phospholipids and thus ensure recruitment to endosomal membranes (Wang et al., 2010). The TOLs, could thus function as crucial switches in integration of different stimuli. The functional significance of UBDs or the phospholipid interactions predicted in TOL proteins are however entirely unknown.

The TOL proteins seems to be responsible for initiating and guiding the ubiquitinated PM protein for degradation to the vacuole (Korbei et al., 2013). However, the detailed mechanism for this starting point is still unclear.

We have already demonstrated that, the TOL proteins plays a crucial function in vacuolar targeting and followed degradation of ubiquitinated PM proteins (Cai et al., 2014; Korbei et al., 2013). The exact localization, distributions and specific function of different TOL members are of crucial interest to us and still mostly unknown. Therefore, the main aim of this thesis was to investigate not only where but also how the TOL proteins are localized in the endomembrane system. In addition, to address their function by understanding determinants that control the TOL distribution and abundance in the endosomal system. I aim to elucidate the individual activities of TOL proteins in the model plant *Arabidopsis thaliana*, since some protein family have been probably evolved and developed independently and acquired specific functional properties in higher plants.

Thus, the outcome of this project will not only close gaps in our knowledge about the endosomal system of plants, but furthermore will serve as a cornerstone for future studies.

### 3 MATERIALS AND METHODS

#### 3.1. Chemicals, reagents and enzymes

Chemicals, reagents and enzymes used in preparation of different working solutions, buffers and medium were purchased from the following companies: Fluka, Roth, Aplichem, MBI Fermentas, Promega, Invitrogen, Roche, Sigma, Merk, NEB, Peqlab, Biorad. In general, the companies provide each specific product with the text description or the protocol for use.

#### 3.2. Oligonucleotides and primers combinations

Lyophilized synthetic Oligonucleotides obtained from MWG-Biotech AG and Invitrogen Company. Primers dissolved in an appropriate volume of ddH<sub>2</sub>O to a stock concentration of 100 µM. Working stocks given an internal number before freezing at -20°C. Abbreviations used: **M** - Mutagenesis, **A** - Amplification and **G** – genotyping (Table 1).

**Table 1 Primer sequences list**

Primer designation	Purpose	Orientation	5`-3` Sequence
TOL6 N73Af	M	forward	GAG ACG TTG GTA AAG GCC TGT GGA G
TOL6 N73Ar	M	reverse	C TCC ACA GGC CTT TAC CAA CGT CTC
TOL6 AAA1f	M	forward	GG GAT GTG ATG GCT GCC GCG GGC GAC ATG
TOL6 AAA1R	M	reverse	GAT GTC GCC CGC GGC AGC CAT CAC ATC CC

TOL6 AAA2f	M	forward	CTC TTG GGC GCC GCG GCA CAA GCT GTG G
TOL6 AAA2r	M	reverse	C CAC AGC TTG TGC CGC GGC GCC CAA GAG
TOL6 W25Af	M	forward	GTTAGGTCCTGATGCGACTACG AATATGGAAATCTGC
TOL6 W25Ar	M	reverse	GCA GAT TTC CAT ATT CGT AGT CGCA TCA GGA CCT AAC
LB1.3	G		A TTT TGC CGA TTT CGG AAC
TOL3u (TOMI152u)	G	forward	G CTC AGG CAA CTG CAT CAG
TOL3d (TOMI152u)	G	reverse	CG GTA TTG GAG TGG GAG CTG
Notlmcherryu	M	forward	G CGG CCG CAT GGT GAG CAA GGG CGA
Notlmcherryd	M	reverse	GCG GCC GCT TAC TTG TAC AGC TCG TCC ATG
TOL6q-f1	G	forward	AC CAG TGA GTC ATC CAC CGT
TOL6q-r1	G	reverse	ACC TCA GTT GCC ATT GCT TCA
TOL6f (TOMIE11u)	G	forward	G TGG ATA TTT TCC CTC TGG ACC
TOL6r (TOMIE11d)	G	reverse	G CGA CGG TGG CTG TTG ATA AAG

TOL6-NotISallr	A	reverse	GGG GGT CGA CGC GGC CGC AAA TCA TTT TCC TTC CTC C
TOL6-Sallu	A	forward	GG GGG TCG ACA TGG CGT CGT CTTC AGC TTC
TOL6-Salld	A	reverse	G GGG GTC GAC GTA AAT CAT TTTCCT TCC TCC
TOL1f (TOMI55-u)	G	forward	CAA TGA ATT GGC TCA ATC GAC
TOL1r (TOMI55-d)	G	reverse	G GGT TTG TTC ATC TCC TCA TAC
TOL5f (TOMI31-u)	G	forward	C CTA CGC TTG TGA AGA TAG
TOL5r (TOMI31-d)	G	reverse	A ACT GGA GTC ATT CTC AGG
TOL3-u	G	forward	G CTC AGG CAA CTG CAT CAG
TOL3-d	G	reverse	CG GTA TTG GAG TGG GAG CTG
BamHITOML31up	A	forward	GG ATC CAT GGC TGC GGA GCT TGT AAG
TOML31NotIBamHld own	A	reverse	GG ATC CGC GGC CGC AGT CAC TGA AGT CTA CGC
prTOL5f	A	forward	CC CGG GCG AAG CGA CGA CGT ATC GTC

prTOL5r	A	reverse	CC CGG GGT TAT CTG TAT GAG CCA GAG
XbaIpTOL6u	A	forward	TCT AGA CCG ATC AAA CAG CTC AAC ACG
KpnIpTOL6d	A	reverse	GGT ACC CAA ACC TAA CAA GAG CAA CTC
UBQEcoRIf	A	forward	G CGA ATT CAT GCA GAT CTT TGT TAA
UBQSallr	A	reverse	CGG TCG ACA GCA GCA CGG AGCCTGA GAA
BamHITOML55up	A	forward	GGA TCC ATG GGT GAC AAT CTT ATG GAC
TOML55NotBamHId	A	reverse	G GAT CCG CGG CCG CAG AAT CGA ATG AGA TCG TCG
prTOL1f	A	forward	GAG CTC GGT GAT ATG GGT AGG CAG
prTOL1r	A	reverse	C CCG GGG CTG ATA CTC AAA AAC CTG

### 3.3. Bacterial strains

#### 3.3.1. *Escherichia coli* (E. coli) strains

Three different strains of *Escherichia coli* used in this study:

**DH10B:** F- *mcrA*  $\Delta$ (*mrr-hsdRMS-mcrBC*)  $\Phi$ 80d*lacZ* $\Delta$ M15  $\Delta$ *lacX74* *endA1* *recA1* *deoR*  $\Delta$ (*ara*, *leu*)7697 *araD139* *galU* *galK* *nupG* *rpsL*  $\lambda$  (Grant et al., 1990).

**BL21 (DE3):** F- *ompT gal [dcm] [lon] hsdSB* (rB –mB -; an *E.coli* strain) with DE3, a  $\lambda$  prophage carrying the T7 RNA polymerase gene (Studier and Moffatt, 1986; Studier et al., 1990).

**DH5 $\alpha$ <sup>TM</sup>:** F-  $\phi$ 80lacZ $\Delta$ M15  $\Delta$ (lacZYA-argF) U169 recA1 endA1 hsdR17 (rk-, mk+) phoA supE44  $\lambda$ - thi-1 gyrA96 relA1 (Invitrogen., 2006).

### 3.3.2. *Agrobacterium tumefaciens* strains

**GV3101 (Rif<sup>R</sup>)** *agrobacterium* with the helper plasmid pMP90RK (Gent<sup>R</sup>) used for transformation (Deak et al., 1986).

## 3.4. Descriptions of Genetic Modified

### Organisms (GMOs) used

Donor/Recipients:    - *Arabidopsis thaliana*,  
                               - *Escherichia coli*,  
                               - *Agrobacterium tumefaciens*,

Vectors:                - pTZ57R/T  
                               - pET-24a  
                               - pPZP221  
                               - pPZP212

## 3.5. *Arabidopsis thaliana* mutants and reporter lines

Wild type ecotype Columbia (Col0) from *Arabidopsis thaliana* was used. The mutants and the reporter lines generated are listed below. The all single TOL TDNA insertion line and the *tolQ* plant line were described previously (Korbei et al., 2013).

List of plant lines used in this study:Mutants:

*tol1-1* (TOL1 single mutant plant line)

*tol3-1* (TOL3 single mutant plant line)

*tol5-1* (TOL5 single mutant plant line)

*tol6-1* (TOL6 single mutant plant line)

*tolQ* (2/3/5/6/9) quintuple mutant (with TOL2, TOL3, TOL5, TOL6, TOL9 mutated proteins).

### 3.6. Cloning Strategies

A clone containing the desired DNA fragment in the correct orientation was identified by restriction enzyme analysis of plasmid DNA. To confirm the correct insert orientation and reading frame integrity all the cloned constructs were confirmed by sequencing. All plant expression vectors were transformed into plants by floral dip method (Clough and Bent, 1998).

I designed constructs for TOLs and mutagenized version of the TOLs for *in vitro* and *in vivo* experiments. For bacterial expression and further *in vitro* binding studies, the cDNAs of the TOLs were cloned into pET24a vector for protein expression. For *in vivo* analysis, non-mutated and mutated TOLs cDNA were subcloned in a binary vector pPZP221 under their endogenous promoter and with a C-terminal Venus tag.

For generation of GST-Ubiquitin constructs, we fused an EcoRI-Sall PCR-fragment (primer pair: UBQEcoRI<sub>f</sub>/UBQSall<sub>r</sub>) ranging from nucleotides 859 to 1461 of *UBQ5* cDNA into **pGEX4T-1** (Amersham), for GST:ubq144A we used a mutagenized ubiquitin version reported previously in (Korbei et al., 2013).

To start with, I amplified the cDNAs of TOL1, TOL5 and TOL6 from pTZ57R/T-TomL cDNA clones previously cloned by Asaf Khan (published in (Korbei et al., 2013)) by PCR with primer pairs BamHITOML55up/TOML55NotBamHId for TOL1, BamHITOML31up/TOML31NotIBamHIdown for TOL5 and TOL6-Sallu/TOL6-NotISallr for TOL6 and introduced the PCR product into a pTZ57R/T vector by ligation with T4DNA ligase via dA overhangs, and confirmed them by sequencing (Fig 8A).

Furthermore, I performed site directed mutagenesis, to generate the different mutated TOL6 (*tol6<sup>mVHS</sup>*, *tol6<sup>mGAT</sup>* and *tol6<sup>mTOTAL</sup>*) constructs, together with a Christina Artner, a Master Student, and the exact mutagenesis procedure is described in details in (C. Artner, Master Thesis 2016). All the constructs were confirmed by sequencing. In brief: For site direct mutagenesis, the TOL6 cDNA into pTZ57R/T (Korbei et al, 2013) first amplified with oligos TOL6 W25Af/OL6W25Ar followed with oligos TOL6 N73Af/TOL6 N73Ar to mutated

*w25A* and *N73A* resulting in *tol6<sup>mVHS</sup>*. At the same time the TOL6 cDNA in pTZ57R/T (Korbei et al, 2013) was amplified with oligos TOL6 AAA1f/TOL6 AAA1f to replace DLL by AAA at position 246-248 and followed by amplification with oligos TOL6 AAA2f /TOL6 AAA2r to replace DML by AAA at position 250- 252, resulting in *tol6<sup>mGAT</sup>*. To obtain the total mutant TOL6 which includes the mutation of both VHS and GAT domains, EcoRI restriction enzyme was used to insert the first 424bp from *tol6<sup>mVHS</sup>* in pTZ57R/T into *tol6<sup>mGAT</sup>* generating *tol6<sup>mTOTAL</sup>* construct.

**For sub-cloning into the pET24a vector** (Fig 8B), I amplified the constructs in the pTZ57R/T vector with specific TOL6 oligos, TOL6-Sallu and TOL6-Salld allowing the introduction of Sall sites at the 5' and 3' end of the PCR product with proof reading polymerase and ligated into the pTZ57R/T via T/A cloning. The PCR product where electroporated into DH10B and positive colonies selected via blue/white screening. Afterwards, the correct inserts were verified by control digestion with Sall and clones confirmed by sequencing. The resulting construct (TOL6-Sall-pTZ57R/T and mutated TOL6-Sall-pTZ57R/T) were then digested by Sall enzyme to remove the pTZ57/R and subcloned into bacterial expression vector pET24a which was dephosphorylated before cloning. The pET24a vector contains all the genetic sequences necessary to produce the



protein of interest including an appropriate promoter to the host cell (T7 promoter), C-terminal His-tag and sequence which terminates transcriptions (T7 terminator). After ligation of the TOL6 and mutated TOL6 into pET24a, it was electroporated into DH10B and positive colonies were confirmed by control digestion using Sall enzyme. Correct insert direction and reading frame was confirmed by control digestion with BamHI or EcoRI restriction endonuclease. The constructs generated: TOL6-pET24a and the various mutated TOL6 versions (*tol6<sup>mGAT</sup>*, *tol6<sup>mVHS</sup>* and *tol6<sup>mTOTAL</sup>*) -pET24a were used for transformation into BL21 *E. coli* strain which is known to be efficient for protein expression and induction (Fig. 8B). I used these constructs for *in vitro* binding analysis.

After all cloning procedure, I obtained the following constructs:

For *in vitro* binding assay: (T7promot+His-tag+T7termin+MCS :pET24a).

*TOL6* in pET24a

*tol6<sup>mVHS</sup>* in pET24a

*tol6<sup>mGAT</sup>* in pET24a

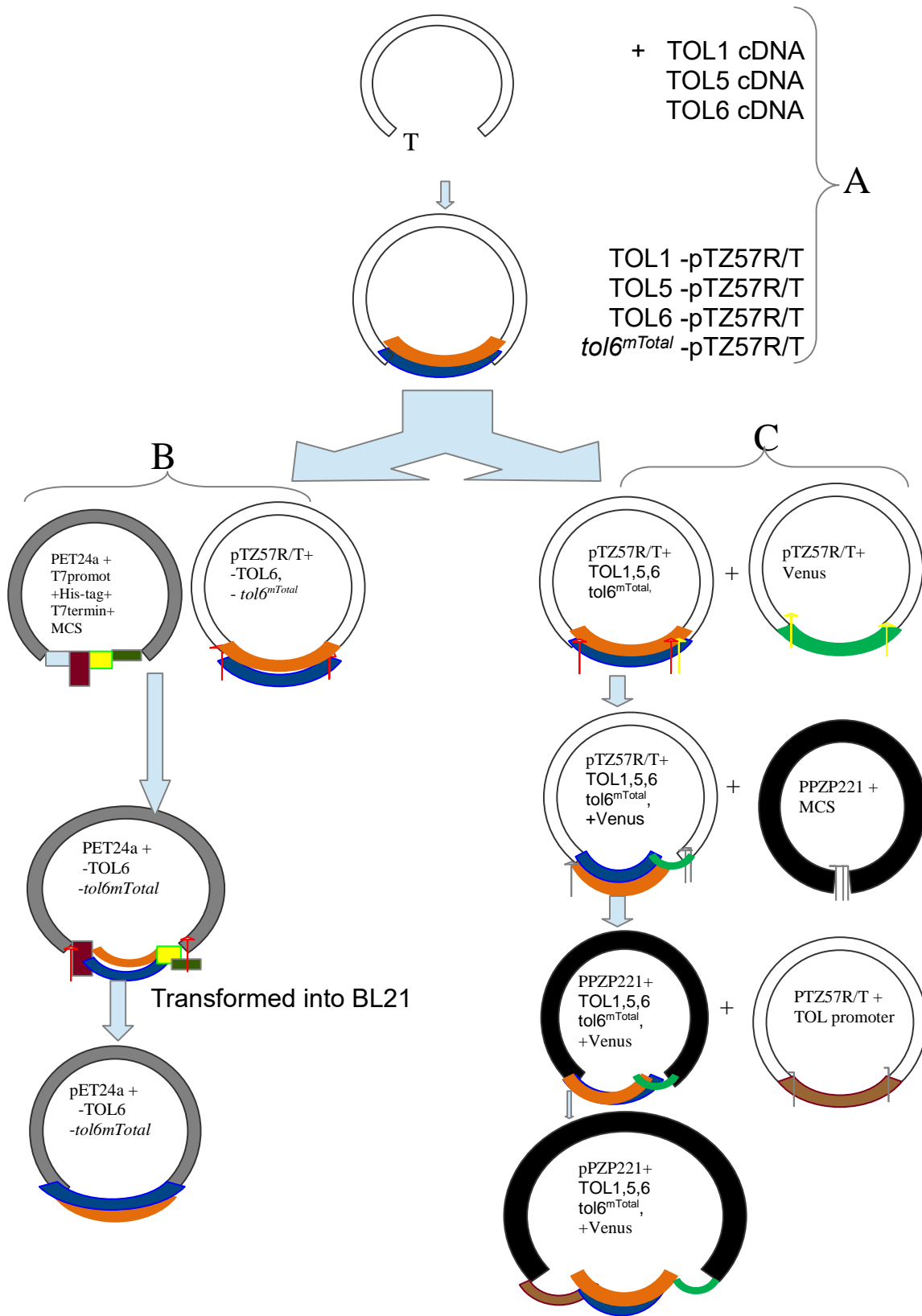
*tol6<sup>mTOTAL</sup>* in pET24a

These constructs were used for induction and expression proteins of mutated and non-mutated TOL6 proteins and used for *in vitro* binding assay.

### **Subcloning into pPZP221 plant vector (Fig. 8C).**

For *in planta* analysis, the TOL cDNAs were subcloned into pPZP221 vector. The pPZP221 vectors already contained 2000bp promoter sequence and a pApA terminator sequence downstream which was previously used for construction of the *pTOL6::TOL6:mcherry*, *pTOL1::TOL1:mcherry* and *pTOL5::TOL6:mcherry* constructs described in (Korbei et al., 2013).

The cDNA of the *TOL1*, *TOL5*, *TOL6* and *tol6<sup>mTOTAL</sup>* in the pTZ57R/T were digested with NotI enzyme and the Venus tag was subcloned into each construct resulting in *TOL1::Venus*, *TOL5::Venus*, *TOL6::Venus* and *tol6<sup>mTOTAL</sup>::Venus* in the pTZ57R/7. The direction of insertions checked with restriction enzyme analysis. The entire cassette was subcloned via Sall enzyme in to the pPZP221, which already contained the appropriated promoter fragment. The direction was once again verified by restriction enzymes analysis (Fig. 8C). This resulted in the constructs: *pTOL1::TOL::Venus*, *pTOL5::TOL5::Venus*, *pTOL6::TOL6::Venus* and *pTOL6::tol6<sup>mTOTAL</sup>::Venus* in pPZP221 which were then electroporated into DH10B and selected via Spectinomycin . Sall enzyme was then used for control digestion to check the presence of the TOL-Venus-pPZP221 construct. The correct orientation of the insertion was then verified by digestion with Pst and HindIII enzymes. These constructs were used for transformation in plants by floral dip method (Clough and Bent, 1998) for *in planta* analysis. Table 2 shows different plant lines generated and used in this study for *in planta* analysis.



Protein expression –  
*In vitro* binding analysis

Agrobacterium transformation-  
*In planta* analysis

**Figure 8 Schematic diagram for cloning strategy :** **A) TOLs and mutated TOLs cloned in pTZ57R/T vector:** Transparent (white) semi-circle is the pTZ57R/T vector; In orange is the mutated TOL6, In blue the non-mutated TOL1, TOL5, TOL6. **B) Subcloning in pET24a:** semi-circle in transparent -pTZ57R/T, semicircle in gray-pET24a, orange- mutated TOL6; dark blue- non mutated TOL6; light blue- T7 promoter; dark red- MCS; yellow-His-tag; dark green- T7 terminator, in red-Sall; **C) Subcloning in binary plant vector (pPZP221)** semi-circle in transparent -pTZ57R/T, orange - TOL6; dark blue- non mutated TOL1, TOL5, TOL6; semicircle in black – pPZP221, In light green – Venus fluorescent protein; in brown – TOL promoter.

**Table 2 Plant lines generated and used during this study**

Reporters:	Notes*
pTOL6: <i>TOL6:mcherry in tol6-1</i>	In this study
pTOL6:Mutated <i>TOL6:mcherry in tol6-1</i>	In this study
pTOL6:: <i>TOL6:GUS in Col0</i>	In this study
pTOL6:: <i>TOL6:Venus in Col0</i>	In this study
pTOL6:: <i>TOL6:Venus in tol6-1</i>	In this study
pTOL6:: <i>TOL6:Venus in tolQ</i>	In this study
pTOL6:: <i>TOL6mTotal:Venus in Col0</i>	In this study
pTOL6:: <i>TOL6mTotal:Venus in tol6-1</i>	In this study
pTOL6:: <i>TOL6mTotal:Venus in tolQ</i>	In this study
pTOL6:: <i>TOL6:Ubiquitin:Venus in tol6-1</i>	Master student (Lisa Jörg)
pTOL6:: <i>TOL6:Ubiquitin:Venus in tolQ</i>	Master student (Lisa Jörg)
pTOL6:: <i>TOL6:Ubiquitin<sup>l44</sup>:Venus in tol6-1</i>	Master student (Lisa Jörg)

pTOL6::TOL6:Ubiquitin <sup>l44</sup> :Venus in <i>tolQ</i>	Master student (Lisa Jörg)
pTOL1::TOL1:Venus in <i>tol1-1</i>	In this study
pTOL1::TOL1:Ubiquitin:Venus in <i>tol1-1</i>	Master student (Lisa Jörg)
pTOL1::TOL1:Ubiquitin <sup>l44</sup> :Venus in <i>tol1-1</i>	Master student (Lisa Jörg)
pTOL3::TOL3:Venus in <i>tol3-1</i>	Bachelor student (Julia)
pTOL5::TOL5:Venus in <i>tol5-1</i>	In this study
pTOL5::TOL5:Ubiquitin:Venus in <i>tol5-1</i>	Master student (Lisa Jörg)
pTOL5::TOL5:Ubiquitin <sup>l44</sup> :Venus in <i>tol5-1</i>	Master student (Lisa Jörg)

\* Notes: Person who produced the plant line.

### 3.7. Antibodies

**Table 3 Antibodies**

Against	Type	Dilution Western	Dilution IP	Notes
TOL6	Rabbit, polyclonal, affinity purified	1:50 (3% BSA)	1:50 (3%BSA)	Local lab (Lucinda)

TOL6 (serum)	Rabbit, polyclonal, not purified	1:500 (3% BSA)	1:500 (3% BSA)	Center for Biomedical Research*
Mouse	Goat IgG HRP	1:20000	1:20000	Dianova
Rabbit	Goat IgG HRP	1:20000	1:20000	Pierce
UBQ (clone P4D1)	Mouse, monoclonal	1:1000 (3% BSA)	1:500 (3% BSA)	Santa Cruz
His epitope	Mouse, monoclonal	1:2000	-	Novagene
GST	Mouse, monoclonal	1:1000	-	Thermo Scientific
GFP	Mouse, monoclonal	1:1000	1:1000	Santa Cruz

\*Center for Biomedical Research, Department of Laboratory Animal Science and Genetics, Medical University Vienna, Austria

### 3.8. General molecular biological methods

#### 3.8.1 Plant genomic DNA isolation by CTAB method

Plant genomic DNA (gDNA) obtained from one rosette leave of approximately 2 weeks old seedlings harvested in 1.5ml Eppendorf tube and frozen immediately in liquid nitrogen. Samples were homogenized by plastic pestle under constant cooling in liquid nitrogen. Alternatively, plant material was grinded with plastic pestle in drilling machine. 200µl of extraction buffer (2xCTAB) was added to the tube, vortexed and incubated at 65°C for 5 minutes gently shaking. 200µl of chloroform was added to the sample, vortexed and then centrifuged for 5 minutes, 13000rpm at RT. The supernatant (aqueous upper phase) was then transferred to a new tube avoiding the tip to touch the interphase. This supernatant was mixed with 2.5 volume of ethanol absolute by inversion. The gDNA was incubated at -20°C for 20 minutes to precipitate. Sample was then centrifuged at 4°C, 13000rpm for 15 minutes. Supernatant was discarded and the gDNA pellet washed with 500µl cold 70%

ethanol (stored at -20°C) and centrifuged for 5 minutes, 13000rpm at 4°C. Supernatant discarded carefully, pellet air-dried and resuspended in 30µl dH<sub>2</sub>O at 37°C, by gently shaking for 15 minutes. From this elution, 1-2µl of gDNA was used to perform PCR reaction. These gDNA was also used for genotyping or cloning.

Extraction buffer (2xCTAB buffer): 2% (w/v) CTAB (Cetyl trimethylammonium bromide, 100 mM Tris/HCl pH 8.0, 20 mM EDTA pH 8.0, 1.4 M NaCl, 1% (w/v) PVP (Polyvinyl pyrrolidone Mr 40000), dH<sub>2</sub>O to an appropriate volume, autoclaved and stored at RT.

The following working stock solutions were prepared, autoclaved and stored at RT:

1 M Tris/HCl pH 8.0: Tris (2-amino-2-hydroxymethyl-1,2-propandiol) dissolved in dH<sub>2</sub>O and brought to the pH 8.0 with concentrated HCl.

0.5 M EDTA pH 8.0: Na<sub>2</sub>-EDTA\* 2H<sub>2</sub>O (Ethylenediaminetetraacetic acid disodium salt dehydrate) dissolved in dH<sub>2</sub>O and brought to a pH of 8.0 with 10 M NaOH.

### **3.8.2 Plasmid DNA isolation with kit**

The highly purity plasmid DNA used for cloning, was isolated from bacterial cell culture by using column-based kits, from Fermentas (Thermo fisher Scientific) company. The DNA was isolated following the manufacture's protocol. The quality and amount of DNA was tested by agarose gel electrophoresis and spectrophotometry.

### **3.8.3 Spectrophotometric quantification of DNA**

The isolated DNA concentration was determined by spectrophotometric quantification method with a Beckmann DU 640 Spectrophotometer using a wavelength of 260 nm (UV). Based on the Beer-Lambert law an OD of 1 (optical density) correspondent to 50 ng/µL for dsDNA and 33 ng/µL for ssDNA. For optimal measurement the OD should range between 0.1 and 1.0. The A<sub>260</sub>/A<sub>280</sub> ratio estimates the purity of the DNA sample. According to the fact, that aromatic amino acids have their absorption maximum at 280nm, the A<sub>260</sub>/A<sub>280</sub> ratio ≥ 1.8 result in a low protein contamination and the A<sub>260</sub>/A<sub>280</sub> ratio ≤ 1.8 in a high protein contamination level of the DNA. Concentration of the samples was calculated with the following equations.

A260 \* dilution factor \* 50 = ng/μL ds DNA

A260 \* dilution factor \* 33 = ng/μL ss DNA

#### **3.8.4 Mini-Preparation of *E. coli* plasmid DNA by the “boiling method”**

Apart from the kits for DNA plasmid isolation, boiling prep method was also used for isolation of *E. coli* plasmid DNA. A single colony was inoculated in about 3-5ml LB or 2xTY liquid medium containing specific selective antibiotic and incubated overnight at 37°C on a rotary plate (180rpm). Next day 1.5ml of the culture were centrifuged at 1300rpm for 2 minutes and supernatant discarded. Pellet was resuspended in 100μl STET buffer. The STET buffer was supplemented with 5μl of freshly made lysozyme. The sample was vortexed and incubated in a heat block at 100°C for 2 minutes to inactivate the lysozyme. Afterwards sample was centrifuged for 30 minutes, 13000rpm at RT. The rubber-like pellet including protein debris was removed using sterile toothpick. 105μl of cold isopropanol (stored at -20°C) was added to the supernatant, vortexed well and centrifuged for 10 minutes, 13000rpm at RT. Supernatant was discarded and pellet washed with 400μl cold 70% ethanol (stored at -20°C) followed by centrifugation for 5 minutes, 13000rpm at RT. Supernatant was discarded and remaining pellet air-dried and dissolved in 35μl of ddH<sub>2</sub>O supplemented with 1μl RNase A (200μg RNase/mL), by gentle shaking for 15 min at 37°C in a heating block.

STET buffer: sucrose (8% w/v), Triton-X (0.05% v/v), Tris/HCl pH 8.0 (50 mM), EDTA (50 mM), dissolved in water, stored at room temperature.

1 M Tris/HCl pH 8.0: Tris (2-amino-2-hydroxymethyl-1,3-propanediol) dissolved in dH<sub>2</sub>O and brought to pH 8.0 with concentrated HCl, autoclaved and stored at room temperature.

Lysozyme solution: 5 mg lysozyme dissolved in 500μL dH<sub>2</sub>O

RNAase A: 100 mg RNAase in 10 mL dH<sub>2</sub>O, heat at 95°C for 10 minutes and cool down slowly. 1 mL aliquots stored at -20°C.

#### **3.8.5 Polymerase Chain Reaction (PCR)**

PCR usually performed in 20μl reaction volume, according to the table 4.



**Table 4 Preparation of 20µl reaction mix**

Component	Volume	Final concentration
Template DNA		10-50 ng
10 x PCR buffer	5 µL	1.5 mM MgCl <sub>2</sub>
2 mM dNTP mix	5 µL	0.2 mM
2 µM oligo forward	2.5 µL	100 nM
2 µM oligo reverse	2.5 µL	100 nM
<i>Taq</i> -Polymerase	1 µL	1 U
dH <sub>2</sub> O	Up to 20 µL	

For direct screening of *E. coli* colonies (colony PCR), colonies were picked from a plate with a sterile toothpick and resuspended in the following reaction mixture (Table 5).

**Table 5 Reaction mix for colony PCR**

Component	Volume
Template DNA	Colony from toothpick
10x PCR buffer	2µl
2mM dNTP mix	2µl
2µM forward oligo	1µl
2µM reverse oligo	1µl
<i>Taq</i> -Polymerase	0.3µl
dH <sub>2</sub> O	13.7µl
Final volume	20µl

PCR was performed with an Eppendorf Thermocycler. A hot start of 5 min at 95°C

was followed by 30-35 cycles according to the table 6.

Eppendorf Thermocycler (or other PCR machine present in the lab) was used to perform PCR.

**Table 6 PCR amplification program designed for the primers**

Step	Temperature	Time
Preheating	95°C	5 ''
Denaturation	98°C	20''
Annealing	Oligo-specific (50-60°C)	60''
Elongation	72°C	30''/kb
Extension	72°C	5'

NOTE: The denaturation, annealing and elongation provide the core amplification part of the method exponentially increasing the DNA concentration with every cycle. They are repeated 19-39 times depending on the sensitivity of the PCR reaction.

10xPCR buffer: 100 mM Tris/HCl pH 9.0, 0.5 M KCl, 15 mM MgCl<sub>2</sub>, 1% v/v Triton X-100, 2 mg/mL BSA, water added to an appropriate volume, divided in small aliquots and stored at -20°C.

Some stock solutions were prepared and stored at adequate temperature, to be used when needed such as:

1 M Tris/HCl pH 9.0: Tris (2-amino-2-hydroxymethyl-1,2-propanediol) dissolved in dH<sub>2</sub>O and brought to the pH 9.0 with concentrated HCl, dH<sub>2</sub>O, autoclaved and stored at RT.

1 M KCl: KCl, dH<sub>2</sub>O to 100 mL, autoclaved and stored at RT.

1 M MgCl<sub>2</sub>: MgCl<sub>2</sub> \* 6 H<sub>2</sub>O, dissolved in dH<sub>2</sub>O, autoclaved and stored at RT.

20% (v/v) Triton X-100: 100% Triton X-100 in dH<sub>2</sub>O, stored at 4°C.

10 mg/mL BSA: bovine serum albumin (BSA, Fraktion V, Fluka) dissolved in dH<sub>2</sub>O and stored in aliquotes at -20°C.

2 mM dNTP mix: 40 µL of each 100 mM deoxyribonucleotide triphosphate stock (dATP, dTTP, dGTP, dCTP), with 1840 µL dH<sub>2</sub>O to a final volume of 2 mL, 500 µL aliquots stored at -20°C.

Oligo stocks (Primers): lyophilized oligonucleotides dissolved in an appropriate volume of dH<sub>2</sub>O to get a 100 µM stock solution. For the 2 µM or 10 µM working solutions the 100 µM stock solution was diluted in water and stored at -20°C until use.

### 3.8.6 Site-directed Mutagenesis by Polymerase Chain Reaction (PCR) with proof-reading Kappa Hifi Kit

Site direct mutagenesis performed with KAPA HiFi HotStart PCR Kit according to manufacturer's manual. PCR was performed in 50µL reaction volume (table 7).

**Table 7 Preparation of 50µl reaction mix for site direct mutagenesis**

Component	Volume	Final concentration
Template DNA	-	30-100 ng
10 x PCR buffer with Mg	10 µL	3 mM MgCl <sub>2</sub>
10 mM dNTP mix	1.5 µL	0.3 mM
10 µM oligo forward	1.5 µL	0.3 mM
10 µM oligo reverse	1.5 µL	0.3 mM
<i>Taq</i> -Hifi-Polymerase	1 µL	1 Unit
dH <sub>2</sub> O	Up to 50 µL	

The denaturation, annealing and elongation steps provide the core amplification part of the method exponentially increasing the DNA concentration with every cycle. Generally, 20 cycles were used. The PCR was performed according to the table 8.

**Table 8 PCR amplification programme designed for the DNA for T/A cloning approaches**

Step	Temperature	Time
Preheating	98°C	3 "
Denaturation	98°C	30"
Annealing	Oligo-specific (50-60°C)	45"
Elongation	72°C	30"/kb
Extension	72°C	10"

30 cycles were used to amplify the desired DNA fragment.

Oligo stocks (Primers): lyophilized oligonucleotides were dissolved in an appropriate volume of dH<sub>2</sub>O to get a 100 µM stock solution. For the 2 µM working stock solutions, 10 µL of the 100 µM stock were diluted in dH<sub>2</sub>O to a final volume of 500 µL, whereas for the 10 µM working solution 50 µL of the 100 µM stock were diluted in dH<sub>2</sub>O to a final volume of 500 µL.

10 mM dNTP mix and 10 x PCR buffer with Mg: were provided by the PCR kit.

### 3.8.7 Polymerase chain reaction (PCR) to get DNA with T/A overhang

For further ligation into pTZ57R/T vector T/A (sticky ends) ends need to be added to a blunt ended insert by using a short PCR reaction (see Table 9).

**Table 9 PCR mixture**

Component	Volume	Final concentration
Template DNA		30-50 ng
10 x PCR buffer	5 µL	1.5 mM MgCl <sub>2</sub>
2 mM dNTP mix	5 µL	0.2 mM
10 µM oligo forward	-	

10 µM oligo reverse	-	
<i>Taq</i> - Polymerase	1 µL	1 U
dH <sub>2</sub> O	Up to 50 µL	

PCR was performed with an Eppendorf Thermocycler, using the standard PCR (Table 10)

**Table 10 PCR amplification program designed for standard PCR**

Step	Temperature	Time
Denaturation	98 °C	3''
Elongation	72 °C	30'
Extension	72 °C	5'

### 3.8.8 DNA gel-electrophoresis

The horizontal gel electrophoresis 1%, 1.2% or 1.5% were used to estimate the size and the amount of plant DNA, bacterial lasted DNA or elution of digested DNA fragment. The gel was prepared by mixing 1x TAE buffer with agarose, heated in microwave until the agates was completely melted. 0.5µg/ml final concentration of ethidium bromide was added to the cooled mixture and poured on a specific strand with desired combs. The DNA sample was mixed with 6x loading dye immediately before loading on agarose gel.

6x orange gel-loading buffer: 0.25% Orange G (w/v), dissolved in 75% glycerol.

50x TAE electrophoresis buffer: 2 M Tris base dissolved in dH<sub>2</sub>O, 1 M glacial acetic acid, 0.05 M Na<sub>2</sub>EDTA\*2 H<sub>2</sub>O or 0.5 M EDTA pH 8.0, added dH<sub>2</sub>O to desired volume, autoclaved and stored at RT.

0.5 M EDTA pH 8.0: Na<sub>2</sub>EDTA\*2 H<sub>2</sub>O dissolved dH<sub>2</sub>O and brought to a pH 8.0 with 10 M NaOH, autoclaved and stored at RT.

Ethidium bromide stock (10 mg/mL): Roth, stored at 4°C.

### **3.8.9 DNA digestion with restriction endonucleases**

The DNA digestion was carried out using the specific enzymes, with supplied buffers and following the manufactures recommendations. Quantitative digestion was performed in 50µL reaction volume and incubated for 1.5 to 2h, for DNA used for cloning. If the DNA was needed for control digestion, the digestion was performed in 20 µL reaction volume and incubated for 1-1.5h according to the enzyme activity. The enzymes were inactivated by heating at 65°C or 80°C according to the enzyme specification. Enzymes were purchased from MBI Fermentas, New England Biolabs and Promega.

### **3.8.10 Purification of DNA fragments from agarose gels**

Following the manufacture's manual, the purified DNA was extracted from agarose gel using a gel extraction kit from Fermentas Company.

### **3.8.11 Dephosphorylation of enzyme-digested DNA ends**

In order to avoid re-ligation of the vector after digestion with restriction endonucleases the Shrimp Alkaline Phosphatase (SAP) was used to remove the 5'-phosphate groups. 1µL of SAP or fastAP was added to the sample immediately after the inactivation of the restriction endonuclease. When using SAP, the dephosphorylation mix was incubated for 1h, whereas when using the fastAP, the time was reduced to 15-30 minutes at 37°C. The SAP and fastSAP enzymes were obtained from MBI Fermentas Company.

### **3.8.12 Cloning of PCR fragments**

The purified DNA from agarose gel was ligated into T/A cloning vector overnight at 14-16°C. 1-3µL of DNA used for transformation into *E. coli* by electroporation. The blue-white selection method was used to identify the positive clones. InsT/A clone PCR product cloning kit, MBI Fermentas.

### 3.8.13 T4 DNA Ligation

DNA quality, amount of purified vector and respective insert were estimated by loading in an agarose gel before the ligation. After confirmation of the quality and amount of the insert and Vector, the ligation was performed in 20µL using 5U of T4 DNA ligase and 2µL of T4 DNA ligase buffer. The molar ration of vector and insert used was approximately 1:3 according to the size of the vector and insert. After ligation, the reaction was incubated for 1h at RT and then at 14 to 16°C overnight. On the next day the T4 DNA ligase was inactivated at 65°C for 10 minutes and then stored at -20°C. T4 DNA Ligase and buffer were purchased from MBI Fermentas, New England Biolabs, Promega.

### 3.8.14 Blue-White Selection of positive clones

The pTZ57R/T plasmid is a *lacZ*-bearing vector backbone, encoding for β-galactosidase. IPTG (Isopropyl-β-D-thiogalactopyranoside) induces the *lacZ* gene expression. X-Gal (5-bromo-4-chloro-3-indolyl- β-D-galactopyranoside) is a substrate for the β-galactosidase, which is cleaved, then dimerizes and oxidizes to form a bright blue insoluble precipitate. If the gene of interest is inserted in the multiple cloning site, expression of the *lacZ* gene is disrupted, no enzyme produced and the X-Gal remains colorless. 75µL of IPTG – X-GAL mixture was spread on the surface of a selective agar plate prior to plating of the bacterial culture. After incubation of the plates at 37°C overnight they were placed at 4°C to promote the formation of blue precipitate. Cells transformed with vectors containing the gene of interest will produce white colonies; cells transformed with only the vector grow into blue colonies.

100 mM IPTG stock: dissolved in dH<sub>2</sub>O and aliquots stored at – 20°C.

X-Gal stock: dissolved in DMF and aliquots stored at – 20°C.

IPTG – X-Gal mixture: 25µL of 100 mM IPTG, 25µL of X-Gal stock, 25µL dH<sub>2</sub>O, mixed before spread on the agar plates.

### 3.8.15 Media and growth conditions for bacteria

For bacterial growth, LB or 2xTY medium containing a specific antibiotic were used. The liquid medium was incubated in rotary shaker (180rpm) and the solid medium in 9 cm Petri

dishes plate (1.5%). The temperature for growing *E. coli* strains was 37°C overnight or few hours according to the experiment. Whereas the temperature for growing *Agrobacterium tumefaciens* was 29°C for two days in solid medium and overnight in liquid medium.

Antibiotics: prepared according to the concentrations (table 11) aliquoted and stored at – 20°C.

**Table 11 Preparation of the different antibiotic used in this study**

Antibiotic	Abreviation	Stock concentration in ddH <sub>2</sub> O	Final concentration for <i>E.coli</i>	Final concentration for <i>A. tumefaciens</i>
Ampicillin	amp	50 mg/mL	50 µg/mL	-
Kanamycin	kan	50 mg/mL	50 µg/mL	50 µg/mL
Gentamycin	Gent	100 mg/mL	-	50 µg/mL
Rifampicin	Rinf	50 mg/mL	-	50 µg/mL
Spectinomycin	Spec	50 mg/mL	50 µg/mL	100 µg/mL

LB medium: 1% peptone (trypton), 0.5 %yeast extract, 172 mM NaCl, added water to the corresponding volume, autoclaved and stored at RT. For solid media, 4.5 g agar was added to 300 mL liquid medium, autoclaved and stored at RT. Prior to use the solid medium was melted in microwave, cooled down to 55°C in water bath or at RT. An appropriate amount of selective antibiotic was added immediately before pouring the medium on plate.

2x TY medium: 1.6 % peptone (tryptone), 1% yeast extract, 86 mM NaCl, dissolved in appropriate amount of water, brought to pH 7.4 with 10 M NaOH, autoclaved and stored at RT. For solid medium the procedure was similar to the LB medium.



**3.8.16 Preparation of electrocompetent *E.coli***

To prepare electrocompetent *E. coli* strain, a specific strain (DH10B or BL21 (DE3)) was streaked out from -80°C, to the LB plate (without antibiotic), and incubated overnight at 37°C. Next day one single colony was inoculated on 5ml of LB medium and grown overnight at 37°C, shaking at 180rpm. From this culture, 2 ml was inoculated in a fresh 500ml LB medium and grown at 37°C, 180rpm. When the bacteria reached the OD600 = 0.5, the culture was transferred to a cold condition, and chilled on ice for 1h. Afterward the cultures were centrifuged for 15 minutes at 5000rpm at 4°C (Hettich Zentrifugen, type 1610 D-78532 Tuttlingen, Rotor E819) in cold 50 ml falcon tubes. The bacterial pellet was resuspended with 200 mL of ice-cold sterile ddH<sub>2</sub>O in each tube and centrifuged again. The water was removed from the tubes, and the washing step repeated once. Within each washing step the number of used tubes was reduced until 2 tubes remain. The pellet was resuspended in 5 ml of cold 10% glycerol for both tubes and centrifuged again. At the end, the pellet was resuspended in 1 ml of cold 10% glycerol. 50µl of the competent cells were aliquoted to the cold Eppendorf tubes, shock frozen in liquid nitrogen and stored at - 80°C.

10 % Glycerol: 100% Glycerol diluted in dH<sub>2</sub>O, autoclaved and stored at 4°C.

**3.8.17 Preparation of electrocompetent *A. tumefaciens***

The preparation of electrocompetent *A. tumefaciens* strain was similar to the electrocompetent *E. coli* cells. A specific strain of *A. tumefaciens* (GV3101) was streaked out from -80°C, to the LB plate (with appropriate antibiotic Rif/Gent), and incubated for two nights at 29°C. A single colony was picked from the plate and inoculated in 5ml LB liquid medium with specific selection antibiotic and grown overnight at 29°C, shaking at 180rpm. Next day, 2 ml of these culture were inoculated in 500ml LB containing specific selection antibiotic and grown at 29°C until reached the OD600 = 0.5 - 0.6. The following steps were the same as described for preparation of electrocompetent *E. coli* strains.

### **3.8.18 Electroporation of *E. coli* and *A. tumefaciens***

To electroporate the plasmid DNA, 50µL of electrocompetent cells from -80°C, were thawed on ice for few minutes and then 1-3µL (corresponding to 1-10ng) of plasmid DNA added to the tube. The suspension was carefully mixed by pipetting avoiding formation of bubbles and immediately transferred to the ice-cold electroporation cuvettes (2mm path length, Equinio, Peqlab). The cuvettes were kept on ice until high voltage pulse was applied at 2.5 kV (for *E. coli*) or 2.2 kV (for *A. tumefaciens*), 200 Ω and 25 µF in a BIO-RAD Gene Pulser™. After application of the electro pulse, 550µL of LB or 2xTY medium was added to the cells, gently mixed and then transferred into a 1.5 mL tube and incubated for 1 hour at 37°C for *E. coli* or at RT in the dark for *A. tumefaciens*. Cell suspension was plated on LB plates with the appropriate antibiotic. For *A. tumefaciens*, the suspension was diluted in water 1 to1 before plating.

### **3.8.19 Preparation of bacterial -80 °C glycerol stocks**

A single colony of the desired clone of *E. coli* grown in 5 mL of selective medium. 600µL of the overnight culture mixed with 600µL 100% glycerol by vortexing in a cryo-tube and directly shock frozen in liquid nitrogen, finally stored at -80°C.

## **3.9. Plant Methods**

### **3.9.1. Seed harvesting and storage**

Dried seeds from mature siliques were harvested and collected into a paper bag or in 1.5ml Eppendorf tubes. The plant materials were removed completely from the seeds using a sieve. The dried seeds were stored at RT.

### **3.9.2. Seed sterilization**

For sterilization, the dried seeds (up to 50µl of seeds) were resuspended in 500µl sterilization solution and incubated for 7 minutes with frequent shaking. Afterwards, the seeds were left to settle down in the bottom of the tubes and the solution removed. Seeds

were washed 3 times with 1 ml sterile water. For large amount of seeds, more than 500µl of seeds (as for T1 seeds selection), 15ml falcon tube was used for sterilization. 3ml of sterilization solutions were added to the tube, and incubated for 7 minutes shaking at RT. After incubation, tubes were centrifuged for 1 minute at 4000rpm and sterilization solution removed. The seeds were washed 3 times with sterile water. In both cases after the washing steps the water was removed and the tubes rinsed with 1% agarose. The sterilized seeds were transferred to a solid/liquid plant medium and then kept at 4°C under dark conditions for 2-4 days for stratification to allow synchronous germination. Alternatively, the sterilized seeds in some ddH<sub>2</sub>O were left in 1.5 ml tube for stratification before transfer to the plant medium.

Alternatively, seeds were also sterilized by soaking them in 70% ethanol in paper bag and allowed to dry in a laminar flow hood, and then resuspended in 0.1% agarose in Eppendorf tube.

Sterilization solution: (6% v/v) sodium hypochlorite, appropriate amount of water, 0.1% v/v Triton X-100. Prepared freshly.

20% (v/v) Triton X-100: 100% Triton X-100 diluted in dH<sub>2</sub>O, stored at 4°C.

### **3.9.3. Cultivation on solid media**

The solid plant nutrient (PN) medium (Haughn et al., 1986) was melted in a microwave and cooled to 55°C in a water bath. 1% (v/v) sucrose final concentration was added to a PN medium in order to obtain PNS (Plant Nutrient with Sugar). For selection of primary transformants (T1) no sugar was added to the plant medium to reduce the contamination with *A. tumefaciens*. Plant hormones or selective drugs were added to the plant medium when necessary. Sterile seeds were resuspended in 0.1% agarose and plated in parallel rows by using a 1 mL pipette tip. For T1 selection a higher amount of seeds was resuspended in 0.1 % agarose and distributed to the solid medium plate by circular movement and allowed to dry in the laminar stream for some minutes.

Dry plates were sealed with surgical tape Leukopor™ and stratified for at least 48 hours at 4°C. Afterwards the plates were transferred into a plant growth incubator/phytotron

(Percifal Scientific Inc.) under following conditions: 12h photo-period, 159  $\mu\text{mol}/\text{m}^2/\text{s}$  light intensity, 50% relative humidity and 22°C. For the T1 selection the plates were incubated in horizontal, for phenotypic analysis plates were incubated in a vertical position.

PN solid medium: 50 $\mu\text{M}$  -  $\text{Na}_2\text{EDTA}\cdot 2\text{H}_2\text{O}$  dissolved in  $\text{dH}_2\text{O}$ , 50  $\mu\text{M}$  -  $\text{FeSO}_4\cdot 7\text{H}_2\text{O}$ , 2.5 mM - 100x  $\text{KPO}_4$  pH 5.5, 5 mM -  $\text{KNO}_3$ , 2 mM -  $\text{Ca}(\text{NO}_3)_2$ , 2 mM -  $\text{MgSO}_4$ , 1x micronutrients mix, correspondent amount of water and brought to pH 5.5 with 1 M KOH. 700 mL of this suspension was filled into a 1000 mL glass bottle containing 1% agar, autoclaved and stored at RT.

Stock solutions were prepared to be used when necessary:

250 mM  $\text{KPO}_4$  pH 5.5: 235 mM -  $\text{KH}_2\text{PO}_4$ , 15mM -  $\text{K}_2\text{HPO}_4$ , dissolved in  $\text{dH}_2\text{O}$ , autoclaved and stored at RT.

500 mM  $\text{KNO}_3$ :  $\text{KNO}_3$  dissolved in  $\text{dH}_2\text{O}$  to 1000 mL, autoclaved and stored at RT.

200 mM  $\text{Ca}(\text{NO}_3)_2$ :  $\text{Ca}(\text{NO}_3)_2\cdot 4\text{H}_2\text{O}$ , dissolved in  $\text{dH}_2\text{O}$ , autoclaved and stored at RT.

200 mM  $\text{MgSO}_4$ :  $\text{MgSO}_4\cdot 7\text{H}_2\text{O}$ , dissolved in  $\text{dH}_2\text{O}$ , autoclaved and stored at RT.

1000x micronutrients mix: 70 mM  $\text{H}_3\text{BO}_3$ , 14 mM -  $\text{MnCl}_2\cdot 4\text{H}_2\text{O}$ , 0.5mM  $\text{CuSO}_4\cdot 5\text{H}_2\text{O}$  1 mM -  $\text{ZnSO}_4\cdot 7\text{H}_2\text{O}$ , 0.2 mM  $\text{Na}_2\text{MoO}_4\cdot 2\text{H}_2\text{O}$ , 10 mM NaCl, 0.01 mM  $\text{CoCl}_2\cdot 6\text{H}_2\text{O}$  dissolved in  $\text{dH}_2\text{O}$ , autoclaved and stored at RT.

1M KOH: potassium hydroxide dissolved in  $\text{dH}_2\text{O}$ , stored at RT.

50% sucrose: sucrose dissolved in  $\text{dH}_2\text{O}$ , autoclaved and stored at RT.

0.1% (w/v) Agarose: agarose dissolved in  $\text{dH}_2\text{O}$ , melted in a microwave oven and aliquoted, autoclaved and stored at RT.

Selection drugs: Antibiotics used for plant selection were divided in 1 mL aliquots and stored at  $-20^\circ\text{C}$  (Table 12).

**Table 12 Preparation of the antibiotics solution for selection**

Antibiotic	Stock concentration in dH <sub>2</sub> O	Final concentration for T1 plants	Final concentration for T2 plants
Gentamycin for pPZP221	50 mg/mL	75 µg/mL	60 µg/mL
Kanamycin For pPZP212	50 mg/mL	50 mg/mL	50 mg/mL

**3.9.4. Plant cultivation on soil**

The soil for plant cultivation was prepared using 3 volumes of Einheitserde E 15 Typ P (Werkverband E.V.) and 1 volume of Granuperl Standard S 0-6 granules (Perlite). To propagate or analyze adult plant phenotype, the soil substrate was filled in small pots (5x5cm), put in plastic tray and soaked with water. Afterwards, 5 plants with 2-3 weeks old were transferred from the agar plates to the soil using tweezers. To avoid the loss of humidity, the plant tray was covered with a transparent plastic during the first days. Plants were grown in climate chambers under long day conditions (16hours of light, 8 hours dark) at 22°C at approximately 100 µM/m<sup>2</sup>/s light intensity and 50% relative humidity.

**3.9.5. *A. tumefaciens* mediated plant transformation by Floral Dip Method**

After electroporation and overnight incubation of *A. tumefaciens* (see section 3.8.4), one single colony of *A. tumefaciens* with the desired construct was inoculated in 5ml LB medium containing all necessary selective antibiotics and incubated overnight at 29°C. Next day the 5mL pre-culture were used to inoculate a large scale culture of 300 - 400 mL LB containing only the antibiotic necessary for selection for the plasmid, and grown at 29°C overnight. The culture was centrifuged for 15 minutes at 4°C in a Sorvall GAS rotor at 3000rpm. The pellet was resuspended in 250mL of infiltration medium and transferred into a 250mL beaker, which fitted to the size of the plant pots. Plant pots were inverted into the *Agrobacterium*-containing medium and the plants were incubated for 5 - 10 minutes at RT (Clough and Bent, 1998). Afterwards the plants were placed horizontally

into a plastic tray overnight (o/n) covered with a plastic wrap to ensure efficient transformation and humidity. Plants were transferred to a vertically position into a plastic tray and incubated in the climate chamber for growth and seed formation.

Infiltration medium: 2.15 g MS salts, 0.5 g MES (2-N-morpholino-ethanesulfonic acid), 50 g sucrose dissolved in 800 mL dH<sub>2</sub>O, brought to a pH 5.7 with KOH, dH<sub>2</sub>O to 900 mL. Before use 300 µL of Silwet L-77 (0.03 % Van Meeunwen Chemicals B.V., Netherlands) was added. Fresh prepared no autoclaving necessary.

### 3.9.6. GUS staining and microscopic preparations

In order to analyze the transgenic seedlings or plant organs carrying GUS reporter constructs, the plant material was harvested and dipped in approximately 3mL of GUS staining buffer in a 6-well culture plate and incubated at 37°C. When staining was complete, the samples were rinsed with H<sub>2</sub>O and de-stained by shaking overnight at RT in 70% ethanol (EtOH). Afterwards the material was placed in water on a microscopic slide, and the slides were ready for microscopy examination.

GUS buffer: 100 mM sodium phosphate buffer pH 7.0, 10 mM EDTA pH 8.0, 0.5 mM K<sub>4</sub>[Fe(CN)<sub>6</sub>], 0.5 mM K<sub>3</sub>[Fe(CN)<sub>6</sub>], 0.1% Triton X-100 (0.1%), added dH<sub>2</sub>O to the appropriate amount and buffer stored at 4°C.

0.5 M Sodium phosphate buffer pH 7.0: 288.5 mM NaH<sub>2</sub>PO<sub>4</sub>·H<sub>2</sub>O, 211.5mM Na<sub>2</sub>HPO<sub>4</sub>·2H<sub>2</sub>O, added dH<sub>2</sub>O, autoclaved and stored at RT. Alternatively, 57.7 parts of 0.5 M sodium phosphate monobasic salt stock mixed with 42.3 parts of 0.5 M sodium phosphate dibasic salt stock.

Working solution:

0.5 M EDTA pH 8.0: Na<sub>2</sub>EDTA·2H<sub>2</sub>O (Ethylenediaminetetraacetic acid disodium salt dihydrate) dissolved in dH<sub>2</sub>O and brought to pH 8.0 with 10 M NaOH, autoclaved and stored at RT.

10 M NaOH: The dissolution of NaOH in H<sub>2</sub>O is a highly exothermic reaction. The 10 M NaOH solution has to be prepared with extreme care in plastic beakers. The NaOH was

slowly added under continuously stirring, until the pellets have dissolved, stored in plastic bottle at RT.

50 mM  $K_4[Fe(CN)_6]$ :  $K_4[Fe(CN)_6] \cdot 3H_2O$  (potassium hexacyanoferrate II trihydrate), dissolved in dH<sub>2</sub>O, autoclaved and stored at 4°C, during time a reddish-orange pellet forms and should not be disturbed.

50 mM  $K_3[Fe(CN)_6]$ :  $K_3[Fe(CN)_6]$  (potassium hexacyanoferrate III), autoclaved and stored at 4°C, during time a reddish-orange pellet forms and should not be disturbed.

20% (v/v) Triton X-100: 100% Triton X-100 diluted in dH<sub>2</sub>O, stored at RT or 4°C.

GUS staining buffer: 19 ml GUS buffer mixed with 1 ml 20 mM X-Gluc stock (1 mM), the staining buffer was prepared just prior use.

20 mM X-Gluc stock: X-Gluc (5-Bromo-4-Chloro-3-Indolyl- $\beta$ -D-glucuronic acid Cyclohexylammonium salt), dissolved in DMF, stored light protected at -20°C.

### 3.9.7. Confocal Laser Scanning Microscopy (CLSM)

To determine the localization of specific-tagged proteins in the root cells, live cell imaging with 6 to 10-days-old seedlings was performed. For image acquisition, a Leica TCS SP5 confocal laser-scanning microscope was used. The Venus-tag was excited at 514 nm (fluorescence emission: 525–578 nm). The GFP excitation at 488 nm (emission: 494-541 nm). Sensitive HyD2 detector detected the fluorescence signals. The image was acquired using 63x water immersion lens. About 4 seedlings were placed onto the object plate, covered with water and a cover slide and then the lens was adjusted to take the image.

The TOL and mutated TOL alleles reporter signal distribution was accessed by determining the ration of the mean fluorescence signal intensity from PM out of cytoplasm (PM/Cytoplasm) for TOL6 and TOL6 mutants. For TOL1 and TOL5 the ration of signal intensity was based on Cytoplasm out of PM (Cytoplasm/PM) due to abundant localization of these TOLs at Cytoplasm. Relative signal intensities from TOL6 and their respective mutants measured by the ration between PM over intracellular relative signal content was obtained by selection of whole cell and intracellular content mean fluorescence with

imageJ/Fiji software. Same procedure was applied for TOL1 and TOL5 with their respective mutants but using the ratio Cytoplasm/PM. In both cases 8 adjacent cells from epidermis of six-day-old roots were measured from three roots each and in three biological repeats. Resulting averages were then used for determination of signal ratios. Average values were depicted as box plots, their statistical significance was calculated using Two-tailed t-test in Sigma Plot (Systat, Chicago, IL, USA). Co-localization coefficients were calculated according to (French et al., 2008).

### **3.9.8. Analysis of plant development**

In order to analyze the plant development of different TOL plant lines as well as different mutated reporter constructs, I started by measuring the root length of 7 days old seedlings. Statistical analysis of the overall root lengths did not show any significance difference, however, there were some clear differences between the mutated and non-mutated plant lines. To address this, I calculate the average of 7 days old root length seedlings from Colombia (Col0) wild type. The average from Col0 was 3.4cm +/-0.5cm. With this number, I divided the roots in three categories: the roots above 3.4 cm considered as long roots (long roots), the roots below 3.4 cm as a regular root, yet the roots with less than 1cm were considered as abnormally short roots. With these categories, I could group the roots and I could perform statistical analysis that allowed me to demonstrate significant phenotypic differences between Col0 and the different TOL plant lines.

For further analysis of the plant growth and development, I counted the rosette leaves when inflorescence stem has 1cm height (Moller-Steinbach et al., 2010). I grew four pots with three plants for two different homozygous plant line under similar conditions in a climate chambers under long day conditions (16hours of light, 8 hours dark) at 22°C at approximately 100  $\mu\text{M}/\text{m}^2/\text{s}$  light intensity and 50% relative humidity. The results were expressed in terms of the mean and the graphics were obtained using Microsoft Excel (Microsoft, USA). Statistical significance was calculated using Two-tailed t-test in Sigma Plot (Systat, Chicago, IL, USA).



### 3.9.9. Computer software

DNA sequences were analyzed and aligned using the DNASTar software (DNASTar Inc., Madison/Wisconsin, USA). Digital images (TIFF, JPEG) were processed with Adobe Photoshop (Adobe Systems, USA) and Microsoft PowerPoint office 2016. Quantification of PCR products resolved by Agarose gel electrophoresis was performed with Quantity One (Bio-Rad Laboratories). Images were processed and analyzed using FluoView (Olympus), Fiji (68), ImageJ-win32, and Photoshop CS6 (Adobe). The graphics were obtained using Microsoft Excel (Microsoft, USA). Statistical significance was calculated using Two-tailed t-test in Sigma Plot (Systat, Chicago, IL, USA).

## 3.10. Biochemical Methods

### 3.10.1 Induction of Protein expression in BL21 (DE3)

For biochemical analysis, plant proteins were expressed from *E. coli* strain BL21 (DE3) *via* induction with IPTG. First step was to streak out the desired construct, which previously had been transformed into BL21 (DE3), from -80 glycerol stock to a LB plate with specific selective antibiotic, and incubated overnight at 37°C. Next day, one single colony was inoculated in 5mL LB medium containing appropriate antibiotic and grown overnight at 37°C, shaking at 180rpm. From this, 1-2mL was inoculated to a fresh 50ml LB medium containing specific selection antibiotic and grown until OD600 = 0.5-0.6. 1mL of the cell culture was separated to an Eppendorf tube, centrifuged and the pellet kept at -20°C for analysis before induction. 100mM of IPTG was added to the culture, to have a final concentration of 0.5 mM IPTG protein expression. The induction of protein expression by IPTG was achieved by incubating the cell culture with IPTG for 5h at 37°C shaking at 180rpm. 1ml of this culture was separated, centrifuged and the pellet saved at -20 for analysis after induction. The culture with induced protein centrifuged in 50mL falcon tube for 15 minutes, 4°C at 5000rpm (Hettich Zentrifugen, type 1610 D-78532 Tuttlingen, Rotor E819). The supernatant was removed and the pellet saved at -80°C to be used for protein extraction, or *in vitro* binding studies.

100 mM IPTG stock: dissolved in dH<sub>2</sub>O, 500μL aliquots stored at – 20°C.

### 3.10.2 Extraction of recombinant proteins from BL21

After induction of protein expression (see section 3.10.1), the protein pellet was resuspended in 1mL of sonication buffer with detergent (SDS) and incubated for 30 minutes at 4°C by rocking. 1mL of sonication buffer without detergent (SDS) was added to the suspension and incubated on ice. Afterwards the cells were disrupted by ultrasonic frequencies during sonication procedure (Vibra cell™, Sonics and Material Danbury.CT. USA). The sonication was applied for 6 times 10 seconds to each sample avoiding formation of bubbles. The samples were always chilled on ice between the sonication pulses. After finishing the sonication step, the samples were centrifuged for 10 minutes, 4°C at maximal speed in a tabletop centrifuge. The supernatant was transferred to a 15mL falcon tube and mixed. 3 mL of RIPA buffer, 500µL of 100% Glycerol and ¼ of the complete mini EDTA free tablet (Roche) were added to the sample in the falcon tube and mixed well. The pellet after centrifugation was analyzed together with 100µL of the sample after extraction, in order to determine the amount of recombinant protein in soluble or pellet fraction. The supernatant was aliquoted and frozen at -80°C and used for the *in vitro* binding assay.

Sonication buffer with SDS: 10 mM Hepes/NaOH pH 7.4, 1 M EDTA pH 8, 0.5 % w/v SDS, appropriate amount of dH<sub>2</sub>O and stored at 4°C. 1 mM PMSF, 1 mM DTE and 1 mM Aprotinin/Leupeptin were added as efficient protease inhibitors immediately before use.

Sonication buffer without SDS: 10 mM Hepes/NaOH pH 7.4, 1 M EDTA pH 8, appropriate amount of dH<sub>2</sub>O and stored at 4°C. 1 mM PMSF, 1 mM DTE and 1 mM Aprotinin/Leupeptin were added as efficient protease inhibitors immediately before use.

RIPA buffer: 50 mM Hepes/NaOH pH 7.4, 1 mM EDTA, 140 mM NaCl, 1 % (w/v) Triton X-100, 0.1 % (w/v) Na-deoxycholate, appropriate amount of dH<sub>2</sub>O and stored at 4°C. Before use 1 mM PMSF, 1 mM DTE and 1 mM Aprotinin/Leupeptin were added as efficient protease inhibitors.

0.5 M Hepes/NaOH pH 7.4: Hepes (4-(2-hydroxyethyl)-1-piperazineethanesulfonic acid) dissolved in appropriate amount of dH<sub>2</sub>O, brought to pH 7.4 with concentrated NaOH, and stored at 4°C.

0.5 M EDTA pH 8.0: Na<sub>2</sub>EDTA\*2H<sub>2</sub>O dissolved in appropriate amount of dH<sub>2</sub>O and brought to a pH 8.0 with 10 M NaOH, autoclaved and stored at RT.

20% SDS: sodium dodecyl sulfate (w/v) dissolved in dH<sub>2</sub>O, autoclaved and stored at RT.

1 M Aprotinin stock: Aprotinin dissolved in H<sub>2</sub>O, aliquots of 50µL were dried and stored at -20 °C.

1 M Leupeptin hemisulfate stock: Leupeptin hemisulfate dissolved in H<sub>2</sub>O, aliquots of 50µL were dried and stored at -20°C.

0.5 M DTE: DTE (2,3-Dihydroxybutane-1,4-dithiol) dissolved in 100µL dH<sub>2</sub>O, stored at -20°C.

100 mM PMSF: PMSF (Phenylmethylsulfonyl fluoride) dissolved in Isopropanol, aliquots for short storage at -20°C.

20% Triton X-100 (v/v): 100 % Triton X-100 diluted in dH<sub>2</sub>O, stored at 4°C.

10% Na-deoxycholate: Na-deoxycholate dissolved in dH<sub>2</sub>O, autoclaved and stored at -20°C.

2.5 M NaCl: NaCl dissolved dH<sub>2</sub>O, autoclaved and stored at RT.

### 3.10.3 Binding Assay with glutathione-magnetic beads

In order to analyze the binding activity of ubiquitin to the TOL proteins *in vitro* (can also be used for different proteins and targets) an *in vitro* binding assay was performed as the following: 100µL of Thermo Scientific Pierce Glutathione magnetic beads were equilibrated with Equilibration Buffer (EB-binding or washing buffer) by washing 3 times, 1mL, 10 minutes at 4°C, gently rocking. The supernatant was removed using a magnetic stand (Promega™ MagneSphere™ Technology Magnetic Separation Stand). 500µl of Equilibration buffer was added to resuspend the beads and then mixed with 500µl of soluble extracted recombinant GST (glutathione-S-transferase)-fusion protein (see section 3.10.2). The sample was incubated for 2 hours at 4°C, gently rocking, allowing the GST-fusion protein to bind to the Glutathione magnetic beads via its GST-tag. After

incubation, the tubes were placed on magnetic stand and the beads settled down. The supernatant was removed and 50µl saved for testing the sample before binding. The ubiquitin coupled Glutathione magnetic beads were washed with EB-binding/washing buffer 3 times, 10 minutes at 4°C by gently rocking. Then the second recombinant protein, which binds to the GST-tagged first protein, was added. The appropriate amount (10-100µl) (depending on the concentration of protein) was diluted in 1 mL Resuspension buffer and added to the beads and incubated overnight at 4°C by gently rocking. From this sample, 20µl was saved before adding to the beads, to analyze the amount of protein before binding.

Next day, the tubes with the samples were placed on magnetic stand to allow the coupled beads, with the potentially bound second protein to settle down and the supernatant was removed. 50µl of the supernatant was saved for analysis after binding. The beads were washed with Resuspension buffer 6 times, 1 mL, 10 minutes, 4°C, gently rocking. After the final washing steps, the beads containing the complex ubiquitin-TOL proteins were resuspended in 50µl Laemmli buffer and incubated for 10 minutes at 98°C. The beads were settled down at magnetic stand and the supernatant transferred to a fresh tube. The sample was saved at -20°C until analysis. Similar procedures were performed as control experiments using just GST.

NOTE: Thermo Scientific Pierce Glutathione Magnetic Beads are composed of iron oxide particles, encapsulated by crosslinked agarose with a mean diameter of 1-10 µm with reduced glutathione (GSH) covalently attached to the surface.

Thermo Scientific Pierce Glutathione Magnetic Beads were stored in 25% slurry of 20% Ethanol with a binding capacity of 5-10 mg of GST fusion protein per 1 mL of settled beads (i.e., 4 mL of 25% slurry).

EB binding/wash-buffer: 1x TBS, 20 mM Tris/HCl pH 7.4, 0.5 % Triton X-100, 5 mM EDTA pH8, 0.5% CHAPS((3-(3-cholamidopropyl) dimethylammonio)-1-propanesulfonate), appropriate amount of water and stored at 4°C. Before use 1 mM PMSF, 1 mM DTE and 1 mM Aprotinin/Leupeptin were added as efficient protease inhibitors.

Resuspension buffer: 20 mM Tris/HCl 7.4, 200 mM NaCl, 1 mM EDTA pH 8, appropriate amount of water and stored at 4°C. Before use 1 mM PMSF, 1 mM DTE and 1 mM Aprotinin/Leupeptin were added as efficient protease inhibitors.

2.5 M NaCl: NaCl dissolved in appropriate amount of dH<sub>2</sub>O, autoclaved and stored at RT.

20x TBS: 1 M Tris (2-Amino-2-(hydroxymethyl)-1,3-propanediol), 3 M NaCl dissolved in dH<sub>2</sub>O, brought to pH 7.5, autoclaved and stored at RT.

1 M Tris/HCl pH 7.4: Tris (2-amino-2-hydroxymethyl-1,2-propanediol) dissolved in dH<sub>2</sub>O and brought to the pH 7.4 with concentrated HCl, autoclaved and stored at RT.

20% Triton X-100 (v/v): 100% Triton X-100 diluted in dH<sub>2</sub>O, stored at 4°C

5% CHAPS: CHAPS ((3-(3-cholamidopropyl) dimethylammonio)-1-propanesulfonate) dH<sub>2</sub>O, aliquots stored at -20°C.

0.5 M EDTA pH 8: Na<sub>2</sub>EDTA\*2 H<sub>2</sub>O dissolved dH<sub>2</sub>O and brought to a pH 8.0 with 10 M NaOH, autoclaved and stored at RT.

1 M Aprotinin stock: Aprotinin dissolved in H<sub>2</sub>O, aliquots of 50µL were dried and stored at -20°C.

1 M Leupeptin hemisulfate stock: Leupeptin hemisulfate dissolved in dH<sub>2</sub>O, aliquots of 50 µL were dried and stored at -20 °C.

0.5 M DTE: DTE (2,3-Dihydroxybutane-1,4-dithiol) dissolved in dH<sub>2</sub>O and stored at -20 °C

100 mM PMSF: PMSF (Phenylmethylsulfonyl fluoride) dissolved in Isopropanol, aliquots, for short storage at -20°C.

### 3.10.4 Discontinuous SDS-Polyacrylamide Gel Electrophoresis (SDS-PAGE)

The proteins extracts were analyzed by discontinuous SDS-PAGE method developed by (Laemmli, 1970). This method uses two gels, a stacking and separating gel which allows the separation of proteins according to their molecular weight. SDS is responsible for protein denaturation, and gives them a constant charge. The stacking gel helps proteins

to start their migration at the same level while the separation gel, is important for separating proteins in accordance to their molecular weight. Between 6% and 14% polyacrylamide was used in the separation gels. Whereas the stacking gels always contained 4% polyacrylamide (Table 13).

**Table 13 Preparation of separation gel**

<b>Chemicals</b>	<b>Volume for 2 gels</b>	<b>Final concentration</b>
30% Acrylamid/Bisacrylamid (37.5:1)	5 mL	10%
4x 1.5 M Tris/HCl pH 8.8	3.75 mL	375mM
20% SDS	75 $\mu$ L	0.1%
dH <sub>2</sub> O	6.25 mL	-
10% APS	75 $\mu$ L	0.05%
TEMED	15 $\mu$ L	0.1%

APS and TEMED were added just before pouring the gels. The components for the separation gel were mixed in a 50mL falcon tube and poured into assembled gel plates using a pipette, but leaving enough space on top for the staking gel to be added later on. To avoid drying out of the separation gel, isopropanol was added on the top of the gel. After at least 30 minutes of gel polymerization the isopropanol was removed and the gel rinsed with water and finally dried with filter paper. Afterwards the staking gel was added on top (Table 14).

**Table 14 Preparation staking gel:**

Chemicals	Volume for 2 gels	Final concentration
30% Acrylamid/Bisacrylamid (37.5:1)	1 mL	4 %
4x 1.5 M Tris/HCl pH 8.8	1.875 mL	375 mM
20% SDS	37.5 µL	0.1%
dH <sub>2</sub> O	4.625 mL	-
10% APS	37.5 µL	0.05%
TEMED	7.5 µL	0.1%

The staking gel was prepared and poured in the same way as the separating gel. The combs were inserted avoiding air bubble formation. After gel polymerization, it was removed from the casting stand and assembled into the chamber for running the electrophoresis. The chamber was filled with 1x running buffer and the protein samples already diluted in 2x Laemmli buffer (1:2) were heated up for 10 minutes at 98°C and then loaded on the gels. The gels were run at 100 V, during the running gel and then the voltage was increased to the 150V until the bromophenol blue dye reached the end of the separating gel.

In case of total membrane protein extraction where the membrane fractions was separated from the soluble fraction urea (3M final concentration) was added to the SDS gel electrophoresis (table 15 and 16).

**Table 15 Preparation 15 mL of the separating gel solution used for Total membrane protein extraction**

Chemicals	Volume (µL)
1M Tris/HCl pH 8.8	6950
10% SDS	150
30% Acrylamid (29:1)	3000 (6%) - 7000 (14%)

10% APS	60
TEMED	15
dH <sub>2</sub> O	fill up to 15 ml

**Table 16 Preparation 6 mL of the separating gel solution used for Total membrane protein extraction**

Chemicals	Volume (μL)
8 M Urea (only for PM extract western)	2800
1 M Tris/HCl pH 6.8	940
10% SDS	112.8
30% Acrylamid (29:1)	1000 (4%)
10% APS	30
TEMED	7.5
dH <sub>2</sub> O	fill up to 6 ml

1.5 M Tris/HCl pH 8.8: Tris (2-amino-2-hydroxymethyl-1,3-propanediol) dissolved dH<sub>2</sub>O and brought to pH 8.8 with concentrated HCl, autoclaved and stored at RT.

20% SDS: SDS (sodium dodecyl sulfate, w/v) dissolved in dH<sub>2</sub>O, autoclaved and stored at RT.

0.5 M Tris/HCl pH 6.8: Tris (2-amino-2-hydroxymethyl-1,3-propanediol) dissolved dH<sub>2</sub>O and brought to the pH 6.8 with concentrated HCl, autoclaved and stored at RT.

10% APS: APS (ammonium persulfate) dissolved dH<sub>2</sub>O, short storage at -20 °C

Running buffer: 25 mM Tris (2-amino-2-hydroxymethyl-1,2-propanediol), 192 mM Glycine, dissolved in dH<sub>2</sub>O, 0.01 % w/v 20 % SDS were added afterwards.



2x Laemmli buffer: 20 % v/v glycerol, 125 mM Tris pH 6.8, 4% w/v SDS, 0.01% w/v bromphenol blue, appropriate amount of dH<sub>2</sub>O, stored at RT. Before use 10% of  $\beta$ -mercaptoethanol was added.

1 M Tris/HCl pH 8.8: Tris (2-amino-2-hydroxymethyl-1,3-propanediol) dissolved and brought to pH 8.8 with concentrated HCl, autoclaved and stored at RT.

1 M Tris/HCl pH 6.8: (2-amino-2-hydroxymethyl-1,3-propanediol) dissolved in dH<sub>2</sub>O and brought to pH 6.8 with concentrated HCl, autoclaved and stored at RT.

8 M Urea: 3 ml Amberlite Mischbettionentauscher beads were washed in a 500 ml bottle with 200 ml dH<sub>2</sub>O for 30 min at RT on a shaker. Water was taken off, 200 ml dH<sub>2</sub>O were again added and washed for 30 min at RT on a shaker. Water was taken off. 50 ml 8 M urea solution (24 g urea in 50 ml dH<sub>2</sub>O) were added and shaken for 30 min at RT. Urea was aliquoted and stored at -20°C.

### **3.10.5 Coomassie blue staining**

After protein separation on SDS-PAGE, the quality of extracted proteins was analyzed by Coomassie blue staining. Coomassie brilliant blue R-250 binds proteins with low specificity. The detection limit of Coomassie blue staining is approximately 0.5 ng protein per band. The polyacrylamide gel was soaked on Coomassie staining solution and gently rocked for 1h at RT. The Coomassie staining solution was removed, and the gel boiled in water in a glass beaker. The boiling step was repeated until the majority of excess dye was removed and the blue bands and clear background were obtained. The gel was incubated overnight in water with a piece of paper towel to soak up the excessive remaining Coomassie brilliant blue.

Coomassie staining solution: 0.25% w/v Coomassie brilliant blue, dissolved in a mixture of dH<sub>2</sub>O, 45% v/v Methanol, and 10% v/v acetic acid, stored at RT.

### 3.10.6 Western Blot and detection

The separated proteins from polyacrylamide gel were transferred to a solid membrane to allow the detection of a particular protein by interaction with specific antibodies. The protein transfer was performed using a mini Trans-Blot cell (BIO-RAD) which transfers the proteins from the SDS-PAGE gel to the nitrocellulose membrane (Roth) or PVDF membrane. PVDF membrane was mostly used to detect ubiquitin with the ubiquitin specific antibody P4D1. After running the SDS-PAGE, the staining gel was removed and the remaining separation gel equilibrated for at least 10 minutes in transfer buffer. Fiber pads, filter paper and nitrocellulose membrane were soaked in transfer buffer at least 15 minutes before assembling on the gel cassette. A PVDF membrane was soaked in 100% methanol before soaking in transfer buffer. The gel cassette was assembled in one layer of fiber pad, at least 2 pieces of filter paper, SDS-PAGE gel, solid membrane (nitrocellulose or PVDF) and the Filter paper again followed by fiber pads. Air bubbles were avoided by trying to assemble the gel cassette within a plastic bowl filled with transfer buffer. The membrane was positioned next to the anode when the gel holder was transferred to the electrode unit. The transfer chamber was filled with transfer buffer and placed into a big plastic bowl filled up with crashed ice for cooling. The transfer was carried out at constant 100 V for 1 hour (depend on the molecular weight of the protein). After transfer the membrane was blocked with 3% BSA in TBST (blocking solution) for 1 hour at RT, rocking gently. The membrane was transferred to an adequately diluted primary antibody in blocking solution and incubated overnight at 4°C, gently rocking. Alternatively, the membrane was incubated for 1h at RT, gently rocking. Next day the primary antibody was removed and the membrane washed 3 times for at least 10 minutes in TBST at RT. After washing steps, the membrane was incubated in an adequate dilution of secondary antibody in blocking solution for 1 hour at RT, gently rocking. After at least 3 washing steps of 10 minutes in TBST at RT, the membrane was transferred onto a plastic plate. The HRP chemiluminescence substrate (Pierce) was distributed on the membrane and incubated for 2 minutes. Afterwards the membrane was transferred onto a plastic slide and excess of substrate was removed with a piece of paper towel. An X-ray film was exposed on the membrane in the dark room for 5 seconds or more and afterwards the film was developed. Alternatively, the FUSION SOLO machine was used to develop.

Transfer buffer: 25 mM Tris, 192 mM Glycine, 10% v/v Methanol, dissolved in dH<sub>2</sub>O, 0.05% w/v SDS were added afterwards. Stored at 4°C, and re-used 3 - 4 times.

Blocking solution: 3% w/v BSA (bovine serum albumin), dissolved in TBST, prepared fresh before use.

20x TBS: 1 M Tris (2-Amino-2-(hydroxymethyl)-1,3-propanediol), 3 M NaCl dissolved dH<sub>2</sub>O, brought to pH 7.5, dH<sub>2</sub>O to 1000 mL, autoclaved and stored at RT.

TBST: 1x TBS, 0.1% v/v Tween 20, dH<sub>2</sub>O, stored at RT.

NOTE: Filter papers were cut slightly smaller than the fiber pad and the nitrocellulose membranes were cut slightly bigger than the polyacrylamide gel.

### **3.10.7 Extraction and purification of HIS-tag recombinant protein from BL21 (DE)**

His-tagged recombinant protein extraction from BL21 (DE) was performed to obtain high level of soluble fraction from His-tagged proteins in a good quality. The frozen pellet from 200mL culture after induction (see section 3.10.1) was resuspended in 5 mL of lysis buffer containing 2% Triton X-100, lysozyme and proteinase inhibitors. For 50 mL induced culture was used 1.25 mL of lysis buffer. Samples were aliquoted in 2 mL tube (approximately 625µl per tube), incubated 15 minutes at 4°C with rocking. Afterwards, 500µL of lysis buffer without Triton X-100 and lysozyme but with proteinase inhibitor was added to each tube. Samples were sonicated 6 times for 10 seconds (setting at 40 outputs). Between sonication pulses, the samples were allowed to chill on ice for at least 2 min. Afterwards the samples were centrifuged at maximal speed for 15 minutes at 4 °C. The supernatant, containing the recombinant his-tagged protein, was mixed together in a 15 mL falcon tube containing 10% glycerol to be frozen at -80°C. 50µl of the sample (correspondent to 1mL of the culture) was saved for testing the extraction and the rest stored at -80°C until purification. Pellet after extraction was also saved to be used in cases of the fusion protein was insoluble.

### **rotein solubilization**

If the fusion protein was in the insoluble fraction (pellet) after extraction, it was solubilized using 4 - 8M urea solution in 100mM NaPO<sub>4</sub>. The sample was incubated for 1hour rocking at RT followed by centrifugation step for 30 min at 4°C 13000rpm. 50µL kept for analyze in Coomassie staining solution. For TOL6-His protein purification, 8M Urea (CH<sub>4</sub>N<sub>2</sub>O or NH<sub>2</sub>CONH<sub>2</sub>) was used to solubilize the insoluble protein.

### **3.10.8 Protein purification**

The purification of the His-tag protein was performed using His-select nickel magnetic agarose beads from Sigma-Aldrich company as following: The Nickel beads were equilibrated with lysis buffer (without lysozyme, Triton and Urea) supplemented with 300mM NaCl, 10mM Imidazole and PMSF, 3 times 1 mL. The soluble protein sample was supplemented with 300mM NaCl, 10mM Imidazole and PMSF. The supplemented proteins sample was added to the equilibrated beads, incubated for 1hour at room temperature by rocking. The tubes were settled in the magnetic rack and the supernatant was removed. 50µl was saved for analyze. The beads were washed with lysis buffer supplemented with 300mM NaCl, 20mM Imidazole and PMSF, 1 mL, 10 minutes, 6 times at 4°C, rocking. When using Urea, the washing steps were reduced. Afterwards the supernatant was removed and the beads eluted with 400µL elution buffer supplemented with 250-500mM Imidazole for 15 min, rocking at 4°C.

Lysis buffer: 50 mM sodium phosphate pH 8, - 300 mM NaCl,

Supplements for lysis Buffer (added when necessary): 2% Triton, Lysozyme 20µL of 1%/mL of buffer (10mg/mL in H<sub>2</sub>O), Proteinase inhibitor, complete mini EDTA free tablet (Roche) (1 tablet /10 mL). If have to be divided, the tablet was dissolved in 1,5 mL water.

Wash buffer: 50 mM sodium phosphate pH 8, 300 mM NaCl, 20 mM Imidazole, add fresh PMSF

Urea wash buffer: 100 mM sodium phosphate pH8, 300 mM NaCl, Urea 4 - 8 M, 20 mM Imidazole, add fresh PMSF.

Elution buffer: 50 mM sodium phosphate pH 8, 300 mM NaCl, 250mM Imidazole, add fresh PMSF

Urea elution buffer: 100mM sodium phosphate pH 8, 300 mM NaCl, 4 - 8 M Urea, 250 mM Imidazole, add fresh PMSF. If the Urea elution with Imidazole was not well eluting the pH of Sodium Phosphate was changed to pH 4, 5 – 6.

### **3.10.9 Affinity purification of rabbit serum containing $\alpha$ -TOL6 antibody**

Bacterially expressed and purified full length TOL6 protein (see section 3.10.8) was sent to Center for Biomedical Research, Department of Laboratory Animal Science and Genetics, Medical University Vienna, Austria for injection into two different rabbits (50 - 200 $\mu$ g/rabbit in ½ mL - 1 ½mL). The serum was collected and sent back to our lab. For TOL6 antibody purification, 300 $\mu$ L of purified full length TOL6 protein was mixed with 300 $\mu$ L 2x Laemmli buffer (with 10%  $\beta$ -mercaptoethanol). Total volume of 600 $\mu$ L was loaded and run in SDS-PAGE gel (one line in all entire gel) and transferred to a nitrocellulose membrane. The membrane was stained in Ponceau S staining solution and the relevant TOL6 protein band (~73kDA) was cut out and destained completely in TBST. The membrane strip was blocked with 3% BSA in TBST for 2h, at RT and left overnight at 4°C in TBST. Next day the TOL6 serum was added to the strip membrane with TOL6 purified protein and incubated for 4.5h, at 4°C gently rocking.

Afterwards the strip membrane was washed 3 times with TBST, and cut into several pieces to fit into a 2 mL tube. Elution of antibodies was performed in a 2 mL tube. Antibodies were stripped off from membrane with 1 mL stripping solution for 1 min on a rocker shaker and quickly neutralized with 150 $\mu$ L neutralization solution. Strips were washed with 0.5 mL TBST and this wash was added to the eluate. The whole elution procedure was carried out three more times. Finally, BSA was added to the eluate to a final concentration of 3%. Aliquots were stored at -80°C.

Ponceau S staining solution: 0.5%, w/v Ponceau S, 0.5 mL acetic acid (1%, v/v), dissolved in dH<sub>2</sub>O, stored at RT.

Blocking solution: 3% w/v BSA (Bovine Serum Albumin) dissolved in TBST. Prepared fresh.

Stripping solution: 20 mM glycine dissolved in dH<sub>2</sub>O and brought to pH 2.3 with concentrated HCl, 500 mM NaCl, 0.5% v/v tween 20 in dH<sub>2</sub>O and stored at 4°C. Before use 1 mg BSA/ml elution buffer (0.1%, w/v) was added.

Neutralization solution: 1 M Tris/HCl pH 7.4 Tris (2-amino-2-hydroxymethyl-1, 3-propanediol) dissolved in dH<sub>2</sub>O and brought to pH 8.8 with concentrated HCl, autoclaved and stored at RT.

### **3.10.10 PIP strip**

To determine the lipid-protein interaction of the TOL6 and TOL2 I used a hydrophobic membrane spotted with 15 different lipids – the PIP Strips membrane. The PIP strip membrane is light sensitive; all the steps were carried out in dark conditions. The PIP strip membrane was blocked with 3%BSA in TBST for 1h at Room temperature (RT) or overnight at 4°C. The blocking solution was discarded. The protein of interest (extract TOL6:His and TOL2: His) was diluted 1:1 with 3% BSA in TBST to a final volume of 4mL or enough to cover the membrane and incubated for 1h at room temperature in dark. Afterwards the membrane was washed 5 times, 5 minutes with TBST at RT. The washing solution was discarded and then an anti-His monoclonal antibody diluted in 1:200 in 3% BSA in TBST was added and incubated for 1h at RT in dark with gentle rocking. The membrane was washed 5 times, 5 minutes with TBST at RT. The washing solution was discarded and the membrane covered with anti-mouse IgG-HRP antibody diluted in 1:10000 in 3% BSA in TBST and incubated for 1h at RT in dark with gentle rocking. The membrane was washed 5 times, 5 minutes with TBST at RT. Washing solution was discarded and the membrane transferred onto a square petri dish and HRP-chemiluminescence substrate was applied. Substrate was allowed to react for 2 min, and then the membrane was removed from the substrate and placed between two sheets of clear autoclave bags. Substrate excess eliminated by gentle pressing with towel paper over the upper plastic sheet. An X- ray film was exposed on the membrane for 1 - 30 min and after that the film was developed. Alternatively, was used the chemidoc equipment to develop.

**3.10.11 Small scale protein extraction for Western blot**

In order to evaluate the protein levels of TOL proteins, and the stability of the fusion proteins in the transgenic plants, a western blot experiment was performed using total plant lysate. 25 seedlings with 5 days after germination (DAG) were harvested in 2mL safe lock Eppendorf tube with 2 of 4mm metal beads and frozen in liquid nitrogen. Plant material was homogenized in a Retsch mixer mill MM2000 for one minute, with the amplitude set at 30. Alternatively, plant material was grinded with plastic pestle in drilling machine. 150 $\mu$ L of 1x sample buffer was added to homogenized sample, and allowed to thaw on ice. After thawing the sample was incubated for 5 minutes at 65°C, gently shaking. The sample was centrifuged for 5 minutes, at RT, maximal speed. The supernatant was transferred to a fresh tube and the sample loaded on SDS-PAGE. Or frozen at -20°C.

1 x Sample buffer: 65mM Tris, pH8, 5%  $\beta$ -mercaptoethanol, 2% SDS, 10% Glycerin, 0.25% Bromophenolblue, 8M Urea. Prepared and stored at RT.

**3.10.12 General plant protein extraction**

Between 50-100mg of plant material with 5 - 6 days after germination (DAG) was harvested in 2 mL safe lock tubes, containing two of 4mm metal beads, and frozen in liquid nitrogen. Plant material was homogenized in a Retsch mixer mill MM2000 for one minute, with the amplitude set at 30. After milling, tubes were again frozen in liquid nitrogen. Alternatively, plant material was harvested in 1.5 mL tubes and homogenized with plastic pestle on drilling machine. 1000 $\mu$ L RIPA buffer was added to the sample, vortexed and the metal beads were removed using a stir bar retriever. If the plant material was homogenized with plastic pestle the RIPA buffer was directly added to the sample and vortexed. Afterwards, the sample was incubated for 1 hour at 4°C on vibrax shaker at 1600rpm and then centrifuged for 10 min, 4°C, and 13000rpm. Supernatant was transferred into a fresh tube, and sample were either stored at -80°C or directly subjected to SDS-PAGE or used for Immunoprecipitation.

RIPA buffer: 50 mM Tris/HCl pH 7.4, 150 mM NaCl, 1%NP-40, 1% (w/v) Sodium Deoxycholate, 0.1%w/v SDS, 20 mM NEM, 1x cOmplete Mini Protease Inhibitor Cocktail (Roche), 1x PMSF dH<sub>2</sub>O to appropriate amount were mixed prior to use.

### **3.10.13 Total membrane protein extraction from *Arabidopsis thaliana***

All steps were carried out on ice and in a cooled microcentrifuge. The method was applied to extract total membranes only from young *Arabidopsis thaliana* seedlings. It is suitable for extracting total seedlings, roots or shoots. Between 10 mg and 200 mg of plant material was harvested in 2 mL safe lock Eppendorf tubes, containing two of 4mm metal beads, and frozen in liquid nitrogen. Plant material was homogenized in a Retsch mixer mill MM2000 for one minute, with the amplitude set at 30. Alternatively, Plant material was grinded with plastic pestle in drilling machine. After homogenization, tubes were again frozen in liquid nitrogen. Prior to extraction of material, a 10% (w/v) PVPP solution was equilibrated with 1x Extraction buffer for 10 min. Per mg of plant material, 0.5 µL of 10% (w/v) PVPP solution (0.05 mg) was transferred into a fresh tube, centrifuged for a few seconds and the extraction buffer was discarded. For small amounts of plant material (up to 20 mg), at least 10µL of 10% (w/v) PVPP solution (1 mg) was used. 1x Extraction buffer was added to grinded plant material and vortexed to quicken thawing of the buffer. If less than 60 mg plant material was extracted, 100 µL of 1x Extraction buffer was added. If material exceeded 60 mg, 1.68 µL of 1x Extraction buffer per mg of plants was added. After thawing, metal beads were removed with a stir bar retriever and the homogenate sample was pipetted to equilibrated PVPP. Samples were alternately vortexed and put on ice for 30 seconds each to ensure efficient extraction without protein degradation. After 5 min, samples were centrifuged at 4°C (2 min, 2120rpm). The supernatant, containing microsomal-type membranes was transferred into a fresh tube. The PVPP/plant material homogenate was again extracted with the same amount of 1x Extraction buffer for 1 min and centrifuged at 4°C (2 min, 2120rpm). The supernatant was mixed with the first supernatant and vortexed. Afterwards the PVPP pellets were discarded at this stage. Supernatants were cleared from minor traces of PVPP by centrifugation at 4°C (2 min, 2120 rpm). Finally, the supernatant was transferred into a fresh tube and centrifuged for 2h, 13000rpm at 4°C to pellet membranes. When the amount of supernatant exceeded 200µL, the sample was aliquoted for the last centrifugation step. After centrifugation, the



supernatant was used as a soluble fraction and pellets were either frozen at -80°C or alternatively directly subjected to immunoprecipitation or SDS-UREA-PAGE.

### Preparation of 1x Extraction buffer:

A stock solution of 1.75x Extraction buffer was prepared and frozen in aliquots at -20°C. Prior to extraction, 1.75x Extraction buffer was diluted to 1x Extraction buffer with sodium molybdate, PAO, water and NEM to inhibit deubiquitinating enzymes. To this 1x Extraction buffer, DTE, Okadaic acid, Benzamidine, Pefabloc-SC, Aprotinin/Leupeptin, E64, Pepstatin, PMSF, borate and ascorbic acid were added and the buffer was ready to use.

1.75x Extraction buffer: 50 mM Tris/HCl pH 7.3, 10mM Tris/HCl pH 8.8, 3.54 M D-Sorbitol, 0.35% (w/v) casein, 10 mM EDTA , 10 mM EGTA, 40 mM Beta Glycerophosphate, 20 mM KH<sub>2</sub>PO<sub>4</sub> buffer pH 7.4 and 50 mM NaF were combined, vortexed, aliquoted and frozen at -20°C. Prior to use 1 mL of 1.75x Extraction buffer was freshly prepared by adding, 1.98 mM Sodium Molybdate and 1.98mM PAO.

1x Extraction buffer: For 1 mL of 1x Extraction buffer, 588µL 1.75x Extraction buffer was diluted with 312 µL dH<sub>2</sub>O and added 20 mM NEM. After vortexing, 9.4 mM borate, 2.4 mM benzamidine, 2 0.94 mM DTE, 1.88 mM Pefabloc-SC, 1.88 nM Okadaic acid, 1.88x Aprotinin/Leupeptin, 1.88x E64, 1.88x Pepstatin, 1.88x PMSF and 9.43 mM ascorbic acid were added and vortexed.

10% (w/v) PVPP: insoluble Polyvinylpyrrolidon was added to dH<sub>2</sub>O. Stored at 4°C.

1 M Tris/HCl pH 7.3: Tris (2-amino-2-hydroxymethyl-1,3-propanediol) dissolved in dH<sub>2</sub>O and brought to pH 7.3 with concentrated HCl, autoclaved and stored at RT.

1 M Tris/HCl pH 8.8: Tris (2-amino-2-hydroxymethyl-1,3-propanediol) dissolved dH<sub>2</sub>O and brought to pH 8.8 with concentrated HCl, dH<sub>2</sub>O, autoclaved and stored at RT.

4.88 M D-sorbitol: D-Sorbitol were dissolved in dH<sub>2</sub>O. stored at 4°C.

7% Casein: casein was dissolved in dH<sub>2</sub>O, aliquots were stored at -20°C.

0.5 M EDTA pH 8.0: Na<sub>2</sub>EDTA x 2H<sub>2</sub>O (Ethylenediaminetetraacetic acid disodium salt dihydrate) dissolved in dH<sub>2</sub>O and brought to pH 8.0 with 10 M NaOH, autoclaved and stored at RT.

0.5 M EGTA: EGTA were dissolved in and brought to pH 8.0 with 10 M NaOH, autoclaved and stored at RT.

1 M  $\beta$ -glycerophosphate:  $\beta$ -glycerophosphate-disodium salt-pentahydrate (C<sub>3</sub>H<sub>7</sub>O<sub>6</sub>PNa<sub>2</sub> x 5H<sub>2</sub>O) were dissolved in dH<sub>2</sub>O and stored at 4°C.

1 M KH<sub>2</sub>PO<sub>4</sub> pH 7.4: K<sub>2</sub>HPO<sub>4</sub> were dissolved in dH<sub>2</sub>O and autoclaved. KH<sub>2</sub>PO<sub>4</sub> were dissolved in 1000 ml dH<sub>2</sub>O and autoclaved. Afterwards, 80.2 mL of 1 M K<sub>2</sub>HPO<sub>4</sub> and 19,8 ml of 1 M KH<sub>2</sub>PO<sub>4</sub> were combined and stored at RT.

2.5 M NaF: NaF were resuspended in dH<sub>2</sub>O. The powder did not completely dissolve. Therefore, extensive vortexing is recommended before each use. Stored at 4°C.

0.5 M sodium molybdate: sodium molybdate-2-hydrate was dissolved dH<sub>2</sub>O. Stored at 4°C.

0.5 M PAO: phenylarsine oxide was dissolved in DMSO. Aliquots were stored at 4°C.

200 mM NEM (N-Ethylmaleimide): For every use, N-ethylmaleimide were freshly diluted in dH<sub>2</sub>O. Do not prepare a stock solution, as NEM is highly unstable. NEM powder is stored at 4°C.

2.7 M borate acid: borate acid were dissolved in dH<sub>2</sub>O. Brought to pH 8.0 with NaOH. Stored at 4°C.

100 mM benzamidine: Benzamidine were dissolved in 50 % glycerol. Stored at -20°C.

0.5 M DTE: DTE were dissolved dH<sub>2</sub>O. Aliquots were stored at -20°C.

200 mM Pefabloc-SC: Pefabloc SC was dissolved in dH<sub>2</sub>O. Aliquots were stored at -20°C.

2  $\mu$ M okadaic acid: A 100 mM okadaic acid solution was prepared first. 80.5 mg okadaic acid was dissolved in 1 mL DMSO. Then it was further diluted with DMSO.

1000x Aprotinin/Leupeptin: Aprotinin and Leupeptin were dissolved in dH<sub>2</sub>O. Aliquots were vacuum-dried and stored at -20°C. When needed, the dried pellet was resuspended in dH<sub>2</sub>O.

1000x E64: E64 were dissolved in MeOH. Aliquots were vacuum-dried and stored at 4°C. When needed, the dried pellet was resuspended in DMSO. Diluted aliquots were stored at -20°C.

1000x Pepstatin: Pepstatin were dissolved in MeOH. Aliquots were Vacuum-dried and stored at 4°C. When needed, the dried pellet was resuspended in DMSO. Diluted aliquots were stored at -20°C.

1000x PMSF: PMSF were dissolved in MeOH. Aliquots were vacuum-dried and stored at 4°C. When needed, the dried pellet was resuspended in DMSO. Diluted aliquots were stored at -20°C.

1 M Ascorbic acid: Ascorbic acid was dissolved in dH<sub>2</sub>O. Aliquots were stored at -20°C.

### **Chloroform/Methanol precipitation of supernatant after membrane protein preparation.**

To analyze the amount of protein remaining in supernatant after the membrane protein extraction, approximately 200 $\mu$ L of the supernatant separated after the 2 hours centrifugation, was precipitated as the following:

From 200  $\mu$ L starting volume was added 800 $\mu$ L methanol, vortexed, 200 $\mu$ L chloroform, vortexed and 600 $\mu$ L ddH<sub>2</sub>O, and vortexed well. After adding ddH<sub>2</sub>O the solutions become cloudy. It was followed by centrifugation step for 2 min, 13000rpm, RT. The top aqueous

layer was removed by pipetting and discarded. Protein exists between layers was visible on thin wafer. To the remaining solution (containing protein) was added 800 $\mu$ L of methanol, vortexed and centrifuged for 3 minutes, 13000, RT. The supernatant was removed by pipetting as much as possible from the tube avoiding disturbing the pellet. The pellet was resuspended in 50 $\mu$ L of sample buffer. Samples were either directly subjected to SDS-UREA-PAGE or stored at -20°C.

### **3.10.14 Immunoprecipitation of whole TOL protein**

All steps were carried out on ice or at 4°C to avoid protein degradation. Approximately 100 mg plant material (4 - 6 DAG, total or roots) were grinded with plastic pestle, in liquid nitrogen, alternatively plant material was homogenized in a Retsch mixer mill MM2000 for one minute, with the amplitude set at 30. 1 mL of RIPA buffer (supplemented with NEM), was added and incubated for 1h at 4°C on vibrax at 1600rpm, followed by centrifugation step for 10 min, 13000, at 4°C. The Supernatant was transferred to a fresh tube and 50 $\mu$ L affinity purified antibody was added. Immunoprecipitation was carried out o/n at 4°C on a turning wheel at 12rpm. Protein A magnetic beads was used for pulling down  $\alpha$ -TOL6 antibody-TOL6 protein conjugate the following day. For other TOL proteins were used anti GFP antibody since the proteins were tagged to the Venus Tag. Therefore 60 $\mu$ L of protein A magnetic beads per sample was rehydrated in 1mL of 1x TBS at 4°C on a turning wheel 12rpm for one hour, followed by three successive washing steps with 1 mL of 1x TBS. For efficient washing, 1x TBS was added to the Protein A magnetic beads, inverted multiple times and settled on magnetic rack to separate the beads to the TBS. After washing in TBS dilution, beads were blocked overnight in 1 mL 1x TBS supplemented with 5% BSA (w/v). The following day, the blocked Protein A magnetic beads were again washed three times in 1 mL of 1x TBS. Then, 150 $\mu$ L of a 50% magnetic beads slurry (i.e. 50 $\mu$ L beads volume and 50 $\mu$ L 1x TBS) were added to the immunoprecipitation reaction and incubated for four hours on a turning wheel at 4°C at 12rpm. Protein A magnetic beads -  $\alpha$ -TOL6/GFP antibody –TOL protein conjugates were then washed five times by inversion with 1 mL of RIPA wash buffer for each washing step. Afterwards, RIPA wash buffer was removed completely. For elution of the antibody - protein complex from Protein A magnetic

beads, 50µL of 1x Laemmli buffer were added to the beads and incubated in a heat block at 98°C 10 min. Tubes were settled in the magnetic rack and the supernatant transferred into a fresh tube. Samples were either directly subjected to SDS-UREA-PAGE or stored at -20°C.

RIPA buffer: 50 mM Tris/HCl pH 7.4, 150 mM NaCl, 1%NP-40, 1% (w/v) Sodium Deoxycholate, 0.1 %w/v SDS, 20 mM NEM, 1x cOmplete Mini Protease Inhibitor Cocktail (Roche), 1x PMSF dH<sub>2</sub>O to appropriate amount. were mixed prior use.

RIPA wash buffer: 50 mM Tris/HCl pH 7.4, 150 mM NaCl (), 1 %NP-40 (), 1 % (w/v) Sodium Deoxycholate, 0.1 % (w/v) SDS, 20 mM NEM and appropriate amount of dH<sub>2</sub>O were mixed prior use. Protease inhibitors were not used during washing steps.

1x sample buffer: 0.5% (w/v) CHAPS, 3% (w/v) SDS, 60mM DTE, 125mM Tris/HCl pH 6.8, 30%l glycerol, 1x Complete Mini Protease Inhibitor Cocktail (Roche) and 1x PMSF were mixed prior use. Bromophenol blue was added with a toothpick. 1x sample buffer was stored at -20°C. After repeated freeze/thaw cycles, PMSF was again added.

1 M Tris/HCl pH 7.4: Tris (2-amino-2-hydroxymethyl-1,3-propanediol) dissolved in dH<sub>2</sub>O and brought to pH 7.4 with concentrated HCl, dH<sub>2</sub>O, autoclaved and stored at RT.

1 M Tris/HCl pH 6.8: Tris (2-amino-2-hydroxymethyl-1,3-propanediol) dissolved in dH<sub>2</sub>O and brought to pH 6.8 with concentrated HCl, dH<sub>2</sub>O, autoclaved and stored at RT.

1 M NaCl: NaCl were dissolved in dH<sub>2</sub>O. Autoclaved and stored at RT.

10% (w/v) sodium deoxycholate: sodium deoxycholate was dissolved in dH<sub>2</sub>O. Stored at -20°C.

10% (w/v) SDS (Sodium Dodecyl Sulfate): Sodium Dodecyl Sulfate was dissolved at 37°C in 100 ml dH<sub>2</sub>O. Stored at RT.

200 mM NEM (N-Ethylmaleimide): For every use, 25 mg N-ethylmaleimide were freshly diluted in 1 ml dH<sub>2</sub>O. Do not prepare a stock solution, as NEM is highly unstable. NEM powder is stored at 4°C.

10x Roche Cocktail: One tablet was dissolved in 1 mL dH<sub>2</sub>O. Aliquots were stored at -20°C.

1000x PMSF: PMSF were dissolved in MeOH. Aliquots were vacuum-dried and stored at 4°C. When needed, the dried pellet was resuspended in DMSO. Diluted aliquots were stored at -20°C.

5% (w/v) CHAPS: CHAPS were dissolved in dH<sub>2</sub>O. Aliquots were stored at -20°C.

0.5 M DTE: DTE were dissolved in dH<sub>2</sub>O. Aliquots were stored at -20°C.

Protein A Magnetic Beads: Protein A magnetic beads 6MB was purchased from GE Healthcare.

### **3.10.15 Immunoprecipitation of the protein by Crosslink method**

Protein A or protein G beads were equilibrated with TBST (1xTBS + 0.04% Triton X-100), two times, and 10 min on a turning wheel at 4°C. 1 mL of TBST was added to the equilibrated beads. 15µL of purified TOL6 antibody or anti GFP antibody was added to the beads and incubated overnight on a turning wheel at 4°C at 12rpm. On the following day beads with antibody, were washed three times briefly with 1mL TBST and crosslinked as following: A coupled beads were washed three times briefly with 1 mL 0.2M Na-borat, pH 9.2. Freshly made 1 mL DMP (20mM DMP in 0.2M Na-Borat pH 9.2) were added to the beads and incubated for exactly 30 min at RT. The crosslinking reaction was stopped by washing with 0.2M Tris-HCL, pH 8.0, two times, 10 min, at RT. The beads were equilibrated with 1 mL TBST two times, 10 min at RT. Afterwards the non-crosslinked antibodies were removed by washing briefly with 0.1M glycine, pH 2.0 two times at RT. The beads were equilibrated by washing briefly with 1 mL TBST three times at RT. Approximately 1 mL of protein extract (100 mg protein per 100µL beads) were added to the crosslinked and coupled beads. Immunoprecipitation was carried out overnight at 4°C

on a turning wheel at 12rpm. Next day, the supernatant was removed and the beads washed briefly, with IP buffer containing detergents (0.1% sodium deoxycholate and 0.5% Triton X-100, see table 17), five times, followed by washing with IP buffer without detergent three times. For elution of the antibody - protein complex from Protein A/G magnetic beads, 70µL of 1x laemmly buffer were added to the beads and incubated in a heat block at 98°C for 10 min. Afterwards, tubes were settled in the magnetic rack and the supernatant transferred into a fresh tube. Samples were either directly subjected to SDS-UREA-PAGE or stored at -20°C.

**Table 17 Preparation 50mL IP buffer**

IP buffer	Stock concentration	Per 50ml
20mM Tris-HCL, pH 7.5	1M	1 mL
150mM NaCl	2.5M	3mL
10% glycerol	70%	7.1mL
2mM EDTA	0.5M	0.2mL
0.1% sodium deoxycholate	10%	0.5 mL
0.5% Triton X-100	20%	1.25 mL

1M Na-Borat: 61.83g boric acid, 10g NaOH dissolved in ddH<sub>2</sub>O and brought to pH 9.2. (Na-Borate solution forms crystals; microwave to redissolve, then cooled at RT. 0.2M Na-Borat pH9.2 solution was prepared prior to use.

20mM DMP (Dimethyl pimelimidate dihydrochloride Sigma D 8388): 5.2 mg/mL in 0.2M Na-borat pH 9.2. for 5 mL – 26g DMP dissolved in Na-borat up to 5 mL. DMP is highly moisture-sensitive; was taken out from -20°C freezer 30 min before use to equilibrate to RT.

### **3.10.16 Immunoprecipitation out of total soluble and membrane fraction protein using crosslinking method**

This protocol for immunoprecipitation out of the total soluble and membrane fraction was published as part of a book chapter in book entitled “Root Development”, which is part of the protocol series "Methods in Molecular Biology", published by Springer Protocols:

*Immunoprecipitation of Membrane Proteins from Arabidopsis thaliana Root Tissue.*

Waidmann S, **De-Araujo L**, Kleine-Vehn J, Korbei B.

*Methods Mol Biol.* 2018;1761:209-220. doi: 10.1007/978-1-4939-7747-5\_16.

### **3.10.17 Protein extraction from plants and immunoprecipitation of TOLs using anti-GFP microbeads**

To pull down the Venus tagged TOLs proteins of the total protein extracts was used anti-GFP coupled microbeads.

All steps were carried out on ice and in a cooled centrifuge. Seedlings from 6-8 DAG were used. At least 1g (distributed in 4-5 tubes with about 250 mg each) of plant material was harvested in 2 mL Eppendorf safe lock tubes, containing 2 of 4mm metal beads and frozen in liquid nitrogen. Plant material was homogenized in a Retsch mixer mill MM200 for one minute, with the amplitude set at 30. After milling, the samples were again frozen in liquid nitrogen. 1x RIPA Buffer (lysis buffer) was added to the grinded plant material and vortexed to quick thawing of the buffer. For 1 mg of plant material was used 2μL of RIPA buffer. After thawing, the metal beads were removed with a stir bar retriever. Sample was incubated at 4°C on a vibrax shaker at 1600rpm for 1h and then centrifuged for 5 minutes at 13000 rpm, at 4°C. The supernatant from the same sample transferred to a new falcon tube and mixed well. 50μL of lysate were transferred to a new Eppendorf tube for analysis. Afterwards 50μL of Anti-GFP coupled Microbeads was added to the falcon tube with lysate and incubated for 30 minutes on ice to allow the formation of the Protein-tag-antibody complex. The μColumn was placed on μMACS™ separator and 200μL of lysate (RIPA) buffer applied to equilibrate the column. The sample lysate was applied onto the center of the column and let it run through by gravity flow. The column was washed with 200μL of wash buffer with detergent 4 times or more and then washed with 100μL of wash buffer without detergent 1 time. During the washing steps, 75μL of lysis buffer was boiled at



## MATERIAL AND METHODS

95°C. 20µL of boiled laemmly buffer was applied onto the center of the column and incubated for 5 minutes. A new 1.5 mL Eppendorf tube was placed under the column to collect the eluate. After 5 minutes, 50µL of boiled laemmly buffer were applied onto the center of the column and the eluate was collected. The samples were frozen at -20°C or directly loaded on SDS-PAGE.

## 4 RESULTS

### 4.1. Affinity purified anti-TOL6 antibody recognizes endogenous and transgenic TOL6

It was already demonstrated that, the TOL proteins work as a molecular players in the first steps in the protein degradation of ubiquitinated PM proteins in plants (Korbei et al., 2013). In order to characterize further the interaction between the endogenous TOLs and other proteins, we wanted to obtain a functional TOL antibody. I started with one of the members of the TOL family, specifically TOL6, which was shown to be more similar to the TOM1L1 which works as an alternative of ESCRT-0 complex in mammalian (Blanc et al., 2009; Puertollano, 2005; Richardson and Mullen, 2011; Wang et al., 2010).

For TOL6 antibody production we needed to obtain a purified ectopically expressed full length TOL6 protein for immunization of the rabbits. Full-length TOL6 protein with a C-terminal His-tag, was bacterially expressed, purified, and sent to the Center for Biomedical Research, Department of Laboratory Animal Science and Genetics, Medical University Vienna, Austria, where it was injected into two different rabbits. After having the serum back in our lab, I purified it with denatured antigen (TOL6::6xHis) immobilized on western blot nitrocellulose membrane. Afterwards, I tested the affinity purified TOL6 antibodies as well as the non-purified TOL6 serum in different plant lysates like Col0, the TOL6 T-DNA insertion plant line *tol6-1*, two different translational reporter lines *pTOL6::TOL6:mCherry* in *tol6-1* and a translational reporter line with a point mutation in the ubiquitin binding domain *pTOL6::mTOL6:mcherry* in *tol6-1* (Fig 9). Figure 9A shows a western blot from total plant lysates of the mentioned plant lines separated with SDS-PAGE and probed with the non-purified TOL6 serum. There is a clear and specific band at approximately 100kDa for the endogenous TOL6 protein in the wild type plant lysate (Fig 9A; open arrow head), which is missing in all the *tol6-1* plant lines. Also, for the transgenic TOL6:mcherry a specific band was shown at approximately 130kDa (Fig 9A; arrow head), as well as the mutated TOL6:mcherry (mTOL6:mcherry in *tol6-1*). Nevertheless, there were also several unspecific bands in the western blot incubated with non-purified TOL6 serum. To reduce the background signal, I boiled the nitrocellulose membrane with the same sample after

blotting and before blocking to test if the unspecific bands could be diminished. The results showed a clear reduction of the unspecific bands after boiling the membrane with the signals for the endogenous and the ectopically expressed transgene still giving prominent signals (Fig 9B, open and closed arrow head), yet some unspecific bands still remained. In addition, I probed the same samples with the affinity purified anti-TOL6 antibody and the results showed that almost all unspecific bands were now removed, while the signals of the endogenous and ectopic TOL6 protein are still clearly discernable (Fig 9C, open and closed arrow head). All this results together showed that, the affinity purified anti-TOL6 antibody not only recognizes the full length endogenous TOL6 in the Columbia ecotype wild type *Arabidopsis thaliana* (Col0), but also the reporter constructs expressed in *tol6* null background (*TOL6:mCherry* in *tol6-1*). As expected there was no signal detected in the *tol6-1* null background (plant lines lacking TOL6). The affinity-purified anti-TOL6 antibody was then used for further western blot detection but also for immunoprecipitation experiments.

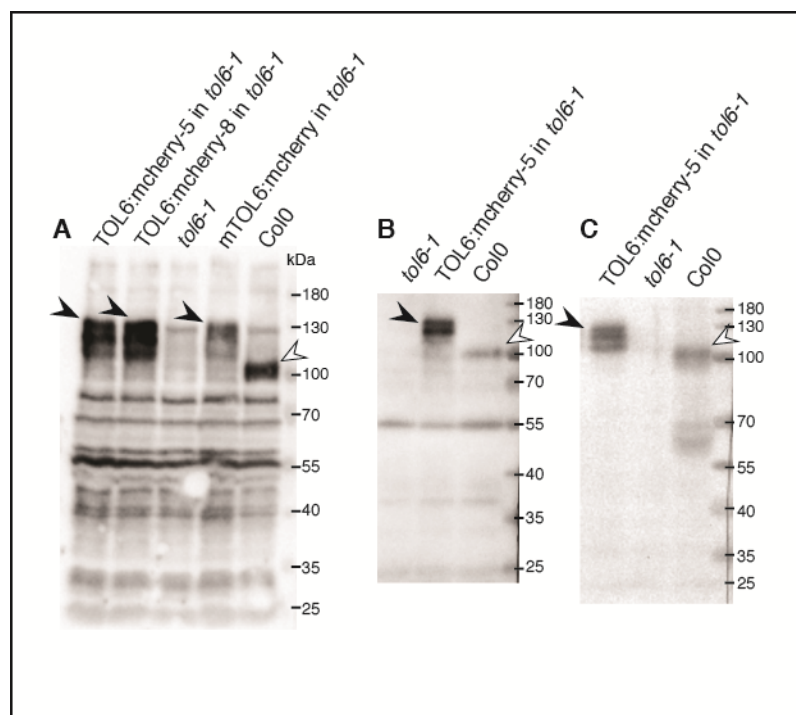


**Figure 9 Western blot of plant lysates with anti-TOL6 serum** : Total protein extracts from *tol6-1*, *TOL6p::TOL6:mCherry* in *tol6-1*, *TOL6p::mTOL6:mCherry* in *tol6-1* and Col0 probed with (A) non-purified anti TOL6 serum (B) non-purified anti TOL6 serum and the membrane was boiled after transfer (C) Affinity purified anti TOL6 antibody (endogenous TOL6 is indicated with an open arrow head and TOL6:mCherry with an closed arrow head).

## 4.2. Expression of TOL protein in planta □

The TOL proteins, which contain two conserved ubiquitin binding domains (UBDs), function as an alternate to the ESCRT-0 complex in plants in recognition of ubiquitinated cargo destined for degradation (Korbei et al., 2013). TOL proteins are a family of nine proteins (TOL1-9) described in *Arabidopsis thaliana*, which recognizes ubiquitinated cargo at plasma membrane and sort them to the ESCRT machinery to ensure their vacuolar targeting for degradation (Korbei et al., 2013). The detailed mechanism, expression, function and distributions of the TOL proteins are still unresolved. As we already have a functional antibody for TOL6 we further wanted reporter constructs for not only TOL6 but also other TOL family members in order to analyze the TOL family members *in planta*. I therefore cloned the TOL expression cassettes, composed of TOL cDNA constructs expressed under their own promoter, into binary vectors with C-terminal Venus-tag. I started with TOL1, TOL5 and TOL6 as well as *tol6<sup>mTOTAL</sup>*, which is a TOL6 construct with both UBDs mutated (see section 4.5.1).

I transformed these constructs into a single knockout specific *tol* plant line and in Col0 lines. I also performed complementation assay by transforming the same constructs into a *tolQ* plant lines lacking five different TOLs (*tol2-1/tol2-1*, *tol3-1/tol3-1*, *tol5-1/tol5-1*, *tol6-1/tol6-1*, *tol9-1/tol9-1*), to access the functionality of the reporter constructs. These lines were used to demonstrate potentially rescue of the severe and pleiotropic *tolQ* phenotype (Korbei et al., 2013).

To continue analyzing the TOL family proteins, I performed western blot experiments using the total plant lysate to evaluate expression levels and the stability of the fusion proteins in transgenic plants. For that, I used an anti-GFP antibody (for Venus-Tag) as well as where applicable the affinity purified anti-TOL6 antibody.

As can be seen in figure 10, I checked the expression levels of several different TOL reporter lines like: *pTOL1::TOL1:Venus* in *tol1-1*, *pTOL3::TOL3:Venus* in *tol3-1*, *pTOL5::TOL5:Venus* in *tol5-1*, *pTOL6::TOL6:Venus* in *tol6-1* and for mutated TOL6, *pTOL6::tol6<sup>mTOTAL</sup>:Venus* in *tol6-1* constructs. For this, I used a total plant lysates, separated it by SDS PAGE and detected via western blot transfer and immunoblot analysis.

The results showed the expression of TOL1:Venus characterized by a specific strong band expressed slightly higher than the expected 73.8 kDa [TOL1(45kDa) +Venus (28,8kDa) = 73,8kDa], which can be seen clearly in figure 10A (left panel). The TOL5:Venus expressed slightly higher than TOL1 showed a specific and strong band also slightly higher than the expected size 78.8kDa [TOL5 (50kDa) +Venus(28.8kDa)=78.8kDa]. The TOL3:Venus protein also ran at slightly higher value than the expected size of 84.8kDa [TOL3 (56kDa) +Venus (28.8kDa) = 84.8kDa] (Fig. 10A, right panel). Similar to TOL1 and TOL5, TOL6:Venus also ran slightly higher than the expected size of 103.8kDa [TOL6 (75kDa) +Venus (28.8kDa) =103kDa] and the same was true for the mutated TOL6 *tol6<sup>mTOTAL</sup>:Venus*, which showed a specific and strong band at a slightly higher value than the expected 103kDa (Fig. 10B, right panel). Furthermore, for TOL6:Venus and *tol6<sup>mTOTAL</sup>:Venus* proteins both in *tol6-1* background, in addition to anti-GFP antibody, I also used affinity purified anti-TOL6 antibody to detect the expression levels of TOL6 proteins (Fig. 10B) and the same bands, which run slightly above calculated size can be observed.

These small differences in the expected, calculated and actual size can either be due to differences in the posttranslational modifications or do to the differences in how these proteins run in the semi native SDS-PAGE Gels.

Additionally, I compared the mutated TOL6:Venus (*tol6<sup>mTOTAL</sup>:Venus*) in *tol6-1* background with *tol6<sup>mTOTAL</sup>:Venus* in Col0 background using anti-GFP antibody and affinity purified anti-TOL6 antibody to check for the endogenous TOL6 in Col0 as well (Fig. 10C). A clear single bands can be seen for the ectopic *tol6<sup>mTOTAL</sup>:Venus* in *tol6-1* and in Col0 lines with both antibodies and in the plant line *tol6<sup>mTOTAL</sup>:Venus* in Col0 a second band, which corresponds to the endogenous TOL6 can be seen as well when, using the affinity purified anti-TOL6 antibody (Fig. 10C; left panel). This band was not detectable when using the anti-GFP (Fig. 10C; right) antibody. This suggest that the affinity purified TOL6 antibody recognizes both the endogenous TOL6 and the transgene, while the GFP antibody clearly and reproducibly recognized all the TOL-Venus tagged proteins.

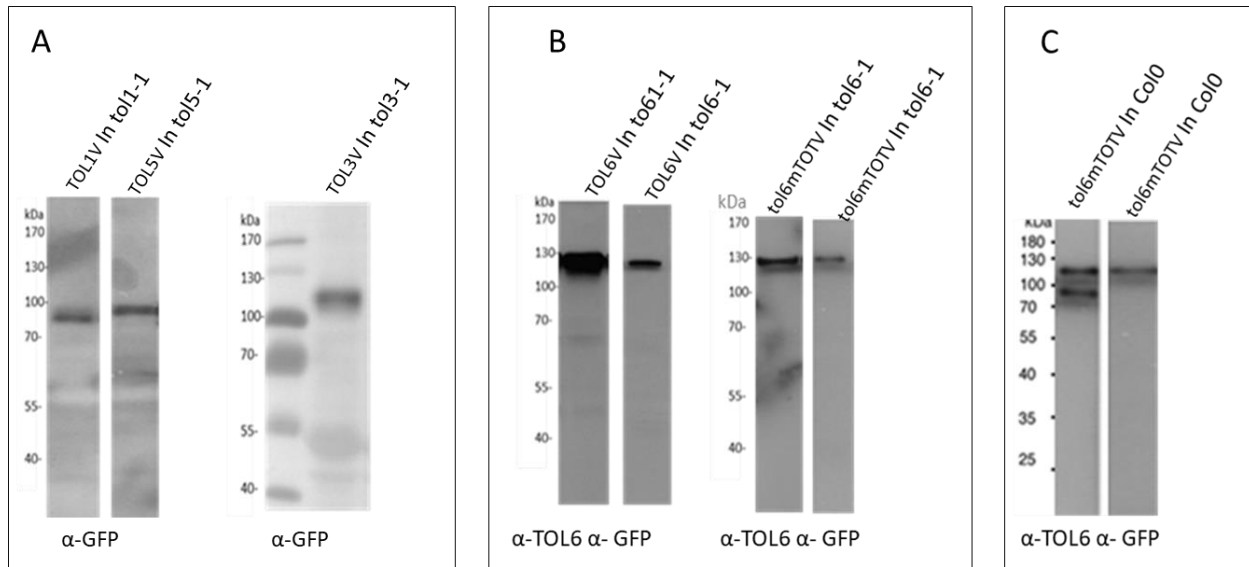


**Figure 10 TOL proteins expression: expression of transgenic TOL proteins in a single knockout plant lines**

: A crude precleared of 6 days old seedling extract was separated by SDS-PAGE and subjected to immunoblotting using the indicated antibodies. **(A)** Left panel: *pTOL1::TOL1:Venus* in *tol1-1* followed by, *pTOL5::TOL5:Venus* in *tol5-1*. Right panel: *pTOL3::TOL3:Venus* in *tol3-1*. Detected with  $\alpha$ -GFP antibody. **(B)** Left panel: *pTOL6::TOL6:Venus* in *tol6-1* using the affinity purified anti-TOL6 antibody for detection and anti-GFP antibody. Right panel: *pTOL6::tol6mTOTAL:Venus* in *tol6-1* using the affinity purified anti-TOL6 antibody for detection and anti-GFP antibody. **(C)** *pTOL6::tol6mTOTAL:Venus* in Col0 using the affinity purified anti-TOL6 antibody (left) and anti-GFP antibody (right) for detection.

### 4.3. TOL proteins have different subcellular localization in plant

The ESCRT machinery in plants seems to be localized earlier in the endosomal system, differently to the animals and yeast (Korbei et al., 2013; Scheuring et al., 2011). Although the exact localization of the initial interactions between ESCRT machinery and ubiquitinated proteins is not clear, as well as the exact localization of some of the TOL proteins, which substitute the function of ESCRT-0 in plants (Korbei et al., 2013; Nagel et al., 2017). To assess the localization of each TOL proteins, I performed localization analysis for at least four different TOL proteins (TOL1, TOL3, TOL5 and TOL6) with fluorescent protein reporter constructs. The subcellular localization of the TOL proteins was assessed by Confocal Laser Scanning Microscopy (CLSM) as well as by cellular fractionation. For cellular fractionation, I separated the cytoplasmic and membrane fraction of total plant cell lysates (Leitner and Luschig, 2014). For this, I used a high-

density buffer, which allow the precipitation of total membrane fraction in a single step and then further precipitation of the total cytoplasmic fraction (Leitner and Luschig, 2014). The protein localization, if it was found in the soluble or the membrane fraction was determined by SDS-PAGE followed by western blotting probed with anti-GFP antibody or with affinity purified anti-TOL6 antibody.

The subcellular localization of the *TOL1:Venus* in *tol1-1* reporter in root epidermal cells of 6 days old seedlings, analyzed by CLSM showed that TOL1:Venus is found mostly in the cytosol but also at the PM (Fig.11, top first panel). This is also reflected in the subcellular localization, where TOL1 is distributed in both fractions with predominant concentration in the soluble fraction and less in the membrane fraction (Fig. 11, bottom first panel). This is in agreement with the localization data for TOL1:cherry, which we published previously (Korbei et al., 2013).

Next, I accessed the localization of TOL3, which in 6 days old root epidermis cells was present predominantly in cytoplasm and found less at the plasma membrane (Fig. 11, top second panel). Similar to the confocal data, the TOL3 subcellular localization using western blot showed its distribution predominantly in the soluble cytoplasmic fraction with less in the membrane fraction (Fig.11, bottom second panel).

The *TOL5:Venus* in *tol5-1* is localized predominantly in the cytoplasm, with potential localization to endosomal structures (Fig. 11 top, third panel). Similar localization was observed when performed a cellular fractionation using a western blot, where the TOL5 is predominantly at the cytoplasmic fraction (Fig.11, bottom third panel), which also agrees with the localization data for TOL5:cherry, which we published previously (Korbei et al., 2013).

I also analyzed 6 days old seedlings of *TOL6:Venus* in *tol6-1* plant lines, which showed a subcellular localization of TOL6:Venus predominantly at the PM (Fig. 11, top last panel). This was also reflected in cellular fractionation where the TOL6 is localized at membrane fraction (Fig.11, bottom third panel), as published previously for TOL6:mCherry (Korbei et al., 2013).

Taken together these results indicating different subcellular localization of different TOL proteins that point towards potentially different functions of the TOLs in the endosomal

system of plants. At the same time, I could also conclude that, the TOL proteins plays role between the PM and cytoplasm, from where they sort ubiquitinated proteins from PM to the ESCRT machinery.

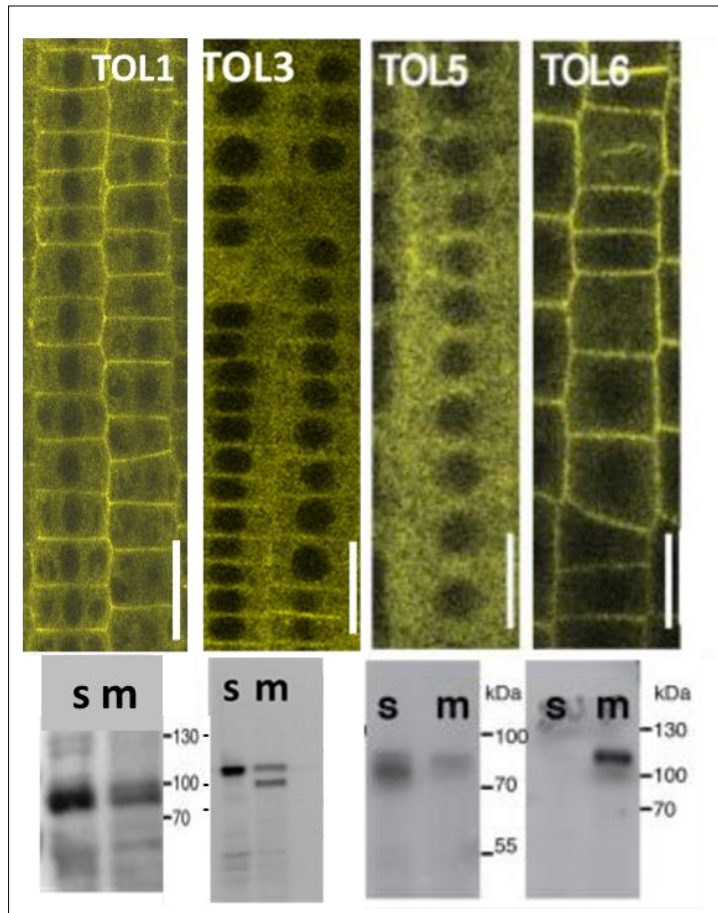


**Figure 11 Subcellular Localization of TOL proteins in planta :** (top) Signal distribution of *TOL1p::TOL1:VENUS* in *tol1-1* (left panel); of *TOL3p::TOL3:VENUS* in *tol3-1* (second panels), of *TOL5p::TOL5:VENUS* in *tol5-1* (third panels) *TOL6p::TOL6:VENUS* in *tol6-1* (last/right panels) in root meristem cells (6 days old seedlings). Scale bars=10 μm. (Bottom) Subcellular fractionation of total protein extracts prepared from roots of seven-days-old seedling from *TOL1p::TOL1:VENUS* in *tol1-1* (left panel); of *TOL3p::TOL3:VENUS* in *tol3-1* (second panels) of *TOL5p::TOL5:VENUS* in *tol5-1* (third panels); *TOL6p::TOL6:VENUS* in *tol6-1* (last/right panels) probed with anti-GFP antibody. Soluble (s) and membrane (m) fraction.

#### 4.4. TOL interaction with phospholipids

The plant PM has a specific electrostatic signature that is driven by PI(4)P and recruits proteins with polybasic sequences (Platre and Jaillais, 2016). Phosphoinositides (PIPs) also recruit coat proteins, such as the Adaptor Proteins (AP) complex involved in Clathrin-coated vesicle formation (Posor et al., 2015). During membrane trafficking, the recognition of ubiquitinated cargo is also regulated by PIPs, that recruit associated adaptors to the appropriate organelle membrane, where for example PIPs lead a ubiquitin ligase to



internal organelle membrane (Dunn et al., 2004). The ESCRT-0 in yeast and mammals recognizes ubiquitinated cargo on early endosomes (Hurley, 2010). The enrichment of endomembrane system of PIP is associated to the early endosomes, via specific PIP binding domain, like the FYVE domain that binds to the PI3P in early endosomes (Katzmann et al., 2003). In plants, the enrichment in the endomembrane system of PIP is different to that of mammals and yeast and therefore FYVE1/FREE1, which contains a FYVE domain does not localize to early endosomes, but to late endosomes where PI3P is accumulated in plant (Platre and Jaillais, 2016).

It was already demonstrated in mammalian and yeast that, the VHS and GAT domain are able to interact with phospholipids (Demmel et al., 2008). Since the TOL proteins have well conserved VHS and GAT domains (Korbei et al., 2013; Sauer and Friml, 2014; Winter and Hauser, 2006), It therefore becomes interesting to investigate if the plants substitute of ESCRT-0 (TOL proteins) also interacts with PIPs. Therefore, I started to determine the interaction of the TOL proteins with phospholipids.

For this propose, I performed an *in vitro* lipid-binding assay with TOL6 and TOL2 proteins representing TOL family. I used the bacterially expressed TOL6:6xHis and TOL2:6xHis to probe a commercially available nitrocellulose membrane spotted with several immobilized phospholipids (PIP-strips: <http://www.echelon-inc.com/index.php>) following the manufactures instructions. The results showed that the TOL6:6xHis bound to phospholipids with acidic head groups, namely phosphatidic acid (PA), as well as to a weaker extend the phosphoinositide phosphates: PtdIns3P, PtdIns4P and PtdIns5P as well as PtdIns(3,4)P2, PtdIns(4,5)P2 (Fig. 12 right). TOL6 did not bind the phospholipids with neutral head groups like phosphatidylcholine (PC) or phosphatidylethanolamine (PE). TOL2:6xHis showed strongest binding to PA (Fig. 12 left). This results suggests that, both TOLs have a strong affinity to phospholipids specifically to the (PA) which indicates that, the TOL proteins might participate in numerous pathways that the PA are involved, like stress response, hormonal pathway and vesicle trafficking (McLoughlin and Testerink, 2013).

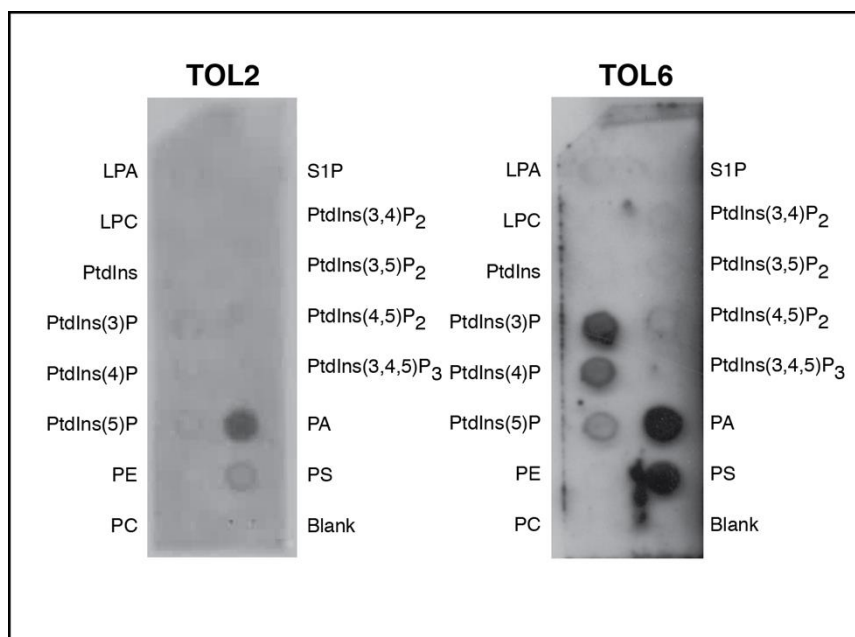


**Figure 12 In vitro lipid binding assay**  
 (A) Purified TOL2:6xHis and (B) purified TOL6:6xHis bind strongly to the phosphatidic acid (PA). TOL6:6xHis also binds to PtdIns3P, PtdIns4P and PtdIns5P as well as PtdIns(3,4)P<sub>2</sub>, PtdIns(4,5)P<sub>2</sub>.

#### 4.5. TOL Interaction with Ubiquitin

The TOL proteins have a crucial function in vacuolar targeting and subsequent degradation of ubiquitinated membrane proteins and TOL proteins contain two well-described and conserved UBDs the VHS domain at N-terminal, followed by a GAT domain (Korbei et al., 2013; Sauer and Friml, 2014; Winter and Hauser, 2006). Besides binding ubiquitin, the VHS domain has also been reported to recognize phosphatidylinositide enriched domains at the PM (Prag et al., 2007). Previously, the interaction of TOL proteins with ubiquitin was tested by *in vitro* binding assay and it was verified that both TOL2 and TOL6 proteins clearly bind to ubiquitin. However, after mutation of ubiquitin at position Isoleucine 44 to an Alanine (I44A) the TOL proteins lost their capacity to bind ubiquitin (Korbei et al., 2013). This finding allowed us to speculate that, the TOL proteins bind to ubiquitin via their two conserved UBDs (VHS and GAT), as those are known to interact with the hydrophobic patch of ubiquitin, centered around I44 (Husnjak and Dikic, 2012). The functional significance of UBDs predicted in TOL proteins is however entirely unknown.

We therefore wanted to assess if the two  $\alpha$ -helical UBDs, the VHS and GAT of the TOL proteins (Winter and Hauser, 2006) behave similar to the ones in mammals and yeast, as these two domains have been demonstrated to be important for binding to ubiquitin (Husnjak and Dikic, 2012).

In the VHS domain, a highly conserved amino acids reported to be important for ubiquitin binding is tryptophan (Hong et al., 2009) at position 26 in the human ESCRT-0 subunit STAM1, which was analyzed using NMR spectroscopy (Hong et al., 2009). Furthermore, it was previously showed that, not only the Tryptophan, but also an Asparagine in the  $\alpha$ -helix of the VHS domain represents highly conserved residue important for ubiquitin binding (Fig. 13 top panel) (Lange et al., 2011). The alignment of the VHS domains of different proteins in plants, mammals and yeast showed that these amino acids are highly conserved, also in the amino acids sequence of all nine TOL proteins (Fig.13 A) (all alignments were done with ClustalW2 - Multiple Sequence Alignment Tool by EMBL-EBI (<http://www.ebi.ac.uk/Tools/msa/clustalw2>)).

There are two ubiquitin binding motifs described in yeast and mammals of GAT domain with the first, formed by the  $\alpha$ -1 helix, being the more conserved one and most important for ubiquitin binding (Prag et al., 2007), while the second one located in the  $\alpha$ -3 helix, is less stringently conserved (Bilodeau et al., 2003). We aligned the amino acid sequences of the GAT domain of different proteins from plants and mammals and found that of the two ubiquitin binding motifs, the first is conserved in all TOL proteins (Fig. 13 B), while the second one is not as conserved.

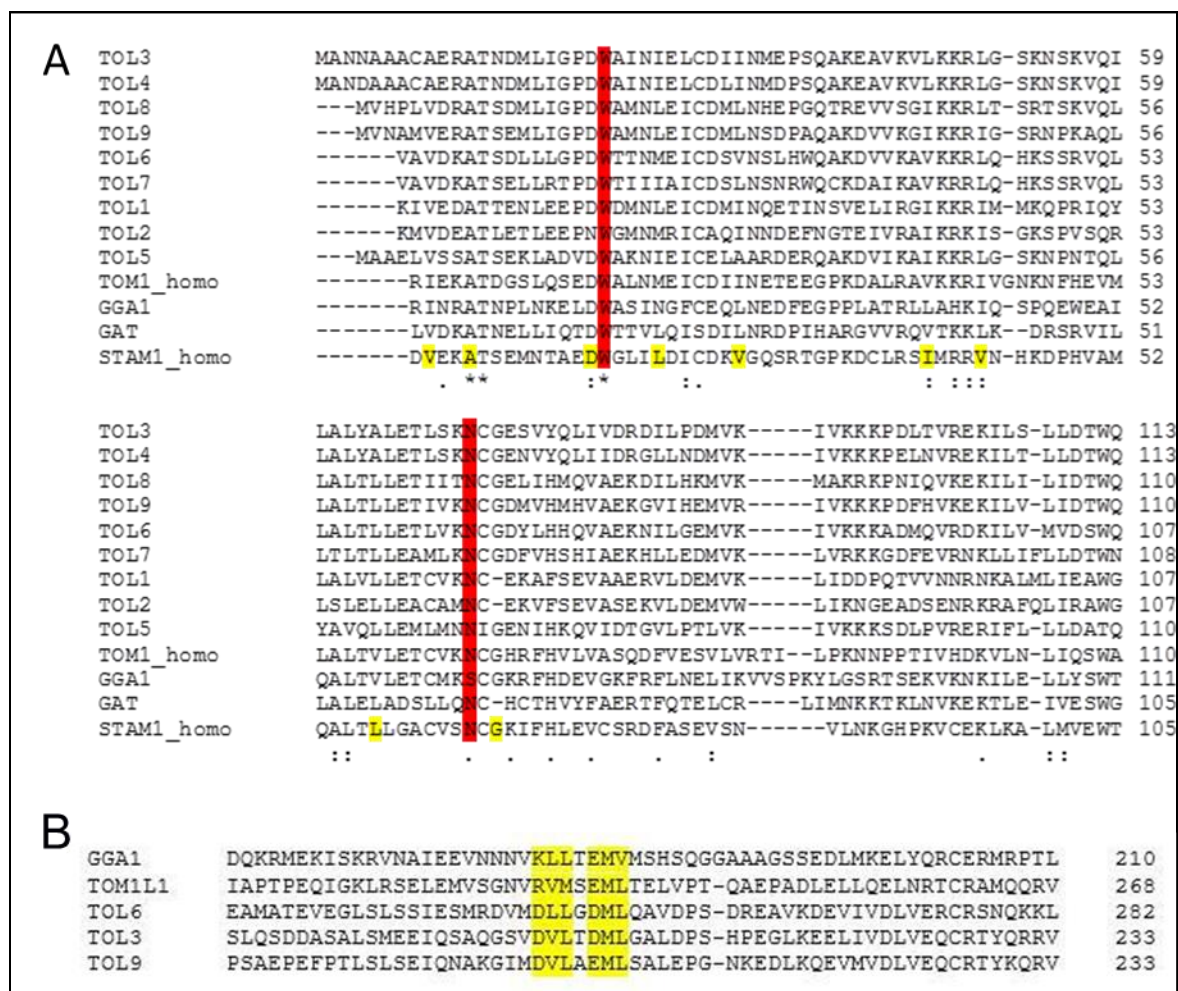


**Figure 13 VHS and GAT domains sequence alignment :** (A) VHS Domain Sequence alignment of TOL1-9 with human TOM1, GGA1 and STAM1, highly conserved amino acids Trp (tryptophan, W) and an Asn (asparagine, N), important for ubiquitin binding highlighted in red Alignment of TOL proteins and ESCRT-0 orthologues: VHS domain between 5-144 amino acids, most conserved amino acids within the alignment were marked in red. (B) GAT Domain sequence alignment of TOL proteins and mammalian orthologues: amino acids 246-252 represent the conserved part of the GAT domain, sequences important for ubiquitin binding marked in yellow. Alignment done with ClustalW2 - Multiple Sequence Alignment Tool by EMBL-EBI (<http://www.ebi.ac.uk/Tools/msa/clustalw2>).

According to our previous data (data not shown), mutation of only one conserved amino acid (the W26) in the VHS domain, showed no significant difference between the mutated and non-mutated TOL6 with respect to the binding of ubiquitin *in vitro*. In order to investigate the capacity of TOL proteins to bind ubiquitin, I therefore, together with a master student (Christina Artner; Master thesis 2016) added a second mutation to previous mutated *tol6*<sup>W25A</sup> at a second highly conserved amino acid, Asparagine (Asn, N). The mutation was at position 73 in the  $\alpha$ -helix 4 of the TOL6 VHS (Fig. 14 A), which we

mutated to Alanine (N73A), and obtained *tol6*<sup>W25A,N73A</sup> constructs, termed *tol6*<sup>mVHS</sup>. At the same time, we also mutated another important ubiquitin binding domain, the GAT domain (Fig. 14 B). Using site-directed mutagenesis, we mutated the amino acids DLL (246-248) to AAA yielding *tol6*<sup>DLL246-248AAA</sup> and DML (250-252) to AAA yielding *tol6*<sup>DLL250-552AAA</sup> of the GAT domain of TOL6 and once again combined these two mutations (yielding *tol6*<sup>DLL246-248AAA,DLL250-528AAA</sup>), which is referred to as *tol6*<sup>mGAT</sup>. Additionally, we made a third construct with combination of both mutations affecting VHS and GAT to obtain a (*tol6*<sup>W25A,N73A tol6<sup>DLL246-248,DLL250-252AAA</sup>) construct and named *tol6*<sup>mTOTAL</sup> (Fig. 14 C). I used these three constructs to perform *in vitro* binding assay.</sup>

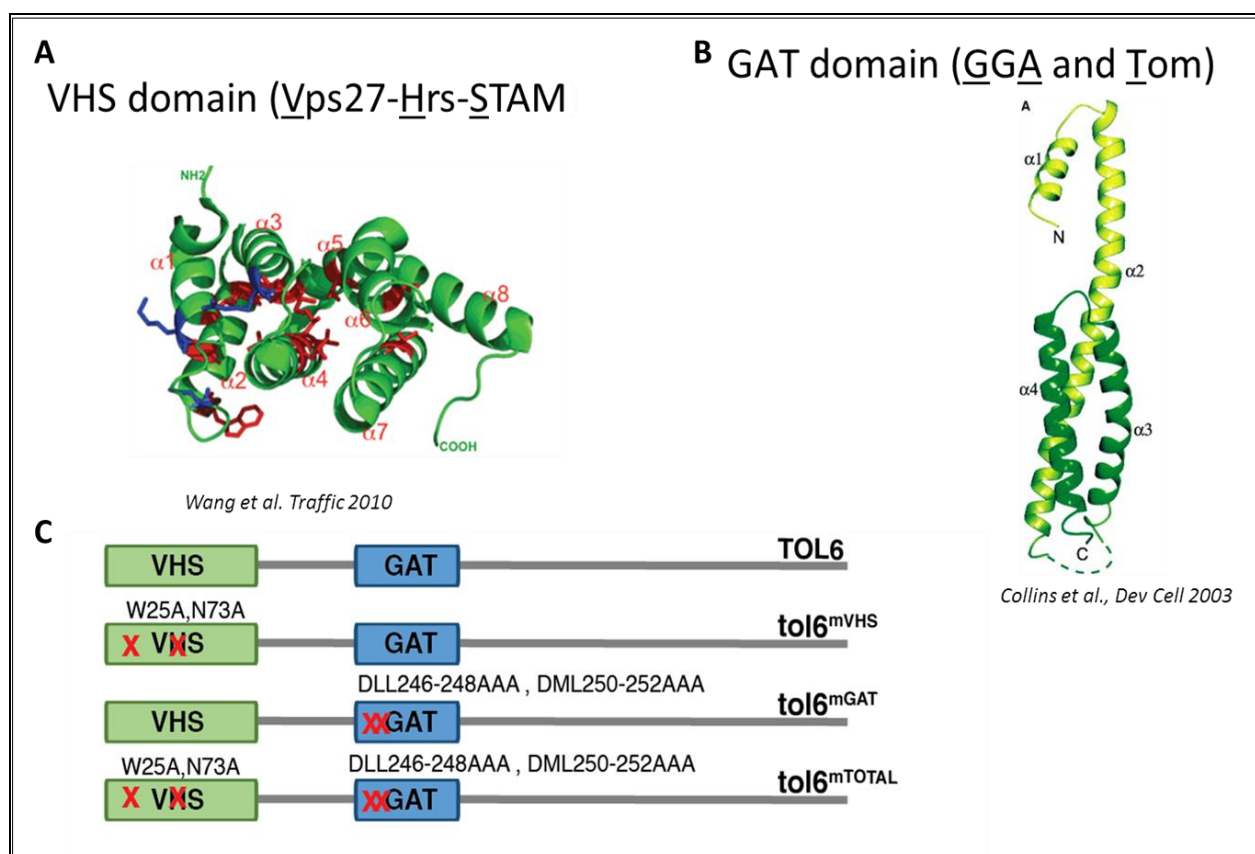


**Figure 14** VHS, GAT domain structure and schematic TOL6 mutations: (A) VHS domain structure. (B): GAT domain structure. (C) *In silico* visualization of TOL6 and the mutated *tol6* alleles from master thesis of Christina Artne.

#### 4.5.1 TOL6 interacts with ubiquitin and alteration of its UBDs interferes with its ability to bind to ubiquitin

For *in vitro* binding assay, I incubated bacterially expressed and purified GST-tagged ubiquitin (or just GST as a control) with glutathione coupled magnetic beads. To these coupled beads bound to the same amounts of GST-ubiquitin (Fig. 15 bottom left panel, open arrowhead) or GST alone (Fig. 15 bottom middle panel, open arrowhead), I added the same amount of bacterially expressed purified His-tagged TOL6 protein or the different His-tagged tol6 mutant proteins (Fig. 15 top right panel, arrowhead). I analyzed the co-precipitation of different constructs of TOL6 by SDS-PAGE and stained with either Coomassie (Fig. 15, bottom panels) for the total protein content or western blots and probed with anti-His antibody for detection (Fig. 15, top panels). The results showed that His tagged TOL6 binds to ubiquitin coupled to the beads with strong affinity (Fig. 15, top-left panel, first lane). The construct with mutated TOL6 in two amino acids of the VHS domain (Fig. 15, top-left panel, second lane; tol6<sup>mVHS</sup>) similarly to the non-mutated construct, also binds to the beads coupled to ubiquitin. The mutated TOL6 in the GAT domain (Fig. 15, top-left panel, third lane; tol6<sup>mGAT</sup>) showed a clear reduction in the binding to the ubiquitin coupled beads in comparison with the tol6<sup>mVHS</sup> and TOL6 construct. The tol6<sup>mTOTAL</sup> (Fig. 15, top-left panel, fourth lane) showed markedly reduced binding affinity to the ubiquitin coupled beads. All the different TOL6 proteins showed no specific binding to the GST-tagged ubiquitin beads alone (Fig. 15 top-middle panels). These results together show that, TOL6 clearly binds to ubiquitin *in vitro*. This ubiquitin binding to TOL6 is not highly affected when two amino acids from the VHS domains are mutated. However, the mutation of six amino acids in GAT domain reduces strongly the capacity of TOL6 to bind ubiquitin. Similar effect happens when we mutated both domains VHS and GAT domain; the capacity of TOL6 to bind ubiquitin is totally abolished. Taken together these results indicates that TOL6 binds to ubiquitin via two well conserved UBDs (VHS and GAT domains), therefore mutation on these domains abolish the capacity of TOL6 to bind ubiquitin. This demonstrates that the UBDs of TOL6 play an important role in the binding to ubiquitin of ubiquitinated proteins and mutation of the UBDs affect the functionality of TOL6 with respect to its binding capacity of ubiquitin.

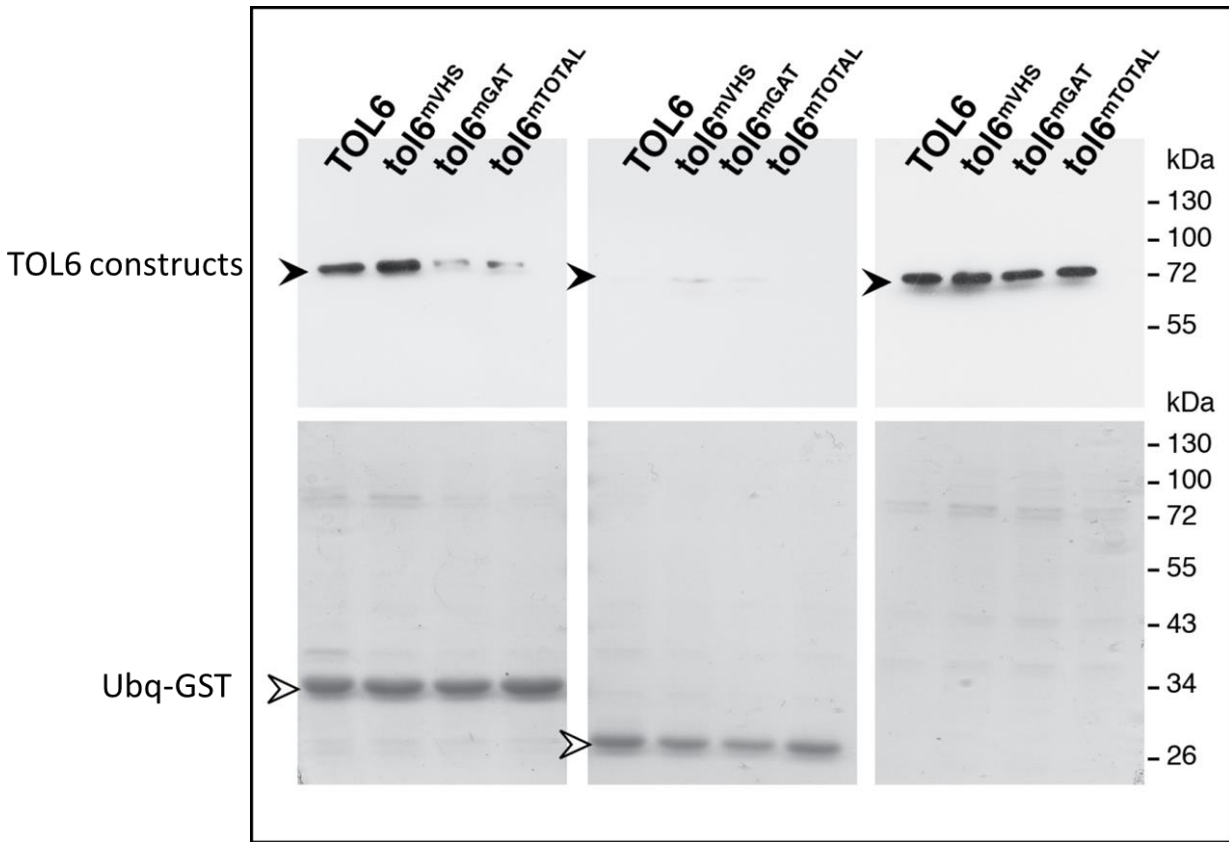


**Figure 15 Typical TOL6 *in vitro* binding assays** : Different TOL6 constructs (TOL6:6xHis, 75 kDa, closed arrow in top panels) were purified and co-precipitated with GST:ubq (34.5 kDa, open arrow bottom left panel) or GST (26 kDa, open arrow bottom central panel) as a control coupled to glutathione magnetic beads. Precipitated proteins were either analyzed by SDS PAGE and Coomassie staining (bottom panels) or were blotted and probed with anti His-antibody (top panels).

#### 4.5.2 Mutations of the UBDs of TOL6 alter the *in planta* localization of TOL6

After demonstrating that the UBD mutated TOL6 (*tol6<sup>mTOTAL</sup>*) lost its capacity to bind to ubiquitin *in vitro*, I also wanted to check if this mutation could also affect the localization of TOL6, when compared with the non-mutated TOL6. In order to verify the localization of different TOL6 alleles *in vivo*, the TOL6 reporters expressed under their endogenous promoter were cloned and transformed in plants. I transformed *pTOL6::TOL6:Venus* and *pTOL6::tol6<sup>mTOTAL</sup>:Venus* into Col0 ecotype (wild type) and in a T-DNA insertion plant line lacking expression of full length endogenous TOL6 (*tol6-1*). As tag I used the fluorescent GFP derived Venus-tag to ensure the detection of transformed proteins expressed in plants.

Subcellular localization of the TOL6:Venus and tol6<sup>mTOTAL</sup>:Venus was assessed with Confocal Laser Scanning Microscopy (CLSM). I also performed cellular fractionation experiments of total plant lysates, that allowed me to verify the protein distribution between soluble and membrane fraction. The subcellular localization of the TOL6:Venus in *tol6-1* reporter in root epidermal cells of 6 days old seedlings, analyzed by CLSM showed that TOL6:Venus is localized at PM (Fig.16A, left). This is also reflected in cellular fractionation, where the TOL6:Venus is localized predominantly in the membrane fraction (Fig. 16 B). Furthermore, the endogenous TOL6 can also clearly be seen in the membrane fraction of the plant lysates from wild type (Col0) (Fig. 16B, left lanes) with a similar distribution to that of the TOL6:Venus transgenic line in *tol6-1* (Fig 16 B, middle lanes).

I performed similar experiments to assess the subcellular localization in root epidermal cells of 6 days old seedlings with the mutated tol6<sup>mTOTAL</sup>:Venus in *tol6-1*. The CLSM showed a striking alteration in the localization of the mutated reporter protein, which unlike to the TOL6:Venus was predominantly in the cytosolic fraction and not at the PM anymore (Fig. 16A, right). This was further confirmed by cellular fractionations experiments, where the protein signal is distributed in both (cytosolic and membrane fraction), but more predominantly in the cytosolic fraction (Fig. 16B, right lanes).

To statistically determine the difference in the localization TOL6 reporter constructs in the *TOL6p::TOL6:Venus* in *tol6-1* and *TOL6p::tol6<sup>mTOTAL</sup>:Venus* in *tol6-1* plant lines I measured the signal intensities of the Venus signal at the PM and in cytosol with image J software and then determined the relative signal intensity between the PM and the cytosolic fraction. These measurements were carried out in root epidermis cells in the meristematic region of 6 days old seedlings. There was a highly significant difference between ratio of the signal intensities in the roots with the non-mutated TOL6 version with respect to tol6<sup>mTOTAL</sup>:Venus (Fig. 16C) indicating that the mutated TOL6 version is more in the cytoplasmic fraction than the non-mutated TOL6, which was also reflected when analyzing the proteins extract from the cellular fractionation experiments. Figure 16D shows that these results are not due to the different expression levels of the *TOL6p::TOL6:Venus* in *tol6-1* and *TOL6p::tol6<sup>mTOTAL</sup>:Venus* in *tol6-1* as they are expressed at similar levels and at the expected sizes when analyzing total plant lysates from both plant lines by SDS-Page and western blot probed with an the purified anti TOL6



antibody (Figure 16D top panel, bottom panel shows a Coomassie stained SDS-PAGE used as normalization control).

Taken together these results indicates that the mutation of both UBDs (VHS and GAT) affects not only the ability of TOL6 to bind ubiquitin but also its localization *in planta*, making the mutated TOL6 localize more in the cytoplasmic fraction.

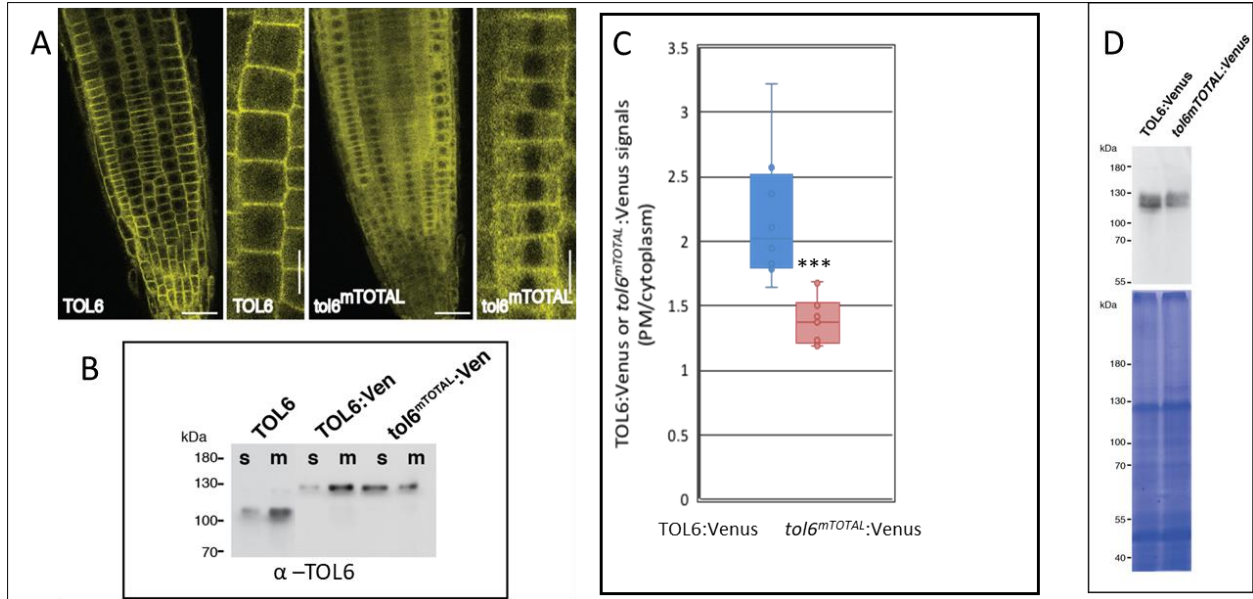


**Figure 16 Signal distribution of TOL6 and mutated TOL6 :** (A) Signal distribution of *pTOL6::TOL6:Venus* in *tol6-1* (left panels) and *pTOL6::tol6<sup>mTOTAL</sup>:Venus* in *tol6-1* (right panels) in root meristem cells (6 days old). Scale bars =10µm. (B) Subcellular fractionation of total protein extracts prepared from roots of seven-day-old seedling: Col0 (TOL6=endogenous TOL6) (left); *pTOL6::TOL6:Venus* in *tol6-1* and *pTOL6::tol6<sup>mTOTAL</sup>:Venus* in *tol6-1* (right), probed with anti-TOL6 antibody. Soluble (s.) and membrane (m.) fraction. (C) Relative signal intensities: *TOL6p::TOL6:Venus* in *tol6-1* and *TOL6p::tol6<sup>mTOTAL</sup>:Venus* in *tol6-1* at the PM at root meristem cells after normalization to cytoplasmic signal intensities (n=number of cells analyzed; n=125 and n=130 respectively; \*\*\*P ≤ 0.001, Student's t-test). (D) **Signal expression:** Expression prepared from total lysate of *pTOL6::TOL6:Venus* in *tol6-1* (left) and *pTOL6::tol6<sup>mTOTAL</sup>:Venus* in *tol6-1* (right).

#### 4.5.3 TOL6 with deficient UBDs is not functional in planta

To continue the investigation of the impact of the mutation of the UBDs of TOL6 on the function of TOL6 *in planta*, I assessed the potential complementation of the construct of the *tolQ* phenotype. For this I transformed the *pTOL6::tol6<sup>mTOTAL</sup>:Venus* as well as the *pTOL6::TOL6:Venus* into a quadruple mutant, which is additionally heterozygous for TOL3 (*tol2-1/tol2-1 tol3-1/TOL3 tol5-1/tol5-1 tol6-1/tol6-1 tol9-1/tol9-1*). I used this plant line because, contrary to the *tolQ* plant line, it can easily be transformed as the *tolQ*

(quintuple plant line lacking expression of TOL2, TOL3, TOL5, TOL6 and TOL9) has very pleiotrophic severe developmental defects (Korbei et al., 2013) and is therefore difficult to transform. While the TOL6:Venus construct could clearly rescue the *tolQ* phenotype characterized by normal development of the 7days old seedlings of TOL6:Venus in *tolQ* (Fig.17A; Top right), similar to the Col0 (Fig.17A top left), the mutated construct (*tol6<sup>mTOTAL</sup>*:Venus) did not rescue the *tolQ* phenotype (Fig. 17A). The *tol6<sup>mTOTAL</sup>* seedlings, characterized by pronounced delays in their development, altered cotyledon formation, (monocots, tricots or fused cotyledons) and short root length demonstrating potential aberrations during embryogenesis (Fig. 17A, bottom right panel). These defects found in the plant line with the mutated constructs, are similar to those described for *tolQ* (Fig. 17A, bottom left panel) plant line (Korbei et al., 2013). 17 days old plants, from TOL6:Venus in *tolQ* showed normal development similar to Col0, demonstrating its capacity to rescue the *tolQ* phenotype (Fig. 17B, first two top panels). On the other hand *tol6<sup>mTOTAL</sup>*:Venus in *tolQ* showed clear defects on rosette leaves formation, with a smaller rosette size and with pronounced delays in development (Fig. 17B, last panel) similar to *tolQ* (Fig. 17B, third panel). In mature plants, while the TOL6:Venus in *tolQ* showed a normal development similarly to the wild type plants (Fig. 17C, first and second pot), the mutated constructs (*tol6<sup>mTOTAL</sup>*:Venus) plant lines are dwarfed, delayed in flowering with anomalous inflorescences (Fig. 17C, fourth pot), similar to the defects in the *tolQ* plant lines (Fig. 17C, third pot) (Korbei et al., 2013).

All these alterations in the *pTOL6::tol6<sup>mTOTAL</sup>:Venus* in *tolQ* plant line, illustrates defects potentially during embryogenesis and development process in plant similar to the defects shown in *tolQ* plant line (Korbei et al., 2013) indicating that the *tol6<sup>mTOTAL</sup>* fails to full rescue the *tolQ* phenotype. Taken together, this indicates that the mutation of the UBD affects not only the capacity of TOL proteins to bind ubiquitin, but also interferes with the sorting mechanism to the ESCRT machinery for further vacuolar degradation thus yielding such a pleiotrophic phenotype, underlining the importance of UBDs for the functionality and localization of the TOL proteins in plants.

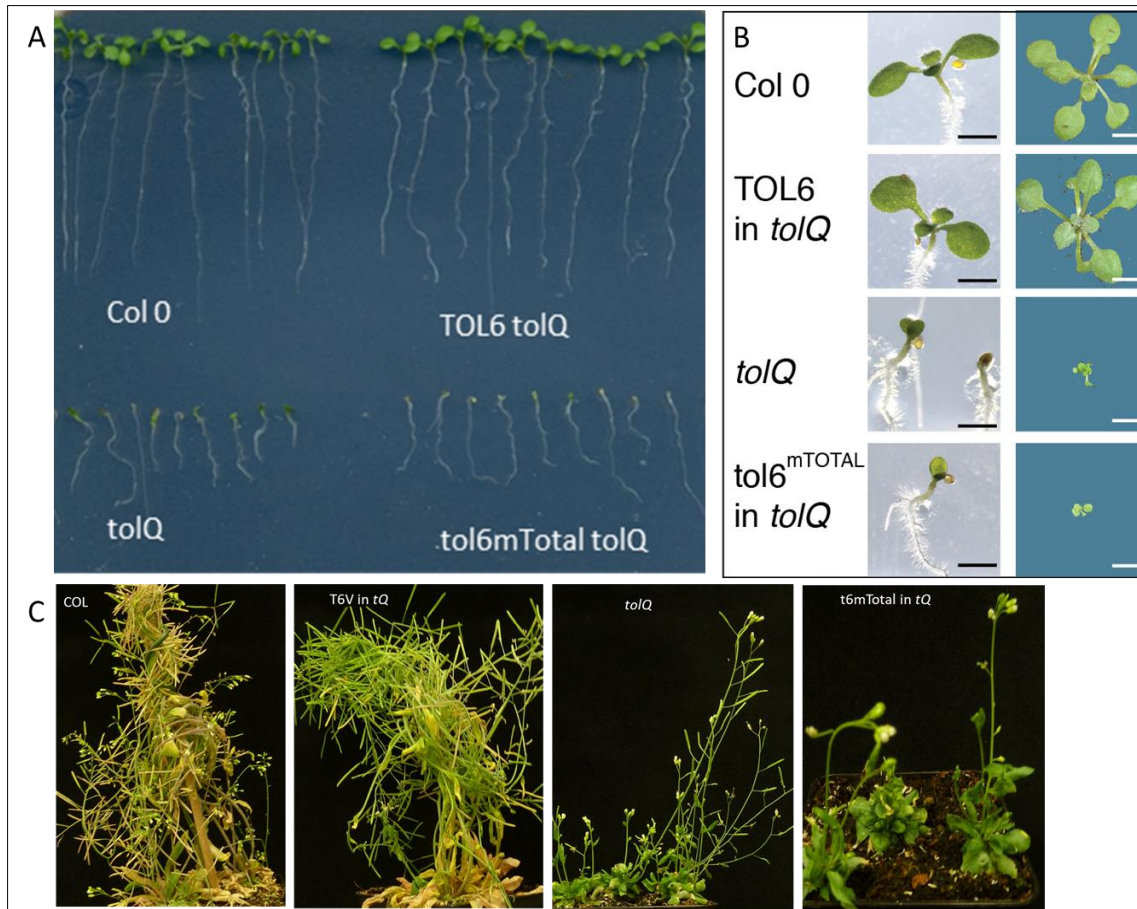


**Figure 17 Rescue of *A.thaliana* tolQ :** (A) Phenotypic analysis of plants expressing *TOL6:Venus* or *tol6mTOTAL:Venus* in *tolQ* background potentially complementing the *tolQ* phenotype (using Col0 as control) in 7 days old seedlings. (B) Phenotypic analysis of plants expressing *TOL6:Venus* or *tol6mTOTAL:Venus* in *tolQ* background potentially complementing the *tolQ* phenotype (using Col0 as control) in 7 days old seedlings (left panel), Scale bars =2mm and 17 days old rosettes (right panel) Scale bars =5mm. (C) Phenotypic analysis: of plants expressing *TOL6:Venus* or *tol6mTOTAL:Venus* in *tolQ* background, potentially complementing the *tolQ* phenotype (using Col0 as control) demonstrating the effect of altered functionality in mature plants.

#### 4.5.4 Mutation of TOL6 UBD affects plant development

I already demonstrated the impact of deficient UBD of TOL6 for the functionality and localization of the TOL6 proteins, where the mutated TOL6 fails to full rescue the *tolQ* phenotype. We then wanted to investigate what happen in plant development, when the ubiquitin binding deficient TOL6 is transformed in *tol6-1* null background. I therefore followed the plant development of the plant lines *TOL6:Venus* in *tol6-1*, *tol6mTOTAL:Venus* in *tol6-1*, *tol6-1* and wild type (Col0 ecotype) (Fig. 18A).

I separated the root length of 7 days old seedlings in three different categories to include variations in the growth of seedlings: very small from 0cm up to 1cm (short roots→

abnormal root development); from 1 cm to 3.4 cm (regular roots → normal root development) and longer than 3.4 cm (long roots). In this experiment, the Col0 plant lines has an average of 3.4 cm  $\pm$  1.2cm. Based on that, I considered all the roots with more than 3.4cm as a long roots, the roots with less than 1cm considered as abnormal root, and roots from 1cm to 3.4 cm considered as regular roots. Statistical analysis demonstrated that, approximately 30% of *tol6-1* roots were abnormal (in short roots category) (Fig. 18B). Similar phenotype was observed for *tol6<sup>mTOTAL</sup>:Venus* in *tol6-1*, while none of the wild type or the non-mutated TOL6:Venus (Fig. 18B ) showed this phenotype. This reveals that, single knockout *tol6-1* might have defects that are not phenotypically very pronounced and when the deficient UBD construct (*tol6<sup>mTOTAL</sup>*) is transformed into the *tol6-1* plant lines, the resulting plant lines shows similar defects.

Morphological plant traits such as size, number of leaves, biomass, and shape are influenced not only by the genes, but also by external environmental factors (Moller-Steinbach et al., 2010). However, the interaction between genes and environmental (and growth) conditions leads to a combinatorial explosion of possible phenotypes, making the understanding of the link between genotype and phenotype a complex task (Houle et al., 2010). Figure 18 C shows growth stage at 35 days old plant from Col0, *tol6-1*, TOL6:Venus in *tol6-1*, *tol6<sup>mTotal</sup> :Venus* in *tol6-1* demonstrating a clear phenotypic difference of *tol6<sup>mTotal</sup> :Venus* in *tol6-1*. Counting the number of leaves in plants is important for plant phenotyping, since it can be used to assess plant growth stages (Telfer et al., 1997). From a phenotyping point of view, the number of leaves in a plant is related to a developmental stage, growth regulation, flowering time, and yield potential (Walter et al., 2015). In order to complement the analysis of the developmental growth, I counted the rosette leaves at the same conditions when the inflorescence stem has 1cm height (Moller-Steinbach et al., 2010) (Fig. 18 D). Statistical analysis, where I compared the number of rosette leaves when they started flowering, showed that, the *tol6-1* plant lines has earlier flowering when compared to Col0 and TOL6:Venus (Fig. 19D). Surprisingly, the *tol6<sup>mTOTAL</sup> V* in *tol6-1* has delayed flowering when compared to Col0 and TOL6:Venus. Thus, *tol6<sup>mTOTAL</sup>* in *tol6-1* has late flowering time while the *tol6-1* has earlier flowering time. This result suggests that, the single knockout *tol6-1* might affect the plant development, but less pronounced. This defect is full rescued by TOL6 full length and not by mutated TOL6 (*tol6<sup>mTOTAL</sup>*). This delay in flowering could be an indirect consequence produced by

dominant negative interference with the function of flowering time genes that affect the developmental stages, growth regulation when associated to deficient UBD of TOL6.

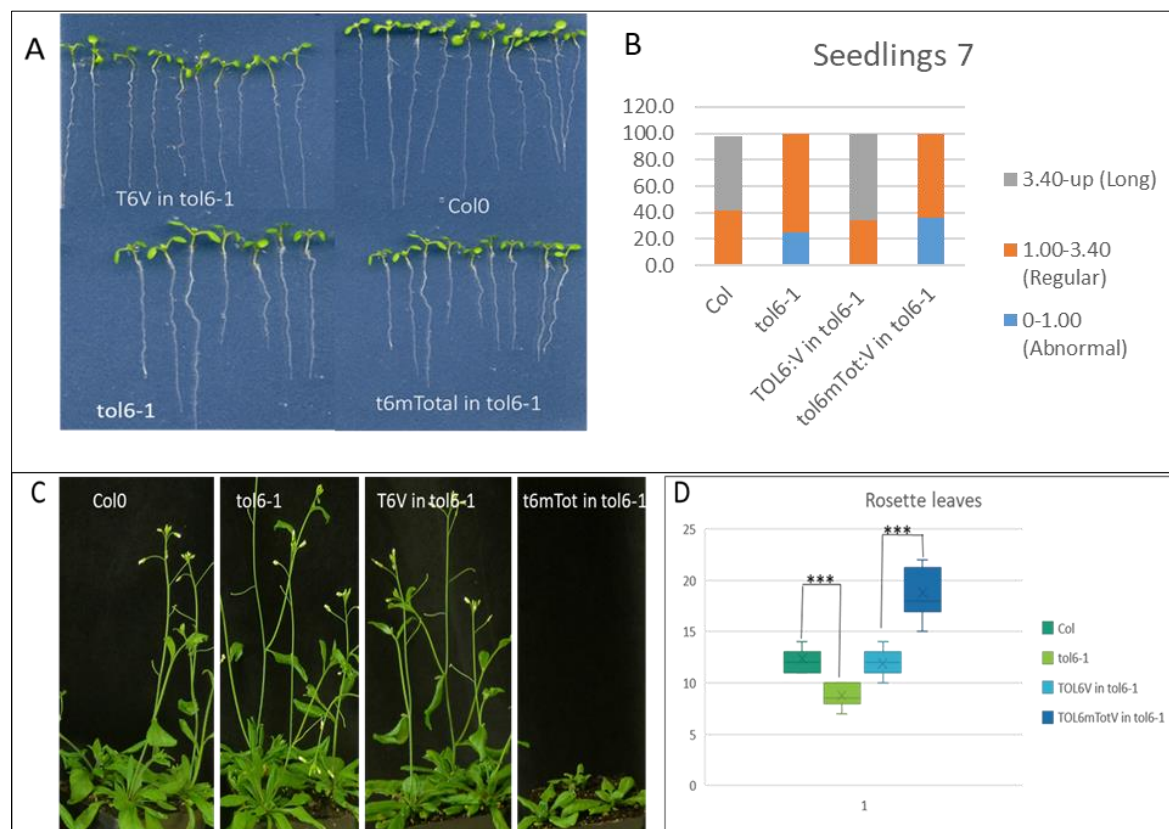


**Figure 18 Mutation of TOL UBD affects the plant development :** (A) Phenotypic analysis of plants expressing *TOL6:Venus* or *tol6mTOTAL:Venus* in *tol6-1* (using Col0 as control) in seedlings at 7days old. (B) Graphic representation of Col0, *tol6-1*, *TOL6V* in *tol6-1*, *tol6mTotal* in *tol6-1* root length of 7 days old separated in three categories. 3.4cm is the average of Columbia in the same conditions. (C) Phenotype of 35 Days old plants of Col0, *tol6-1*, *TOL6:Venus* in *tol6-1*, *tol6mTotal :Venus* in *tol6-1*, showing late flowering of *tol6mTotal* in *tol6-1* (D) Graphic representation of rosette leaves counted after all the plants were flowering showing late flowering of *tol6mTotal* in *tol6-1* and earlier flowering of *tol6-1*.

## 4.6. TOL Proteins are ubiquitinated in planta

### 4.6.1 TOL6 is ubiquitinated *in planta*, specifically in its cytoplasmic fraction

Ubiquitination, or the covalent addition of an ubiquitin molecule to a protein, is an important post-translational protein modification responsible for signaling, proteosomal degradation, reparation of DNA, membrane transport events like endocytosis and cell cycle control (Hurley et al., 2006). Proteins, termed ubiquitin receptors, bind to ubiquitinated cargo via UBDs like the VHS and GAT domains, and then assist in the regulation of the abundance,

the function, the localization and the interactions of the ubiquitinated proteins (Haglund and Stenmark, 2006). Ubiquitin receptors, like the subunits of the ESCRT-0 and ESCRT-I, which function as a recruitment site for ubiquitinated cargo in the sorting machinery of the ESCRT pathway (Klapisz et al., 2002), are known to be ubiquitinated themselves and this ubiquitination seem to affect their function (Hoeller and Dikic, 2010). This process of monoubiquitination of UBD containing proteins is called "coupled monoubiquitination" (Fig. 19) (Hoeller et al., 2006; Kim et al., 2007; Woelk et al., 2006). Ubiquitination of proteins containing UBDs of the endosomal sorting machinery could have several different effects. Ubiquitination could allow for regulation of the abundance of the ubiquitinated subunits of the endocytic sorting machinery a protein by leading to their proteosomal degradation (Husnjak and Dikic, 2012). Furthermore, ubiquitination of subunits could also help in the generation of interactions networks between ubiquitinated proteins and proteins with UBDs, by allowing proteins to reversibly bind each other, which is important for organizing the machinery (Hoeller et al., 2006; Hoeller and Dikic, 2010). Furthermore, coupled monoubiquitination could prevent binding to the ubiquitinated cargo, as the UBD is already occupied either by intra- or by intermolecular ubiquitin binding (Fig. 19) (Hoeller et al., 2006). This has been shown for endocytic components of the mammalian sorting machinery (EPS15, epsin 1 and 2, HRS, STAM), which are subjected to intramolecular binding of their UBDs to monoubiquitin, leading to their inactivation (Blanc et al., 2009). Two of these proteins, HRS and STAM form the mammalian ESCRT-0 complex, whose interaction with ubiquitin is regulated by two well-conserved UBDs the VHS and GAT domain (Dikic et al., 2009; Shields and Piper, 2011). In plants this initial interaction of ubiquitinated PM proteins, is carried out by the TOL proteins, which share the same conserved domains as the ESCRT-0 (VHS and GAT domains) (Korbei et al., 2013). Thus, I wanted to check if the TOL proteins are subjected to the same regulatory mechanism of coupled monoubiquitination as their mammalian counterparts.



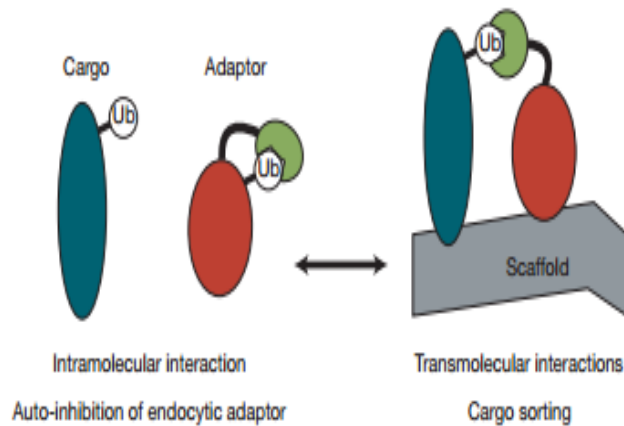


**Figure 19 Coupled Monoubiquitination** : (adapted from (Hoeller et al., 2006) Proposed mechanism of monoubiquitin-mediated regulation of endocytic adaptor proteins: In solution, monoubiquitinated UBD-containing proteins adopt a closed, auto-inhibited conformation due to intramolecular UBD–ubiquitin interactions. This pool of proteins will be inactive with respect to transmolecular binding to ubiquitinated targets; for example, cargo sorting.

To assess if TOL6 protein is ubiquitinated *in vivo*, I performed the immunoprecipitation (IP) experiments, where I precipitated endogenous TOL6 out of wild type (Col0) plant lysates using protein A magnetic beads cross-linked with the affinity purified anti-TOL6 antibody. The precipitates were then separated via SDS-PAGE and detected by western blot using the TOL6 antibody as well as an antibody used for the detecting of ubiquitination. The results showed a strong band for the IP out of the wild type plant lysates at the correct size of TOL6 (Fig. 20A left panel, open arrowhead) and no corresponding band at the expected TOL6 size in the IP out of the TOL6 null plant line *tol6-1* indicating that the IP is specific. I then tested the same IP precipitate with an anti-ubiquitin antibody ( $\alpha$ -UBQ; Fig. 20A right panel) once again using the precipitate out of the *tol6-1* plant line as a negative control. A specific signal for ubiquitin characterized by strong smear and a specific band at TOL6 size was detected in Col0 precipitate (Fig. 20A right panel, arrowhead), which demonstrated that the endogenous TOL6 is ubiquitinated. Unlike Col0, the *tol6-1* IP did not show any smear indicating that the signal is specific for TOL6. These results demonstrate the ubiquitination of endogenous TOL6.

To continue investigation of TOL6 ubiquitination, I precipitated Venus tagged TOL6 out of a *pTOL6::TOL6:Venus* in *tol6-1* background transgenic line with anti-GFP microbeads and used Col0 plant lysates as a negative control. Precipitation of the TOL6:Venus tagged reporter construct out of the transgenic plant lysate showed clear band at correct size of TOL6 (approximately 130kDa) when probed with anti-TOL6 antibody ( $\alpha$ -TOL6; Fig 20B left panel, arrowhead). As expected, the precipitate out of the Col0, wild type, plant lysate

did not show any band at the TOL6 size, indicating that there is no unspecific precipitation of Col0 lysates, when using the anti-GFP microbeads. Next, I used the same precipitate to check for ubiquitination using an anti-ubiquitin antibody ( $\alpha$ -UBQ; Fig 20B right panel). An ubiquitin specific signal at the size of TOL6, as well as a smear were detected only in the IP from the transgenic plant line expressing the TOL6:Venus reporter construct and there was no signal observed in Col0 precipitate demonstrating that the ectopically expressed TOL6:Venus itself is also ubiquitinated (Fig. 20B, right panel, arrowhead).

I went further and performed subcellular fractionation experiments to separate membrane and cytosolic fraction from Col0 and *tol6-1* plant lysates. Out of these fractions I then performed immunoprecipitation using protein A magnetic beads cross-linked to affinity purified anti-TOL6 antibody. The IP showed the TOL6 protein mostly concentrated in the membrane fraction characterized by strong band at the correct size of TOL6 (Fig. 20C, left panel, arrowhead) while less could be pulled down from the cytosolic fraction. This is in accordance with results obtained from the subcellular localization experiments described in section 4.4, where TOL6 was also mainly found in the membrane fraction. The negative control, precipitation out of *tol6-1* plant lines, did not show any TOL6 bands neither in the cytosolic, nor in the membrane fraction. I then used these precipitates to check for ubiquitination by blotting with anti-ubiquitin antibody (Fig. 20C, right panel).

Interestingly, only in the precipitate out of the cytosolic fraction of Col0, where smaller amounts of endogenous TOL6 were precipitated, there was a specific ubiquitination signal, characterized by smear, extending upwards from the predicted size of endogenous TOL6 (Fig. 20C right panel), which can neither be found in the precipitate out of the membrane fraction, where more TOL6 is present. This smear is specific for the TOL6 out of the soluble fraction, as it is also not found in the precipitates out of the membrane and soluble fraction of the lysates from the TOL6 null plant line *tol6-1*. This indicates that, only the cytosolic fraction of TOL6 proteins is ubiquitinated. Taken together these results



demonstrates that the soluble fraction of TOL6 is ubiquitinated while the membrane fraction is not ubiquitinated, even though the TOL6 is more abundant at the membrane.

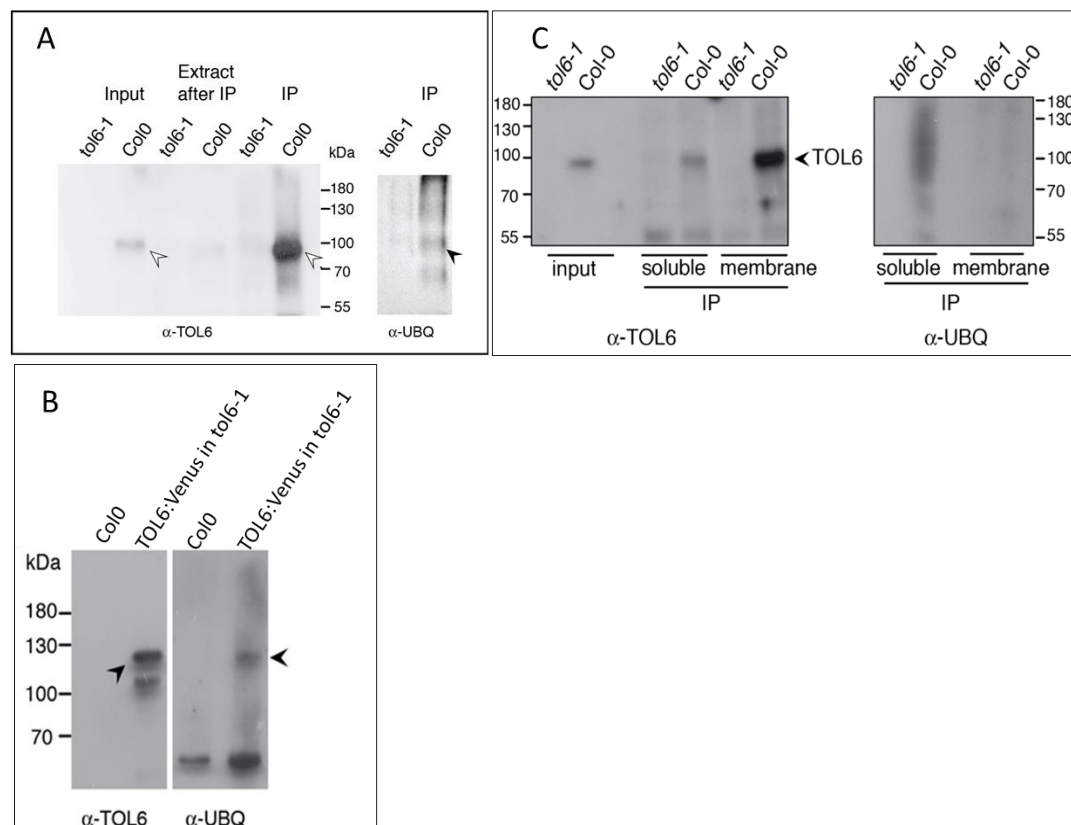


**Figure 20 Immunoprecipitation (IP) of TOL6 :** (Left panel) with protein A magnetic beads coupled to and crosslinked with affinity purified anti-TOL6 serum from *tol6-1* or *Col0* plant extracts. Endogenous TOL6 is clearly visible in the *Col0* lysate as well as after IP and indicated with an open arrowhead. (Right panel) IP probed with an anti-ubiquitin antibody (P4D1). A clear band can be seen in the IP from *Col0*, (arrowhead) which is missing in *tol6-1* control. (B) **Immunoprecipitation of TOL6:** *TOL6p::TOL6::Venus* in *tol6-1* and *Col0* seedlings (6DAG) were used for the IP using anti-GFP coupled microbeads. TOL6::Venus is clearly precipitated while the *Col0* (left panel) when probed with  $\alpha$ -TOL6 antibody. The precipitate probed with  $\alpha$ -Ubiquitin (P4D1) antibody showed a clear band at the same height as TOL6::Venus, demonstrating the ubiquitination of TOL6, which is not visible in *Col0* (right panel). The lower bands corresponds to the antibody. (C) **TOL6 immunoprecipitation out of the soluble and membrane fractions.** IPs were performed from *tol6-1* and *Col0* *Arabidopsis thaliana* root extracts with protein A magnetic beads coupled and cross-linked to affinity purified anti-TOL6 antibody. (Left panel) The left lanes show the input amount, while right lanes represent the eluted protein from the beads. Endogenous TOL6 is clearly visible in the precipitates of both *Col0* membrane and soluble fractions (black arrowhead), which are missing in *tol6-1* control extracts (right panel). The precipitates probed with  $\alpha$ -Ubiquitin (P4D1) antibody showed a band at the same height as TOL6, demonstrating the ubiquitination of TOL6, which is not visible in *tol6-1* but only on the soluble fraction, not in the membrane fraction, where more TOL6 was precipitated, indicating that is the soluble TOL6, which is ubiquitinated.

#### 4.6.2 Ubiquitination of other TOL family members

Recent plant ubiquitome studies have shown that several endocytic adaptors, including the TOLs (TOL1, TOL2 and TOL3) are ubiquitinated (Svozil et al., 2014; Walton et al., 2016). It thus became interesting to verify if other members of the TOL protein family are also ubiquitinated, like TOL6. I therefore performed immunoprecipitation experiment using the available transgenic plant lines *pTOL1::TOL1:Venus in tol1-1*, *pTOL3::TOL3:Venus in tol3-1* and *pTOL5::TOL5:Venus in tol5-1*. To precipitate the Venus tagged of TOL proteins TOL1, TOL3 and TOL5, I used anti-GFP microbeads. Stringent washing conditions were applied and N-Ethylmaleimide (NEM), which inhibits the activity of deubiquitinase enzymes was added to all buffers to avoid deubiquitination. For detection of the Venus tagged TOL proteins, I used the anti-GFP antibody that is able to detect the Venus tag. The results clearly showed that with the anti-GFP microbeads I managed to precipitate sufficient amounts of TOL1:Venus (Fig. 21A left panel open arrowhead), TOL3:Venus (Fig. 21B left panel open arrowhead) and TOL5:Venus (Fig. 20C left panel open arrowhead). To test if these precipitated proteins were ubiquitinated, I used the same precipitates and probed the western blot with an anti-ubiquitin antibody ( $\alpha$ -UBQ, P4D1). The results showed clearly a specific smear which always starts approximately at the size of the respective TOL and characterizes ubiquitination of the TOL1:Venus, TOL3:Venus and TOL5:Venus (right panels of Fig. 21 A, B, C respectively black arrow heads). As negative control, I used the precipitated obtained by performing the immunoprecipitation with the anti-GFP microbeads out of Col0 wild type plant lysates (Fig. 21 B), which showed a weaker, background staining when probed with the anti-ubiquitin antibody. As second control, I also performed the extraction of TOL3 using buffer lacking NEM, thus leading to faster deubiquitination of the sample. From this sample buffer I could also show that TOL3: Venus was clearly precipitated, characterized by strong band at the expected size of TOL3 (Fig. 21B, left panel, third lane). When I used the same precipitate and probed with the anti-ubiquitin antibody, I found a signal reminiscent of the signal obtained with the Col0 negative control (Fig. 21B, right panel, third lane) and in strong contrast to the strong signal obtained when probing the samples where NEM was added to the buffer (Fig. 21B, left panel, first lane). This indicates that there is no ubiquitination of TOL3:Venus when using a buffer lacking NEM and shows that the ubiquitination of TOL3:Venus is specific.

Together, these results suggest that several members of the TOL family members tested in this study are ubiquitinated.

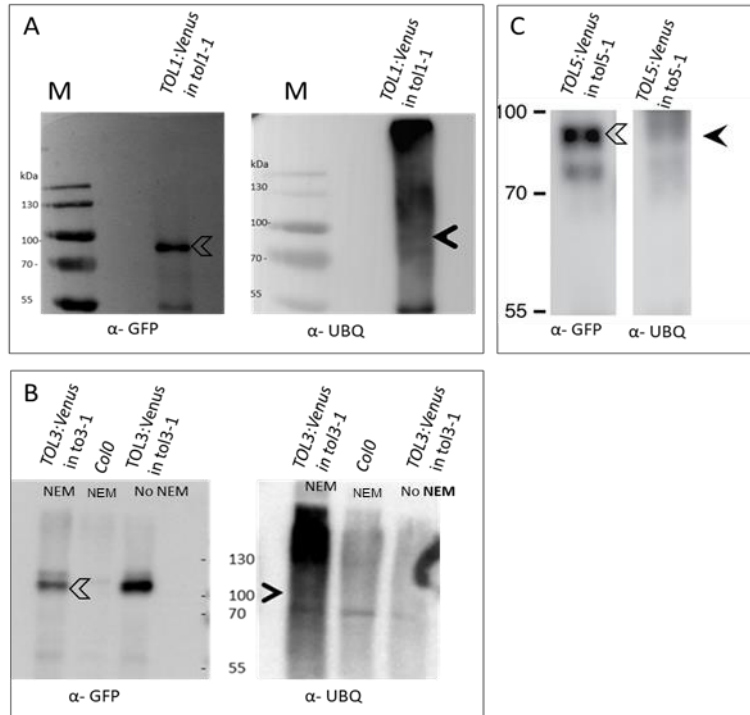


**Figure 21 Ubiquitination of other TOL family members:** (A) Ubiquitination of TOL1, seedlings with 6 days old pTOL1::TOL1:Venus in tol1-1 extracted and used for IP with anti-GFP microbeads and then probed with anti-GFP antibody (left panel) and the precipitate was also probed with anti-ubiquitin antibody (right panel). (B) Ubiquitination of TOL3 – 6 days old seedlings from pTOL3::TOL3:Venus in tol3-1 precipitated with anti-GFP microbes and incubated with anti-GFP antibody (left panel) as well as with anti-ubiquitin antibody (right panel). (C) Ubiquitination of TOL5 – 6days old seedlings from pTOL5::TOL5:Venus in tol5-1 precipitated with anti-GFP microbeads and incubated with anti-GFP antibody (left panel) as well as with anti-ubiquitin antibody (right panel). (D) Ubiquitination of TOL6 – 6 days old seedlings from pTOL6::TOL6:Venus in tol6-1 precipitated with anti-GFP microbeads and incubated with anti-GFP antibody (left panel) and with anti-ubiquitin antibody (right panel).

#### 4.7. Constitutively ubiquitinated TOL proteins affects the plant regulatory mechanism

Now that we know that TOLs are ubiquitinated *in planta* (see section 4.6), we need to try to find out the purpose of this ubiquitination and to assess if it is a mere signal for degradation or has a regulatory role. For this purpose, we generated constitutively ubiquitinated TOL proteins and expressed them *in planta*. As negative control, to dissect the effect of the ubiquitination from any potential steric effects that addition of a large tag to our TOL proteins could have, we added a mutated ubiquitin version. This mutated

ubiquitin (ubq<sup>I44A</sup>) loses its ability to bind UBD containing proteins (Dikic et al., 2009). The amino acid Isoleucine at position 44 is known to be important for ubiquitin to bind UBDs, thus the mutation in this position will alter the ability of the UBD to bind ubiquitin (Hurley et al., 2006) (Fig. 22).

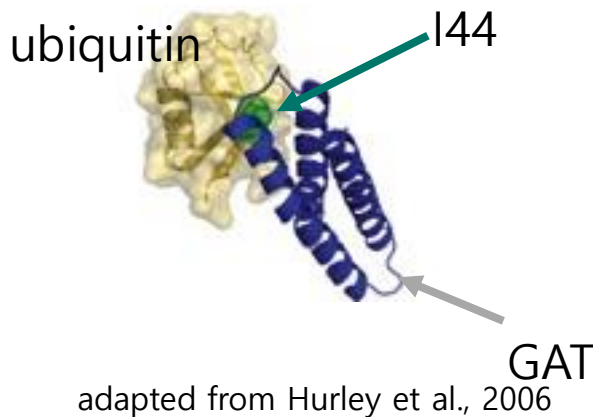


**Figure 22 Helical ubiquitin-binding domain structures :** Ubiquitin molecule (yellow) in ribbon and surface representations is shown with corresponding helical domain (blue) in ribbon representation . Ile44, the centre of the hydrophobic recognition patch on the ubiquitin, is shown as green spheres. adapted from (Hurley et al., 2006).

In order to investigate if TOL protein are regulated by coupled monoubiquitination, a master Student in our lab, Lisa Jörg, cloned constitutively ubiquitinated TOL construct as well as constructs fused to the mutated non-functional ubiquitin. Different constructs for plant expression, where the cDNA of three different TOLs (TOL1, TOL5 and TOL6) under their endogenous promoters with a C-terminal ubiquitin or ubiquitin<sup>I44A</sup> fused in frame to a Venus tag were cloned, resulting in: *pTOL1:TOL1:ubq:Venus*; *pTOL1:TOL1:ubq<sup>I44A</sup>:Venus*; *pTOL5:TOL5:ubq:Venus*; *pTOL5:TOL5:ubq<sup>I44A</sup>:Venus*; *pTOL6:TOL6:ubq:Venus* and *pTOL6:TOL6:ubq<sup>I44A</sup>:Venus* (for the cloning procedure see: Master thesis Lisa Jörg, 2017). Figure 23A, 26A and 28A shows schematics of the constructs used in this study for TOL6, TOL1 and TOL5 respectively. These constructs were transformed into single knockout plant lines that lacks respective TOL protein (*tol1-1*, *tol5-1* and *tol6-1*). With this transformation the following plant lines were obtained *pTOL1:TOL1:ubq:Venus* in *tol1-1*, *pTOL5:TOL5:ubq:Venus* in *tol5-1*, *pTOL6:TOL6:ubq:Venus* in *tol6-1* and with mutated ubiquitin *pTOL1:TOL1:ubq<sup>I44A</sup>:Venus*

in *tol1-1*, *pTOL5:TOL5:ubq<sup>I44A</sup>:Venus* in *tol5-1* and *pTOL6:TOL6:ubq<sup>I44A</sup>:Venus* in *tol6-1*. Besides that, the TOL6 constructs were also transformed into the quintuple mutant *tol/Q* plant line in order to analyze the complementation of the *tol/Q* phenotype. Having these constructs, with the ubiquitin chimera (TOL1ubq:Venus, TOL5ubq:Venus and TOL6ubq:Venus), which mimics permanent monoubiquitination and the mutated ubiquitin (TOL1ubq<sup>I44A</sup>:Venus, TOL5ubq<sup>I44A</sup>:Venus and TOL6ubq<sup>I44A</sup>:Venus), that is not functionally monoubiquitinated, I was able to analyze the importance of monoubiquitination of TOL proteins in plant cells.

#### 4.7.1 Constitutively ubiquitinated TOL6 affects its distribution and function in plant

After having obtained the constructs described above, I started to analyze the TOL6 proteins, with the ubiquitin chimera (TOL6ubq:Ven), which mimics permanent monoubiquitination and the mutated ubiquitin chimera (TOL6ubq<sup>I44A</sup>:Ven). Figure 23A shows the schematic representation of ubiquitin chimera used for TOL6, where the VHS and GAT domains of TOL6 are represented in green and blue boxes respectively, the red circle represents ubiquitin and the red circle with X represents the mutated ubiquitin I44A. I performed the western blots of total plant lysates of the reporter plants lines to verify if the proteins are expressed in comparable amounts and at the expected size. All three TOL6 constructs (TOL6:Ven, TOL6:ubqVen and TOL6:ubq<sup>I44A</sup>Ven) are expressed at roughly the correct size and in similar amounts (data not shown).

In order to analyze the importance of monoubiquitination of TOL6 in plant cells, I checked if the constitutively ubiquitinated TOL6 (TOL6:ubqVen) could affect the localization of TOL6 when compared to the TOL6 (TOL6:Ven) as well as constitutively TOL6 with mutated ubiquitin (TOL6:ubq<sup>I44A</sup>Ven). Confocal Laser Scanning Microscopy (CLSM) was used to access the subcellular localization of the TOL6:Venus, TOL6:ubqVenus and TOL6:ubq<sup>I44A</sup>Venus. I also performed cellular fractionation experiments of total plant lysates, to verify the protein distribution between soluble and membrane fraction. The subcellular localization of the TOL6:Venus reporter in *tol6-1* root epidermal cells of 6 days old seedlings, analyzed by CLSM showed that TOL6:Venus is localized at the PM (Fig. 23B, left panel). This is also reflected in cellular fractionation, where the TOL6:Venus is

localized predominantly in the membrane fraction (Fig. 23C left panels), with a similar distribution already showed in section 4.3.

I performed similar experiments with *pTOL6:TOL6:ubq:Venus* in *tol6-1*, *pTOL6:TOL6:ubq<sup>I44A</sup>:Venus* in *tol6-1*, where I accessed the subcellular localization of root epidermal cells of 6 days old seedlings. The CLSM showed that, the constitutive ubiquitination of TOL6 (TOL6:ubqVen) caused alteration of the localization of the TOL6, which is no longer localized predominately at the PM, but it is also in the cytoplasm (Fig. 23B middle). These results were further confirmed by cellular fractionation experiments, where protein signal is no longer predominant in the membrane fraction but distributed in both (cytosolic and membrane fraction) but more predominantly in the cytosolic fraction (Fig. 23C, middle panel). Furthermore, subcellular localization of constitutive ubiquitination of TOL6 with mutation in ubiquitin chimera (TOL6:ubq<sup>I44A</sup>Venus) when analyzed by CLSM, showed a signal more at the PM (Fig. 23 B right panel) restoring the signal to a similar distribution as the non-ubiquitinated TOL6 (Fig. 23B, left panel) and the endogenous TOL6 (section 4.3). This is also reflected in cellular fractionation where the protein signal is predominantly at the membrane fraction (Fig. 23C right panel).

To confirm the differences in localization I performed statistical analyzes where I quantified the fluorescence signal from TOL6:Ven, TOL6ubq:Ven and TOL6:ubq<sup>I44A</sup>Venus at the PM with respect to the signal in the cytosol with Image J in the epidermis cells of root meristem cells of 6 days old seedling. Statistically, the difference in localization showed to be highly significant between the TOL6:Ven and the TOL6ubq:Ven reporter line both in the *tol6-1* background as well as the between TOL6ubq:Ven and the I44A ubiquitin chimera (Fig. 23D) suggesting that a functional ubiquitin tag clearly alter the localization of the TOL6 in planta.

This brings us to the previously proposed model by (Hoeller et al., 2006) in which, the monoubiquitination of UBD-containing proteins does not serve to target the proteins for degradation but rather has a regulatory role, which in our case could be an alteration in the localization of TOL6 thus affect the functionality of the protein. These results indicate that the posttranslational modification of TOL6 with ubiquitin could alter the function of the protein, thus serving to fine-tune the protein function.

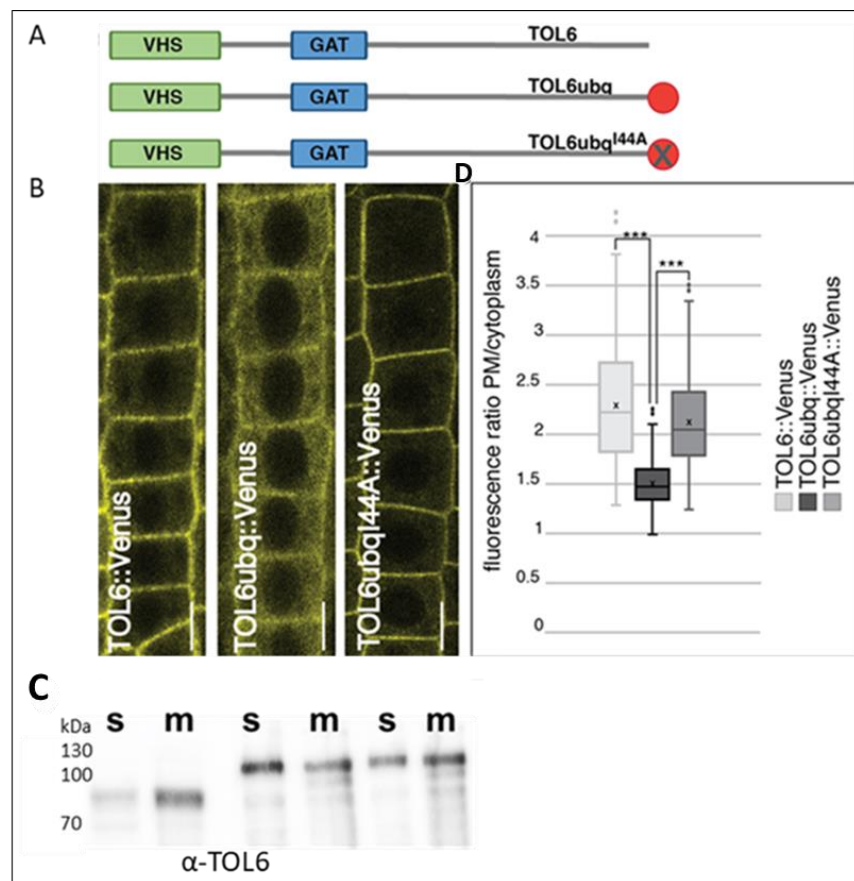


**Figure 23 TOL6ubq:Venus interfere with the localization :** **(A)** Schematic representation of ubiquitin chimera that were used for the described experiments. Red circle represents ubiquitin, red circle with X the mutated ubiquitin I44A. **(B)** Signal distribution of TOL6p::TOL6:Venus, TOL6p::TOL6:ubiquitin:Venus and TOL6p::TOL6:ubiquitinI44A:Venus in root meristem cells (6 days old seedlings of *tol6-1* plants). Scale bars =10μm **(C)** Subcellular localization of TOL6p::TOL6:Venus, TOL6p::TOL6:ubiquitin:Venus and TOL6p::TOL6:ubiquitinI44A:Venus (S=soluble, m=membrane). TOL lysate were separated out of soluble and membrane fraction with long centrifugation and incubated with affinity purified anti-TOL6 antibody. **(D)** Graphic Representation for Relative signal intensities of the above mentioned TOL6 ubiquitin chimera at the PM of

*tol6-1* root meristem cells after normalization to cytoplasmic signal intensities (n=number of cells analyzed; n=133, n=153 and n=139 respectively; \*\*\* $P \leq 0.001$ , Student's t-test-test).

#### 4.7.2 Constitutively ubiquitinated TOL6 has a diminished functionality in planta

After demonstrating the impact of constitutive ubiquitination on the localization of TOL6, I went further to analyze the functionality TOL6ubq:Venus *in planta*. The plant lines *pTOL6::TOL6ubq:Venus* and *pTOL6::TOL6ubq<sup>I44A</sup>:Venus* were transformed into the single knock out plant line *tol6-1* and the quintuple mutant *tolQ* plant by a master student in our lab Lisa Jörg (Master Thesis Lisa Jörg, 2017).

I performed complementation experiments to investigate if the *pTOL6::TOL6ubq:Venus* is able to fully rescue the *tolQ* phenotype which allows to check if these changes we saw in the localization also affects the functionality. Seven days old seedlings from *pTOL6::TOL6ubq:Venus* in *tolQ* revealed a phenotype where the roots were shorter and had defects in their cotyledon formation (Fig. 24A; bottom left). These defects were not

observed in Col0 (Fig. 24A, top left), in *TOL6p::TOL6:Venus* in *tolQ* (Fig. 24A, top right), and *pTOL6:TOL6:ubq144A:Venus* in *tolQ* (Fig. 24A, bottom right) plant lines, indicating that these defects are specific to the constitutively ubiquitinated version and are not found in the TOL6 version fused to the non-functional ubiquitin, serving as a control. Rosettes from 17 days old plants, from *TOL6:Venus* in *tolQ* showed normal development similar to Col0, demonstrating its capacity to rescue the *tolQ* phenotype (Fig. 24B, first two top panels) similarly to the *TOL6:Venus* in *tolQ* background, which we showed before (Fig. 17B). However, not only in the 7day old seedlings but also in the 17 day old plants, the *pTOL6:TOL6:ubq:Venus* in *tolQ* showed pronounced phenotypic differences, characterized by a smaller rosette with less number of rosette leaves (Fig. 24B, bottom panel last row), although not as drastic as the defects described for the *tolQ* plant lines (Fig. 24B, third panel last row) (Korbei et al., 2013). Mature plants from *pTOL6:TOL6:ubq:Venus* in *tolQ* were slightly dwarfed and showed delayed growth, when compared to wild type plants lines as well as the fully complementing *TOL6:Venus* in *tolQ* and the *TOL6ubq144:Venus* in *tolQ* (Fig. 24C). This indicates that the constitutively ubiquitinated TOL6 fails to fully rescue the *tolQ* phenotype.

As shown before, the *TOL6ubq:Venus* also changes its localization to the cytosolic fractions, albeit to a lesser degree than the UBD mutated version of TOL6, thus potentially promoting alteration in the sorting of ubiquitinated proteins to be degraded, which is also demonstrated by the fact that this construct fails to fully rescue the *tolQ* phenotype. Taken together this result suggests that, TOL6 could be regulated by coupled monoubiquitination, thus allowing for fine tuning in the degradation of ubiquitinated PM proteins.



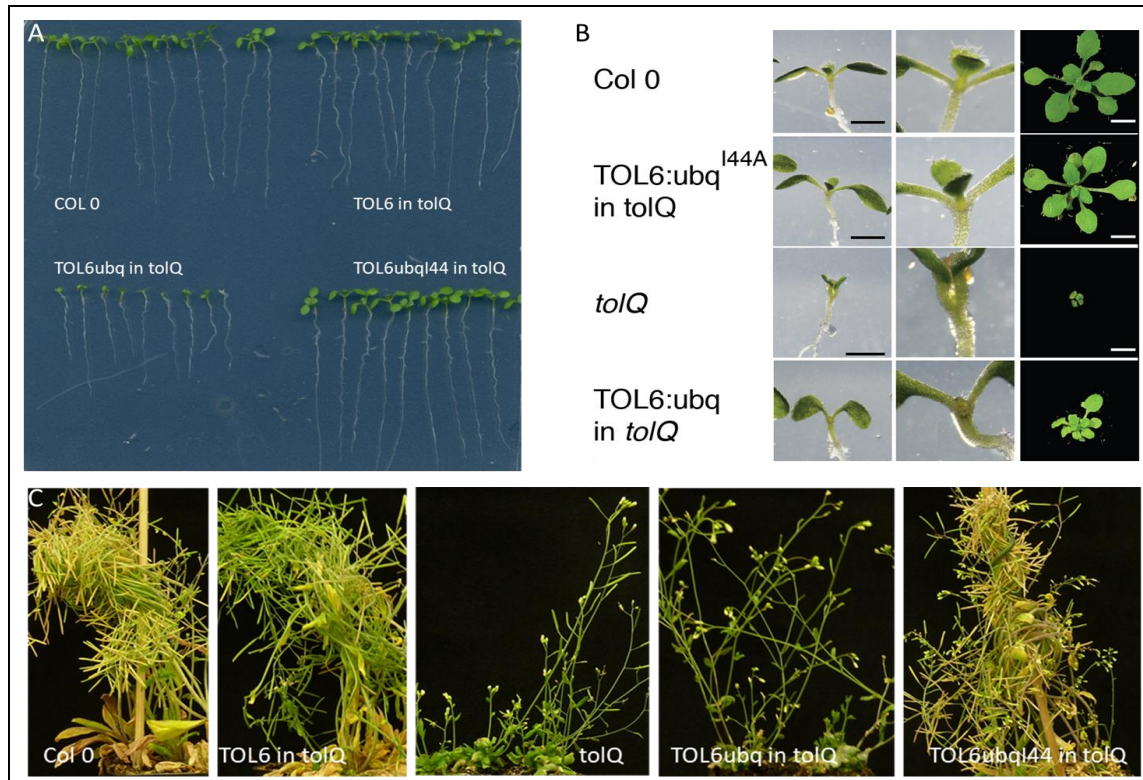


**Figure 24 Monoubiquitinated TOL6 has diminished functionality in planta :** (A) Phenotype of Columbia, TOL6:Venus in *tolQ*, TOL6ubq:Venus in *tolQ* and TOL6ubqI44A in *tolQ* seven days old seedlings scan photograph of seedling on plate. (B) Comparison of Columbia TOL6:Venus in *tolQ*, TOL6ubq:Venus in *tolQ* and TOL6ubqI44A:Venus in *tolQ* and *tolQ* seedlings 7 DAG (left panel scale bar =2mm). Close up of shoot apical meristem (middle row) and 17 days old showing rosette development (right panel scale bar =5mm). (C) Phenotype of Columbia, TOL6:Venus in *tolQ*, TOL6ubq:Venus in *tolQ* and TOL6ubqI44A:Venus in *tolQ* and *tolQ*, adult plants (35 days old).

#### 4.7.3 Monoubiquitination of TOL6 affects plant development

After demonstrating that the constitutive ubiquitinated TOL6 (TOL6ubq:Ven) affects the localization and the functionality *in planta*, I wanted to investigate if it also affected the plant development in the single mutant line. I followed the plant development of the *pTOL6p:TOL6:Venus* in *tol6-1*, *pTOL6::TOL6ubq:Venus* in *tol6-1*, and *pTOL6::TOL6ubq<sup>I44A</sup>:Venus* in *tol6-1*. I started by measuring the root length of 7 days old seedlings and separated in three different categories to include variations in the growth of seedlings (see 3.10.8). Statistical analysis demonstrated that, approximately 30% of *tol6-1* roots were abnormal (in short roots category) (Fig. 25A). Similar phenotype was also observed in *pTOL6:TOL6:ubqVenus* in *tol6-1*, while neither the wild type Col0, or *pTOL6::TOL6:Venus* in *tol6-1* and *pTOL6:TOL6:ubq<sup>I44A</sup>Venus* in *tol6-1* showed this phenotype. This reveals that, single knockout *tol6-1* plant lines might have defects that

are not phenotypically pronounced but these subtle defects are not fully rescued by the TOL6ubq:Venus protein but they are clearly rescued by full length TOL6 (TOL6:Venus) and the TOL6:UbqI44A:Venus.

Reduced number of rosette leaves indicative of an earlier flowering time, were observed in *tol6-1* plant lines as well as in *pTOL6:TOL6ubq:Venus* in *tol6-1* plant lines, while not in *pTOL6:TOL6:Venus* in *tol6-1*, and *pTOL6:TOL6:ubqI44A:Venus* in *tol6-1* when compared to Col0. This was confirmed by statistical analyzes which showed highly significance difference between the amount of rosette leaves at the time point when the stem is 1cm in height (Fig 25B).

Rosettes sizes from 21 days old plants also showed defects in growth development and were smaller in diameter for *tol6-1* when compared with Col0. *TOL6ubq:Venus* in *tol6-1* failed to rescue this phenotype, while the TOL6:Venus and TOL6ubq<sup>I44A</sup>: Venus in *tol6-1* fully rescued the phenotype and their rosette diameters resembled those of Col0 plants (Fig. 25C). Surprisingly the *tol6-1* plant line did not show any defects in the mature plants, indicating that, the defects are pronounced in juvenile plants but not in adult plants (see Fig. 18C).

In summary, these results suggest that, TOL6ubq is not fully functional, which is not due to the size or steric hindrances of the ubiquitin tag. Thus, reduced functionality could be caused by for example an intramolecular binding of the ubiquitin to its UBD and therefore auto-inhibition of the TOL6 protein, as is suggested by the coupled monoubiquitination regulatory mechanism (Hoeller et al., 2006). TOL6:ubq consequently cannot functionally substitute TOL6 in the early steps in the transport of ubiquitinated cargo from the PM to vacuolar for degradation. This is demonstrated in deficiencies in plant growth and development, highlighting therefore, that the potential regulatory role that ubiquitination of TOL6 proteins plays a vital part in plant development.

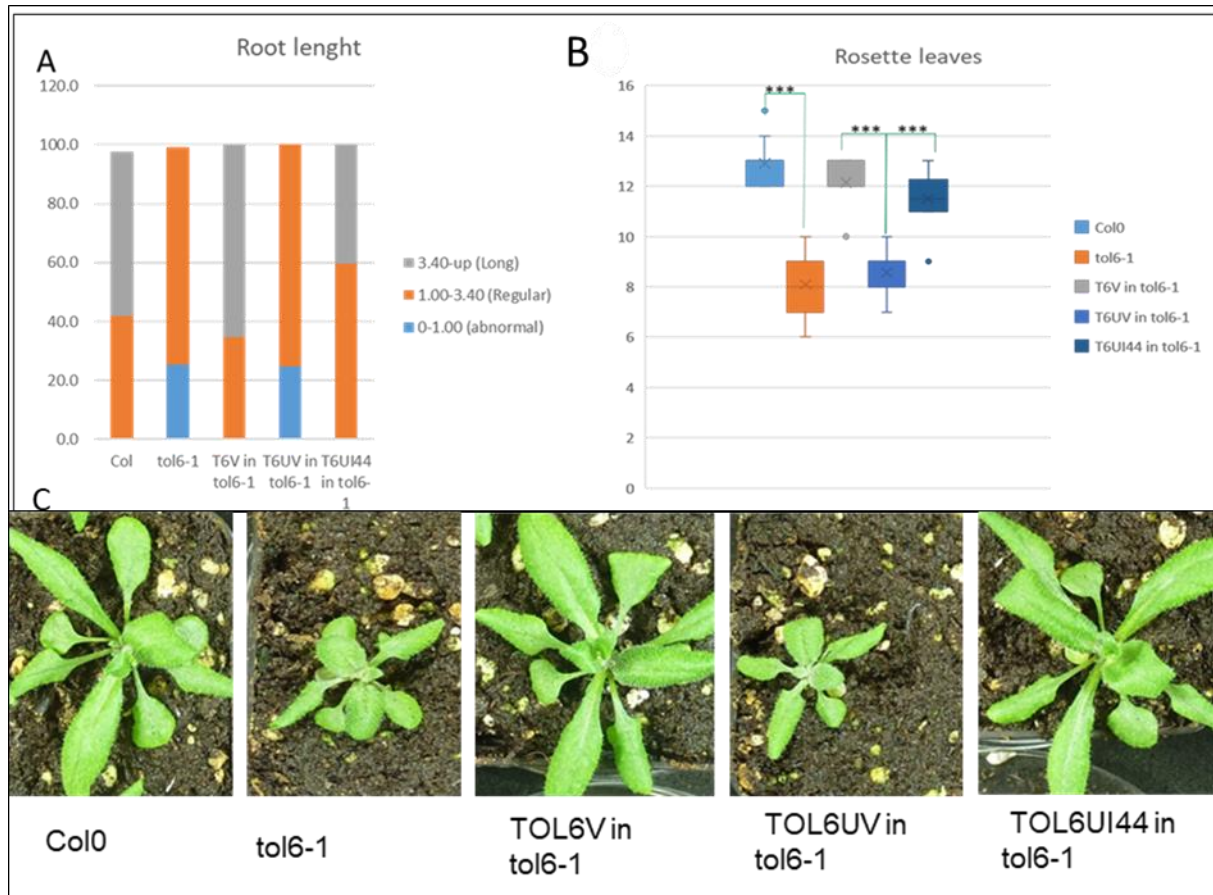


**Figure 25 Monoubiquitination of TOL6 affects with the plant development :** (A) Graphic representation of Col0, *tol6-1*, TOL6V in *tol6-1*, TOL6ubq in *tol6-1* and TOL6ubqI44A in *tol6-1* root length of 7 days old seedlings separated in three categories. 3.4cm is the average of Columbia in the same conditions. . (B) Graphic representation of rosette leaves counted after all the plants were flowering at the time point when the stem is 1cm in height. (C) Phenotype of 21 Days old plants of Col0, *tol6-1*, TOL6V in *tol6-1*, TOL6ubq in *tol6-1* and TOL6ubqI44A . TOL6V=TOL6:Venus; TOL6UV=TOL6ubq:Venus; TOL6UIV=TOL6ubq<sup>I44A</sup>:Venus.

#### 4.7.4 Constitutively ubiquitinated TOL1 alters its distribution and function in plant

As mentioned before, In addition to TOL6, I also analyzed the constitutively ubiquitinated TOL1 where I used the *pTOL1::TOL1:Venus* in *tol1-1*, *pTOL1:TOL1:ubq:Venus* in *tol1-1* and *pTOL1:TOL1:ubqI44A:Venus* in *tol1-1* (Fig. 26A). Confocal Laser Scanning Microscopy (CLSM) was used to access the subcellular localization. I also performed cellular fractionation experiments of total plant lysates, to verify the protein distribution between soluble and membrane fraction (Fig. 26D).

For the *TOL1:Venus* in *tol1-1* reporter I could show that the subcellular localization in the root epidermal cells of 6 days old seedlings is at the cytoplasm as well as the PM similar to the results described in section 4.3 (Fig 26B, left panel), which was confirmed by the cellular fractionation assay (Fig. 26D, first two lanes). When the ubiquitin is constitutively fused to the C-terminus of the TOL1 protein (TOL1ubq:Venus), it showed an altered signal localization, as it became more diffused and showed an enhanced concentration in the cytoplasm (Fig. 26B, middle panel), which was not as prominent in the TOL1ubqI44A:Venus expressing plant line, exhibiting the tendency of restoring to the signal to that of TOL1:Venus (Fig. 26B, right panel).

Relative signal intensities from TOL1:Ven, TOL1ubq:Ven and TOL1:ubq<sup>I44A</sup>Venus were measured with Image J software via the ration between the cytoplasmic intracellular signal respect to the signal at the PM in 6 days old epidermal root cells. Statistically, the difference in localization showed to be highly significant between the TOL1:Ven and the TOL1ubq:Ven reporter line as well as the I44A ubiquitin chimera TOL1ubq<sup>I44A</sup>:Venus, albeit to a slightly smaller degree (Fig. 26C). This shows that a functional ubiquitin tag modifies the localization of TOL1:Venus in the endosomal system of plants.

This was not so well reflected when I performed the subcellular fractionation experiments. The signal distribution of TOL1:Venus is predominantly in the cytoplasm as shown in section 4.3. and this is not significantly altered when the ubiquitin was constitutively attached to the TOL1 (TOL1ubq:Venus) (Fig. 26D middle). The TOL1ubq<sup>I44A</sup>:Venus showed its localization mostly in the cytosolic fraction, similar to the TOL1:Venus distribution (Fig. 26D right). These differences could be due to the fact that the PM localized TOL1:Venus, is not tightly associated with the PM and is therefore not found in the membrane fraction in the cellular fractionation experiment. A more detailed analysis of the exact localization of TOL1 should help to elucidate this issue, but was beyond the scope of this thesis.

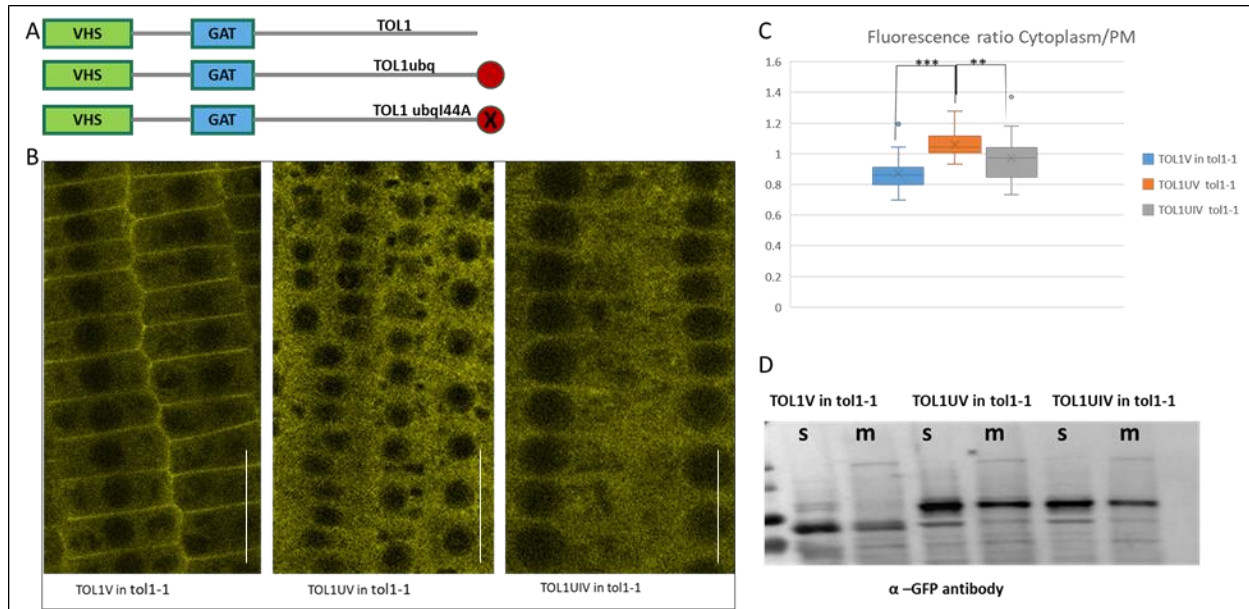


**Figure 26 TOL1ubq:Venus interfere with the localization :** **(A)** Schematic representation of ubiquitin chimera that were used for the described experiments. Red circle represents ubiquitin, red circle with X the mutated ubiquitin I44A. **(B)** Signal distribution of *TOL1p::TOL1:Venus* in *tol1-1*, *TOL1p::TOL1:ubiquitin:Venus* in *tol1-1* and *TOL1p::TOL1:ubiquitin<sup>I44A</sup>:Venus* in *tol1-1* plant lines in root meristem cells of 6 days old seedlings. Scale bars = 25 μm **(C)** Graphic representation for Relative signal intensities of the above mentioned TOL1 ubiquitin chimera at the cytoplasm of *tol1-1* root meristem cells after normalization to PM signal intensities (n=number of cells analyzed; n=72, n=75 and n=70 respectively; \*\*\*P ≤ 0.001, Student's t-test). **(D)** Subcellular fractionation of *TOL1p::TOL1:Venus*, *TOL1p::TOL1:ubiquitin:Venus* and *TOL1p::TOL1:ubiquitin<sup>I44A</sup>:Venus* (S=soluble, m=membrane). TOL lysate were separated out of soluble and membrane fraction with long centrifugation and incubated with anti-GFP antibody. TOL1V=TOL1:Venus; TOL1UV=TOL1ubq:Venus; TOL1UIV=TOL1ubq<sup>I44A</sup>:Venus.

I also analyzed if the constitutively ubiquitinated TOL1 (TOL1ubq:Venus) has an effect on the functionality and role of TOL1 in plant growth. For this purpose I assessed the differences between the three plant lines *TOL1:Venus* in *tol1-1*, *TOL1ubq:Venus* *tol1-1* and *TOL1ubq<sup>I44A</sup>:Venus* in *tol1-1* and compared them to Col0.

When measuring the root lengths of 7 days old seedlings (see 3.10.8), the *tol1-1* single knockout showed around 35% of small roots (root with abnormal development). The same results were observed on *TOL1ubq:Venus* in *tol1-1* seedlings, differently to the *TOL1:Venus* in *tol1-1*, Col0 wild type and *TOL1ubq<sup>I44A</sup>:Venus* in *tol1-1* plant lines (Fig. 27A), where no differences were observed. This demonstrate that, the single knockout *tol1-1* itself shows a subtle root growth defect, which is rescued by expressing TOL1:Venus and TOL1ubq<sup>I44A</sup>:Venus but not TOL1ubq:Venus.

I also compared the amount of rosettes leaves, when the inflorescences are 1cm in height between these plant lines, and observed that the T-DNA insertion plant line *tol1-1* produce



less rosette leaves (Fig. 27B second panel) which leads to earlier flowering. Similar results were observed for the *TOL1ubq:Venus* in *tol1-1* reporter line (Fig. 27B, fourth panel), which also produced less number of rosette leaves demonstrating its earlier flowering. This defects where not observed in Col0 (Fig. 27B, first panel) and the expression of TOL1:Venus (Fig 27B, third panel), as well TOLubq<sup>l44A</sup>:Venus (Fig. 27B, last panel) in *tol1-1* rescued this early flowering phenotype. These differences on the number of rosette leaves turns out to be extremely statically significant between the *tol1-1* and *TOL1ubq:Venus* in *tol1-1* when compared to Col0, *TOL1:Venus* in *tol1-1* as well as *TOLubq<sup>l44A</sup>* in *tol1-1* (Fig. 26 C), suggesting that the monoubiquitination of TOL1 affects its functionality *in planta*.

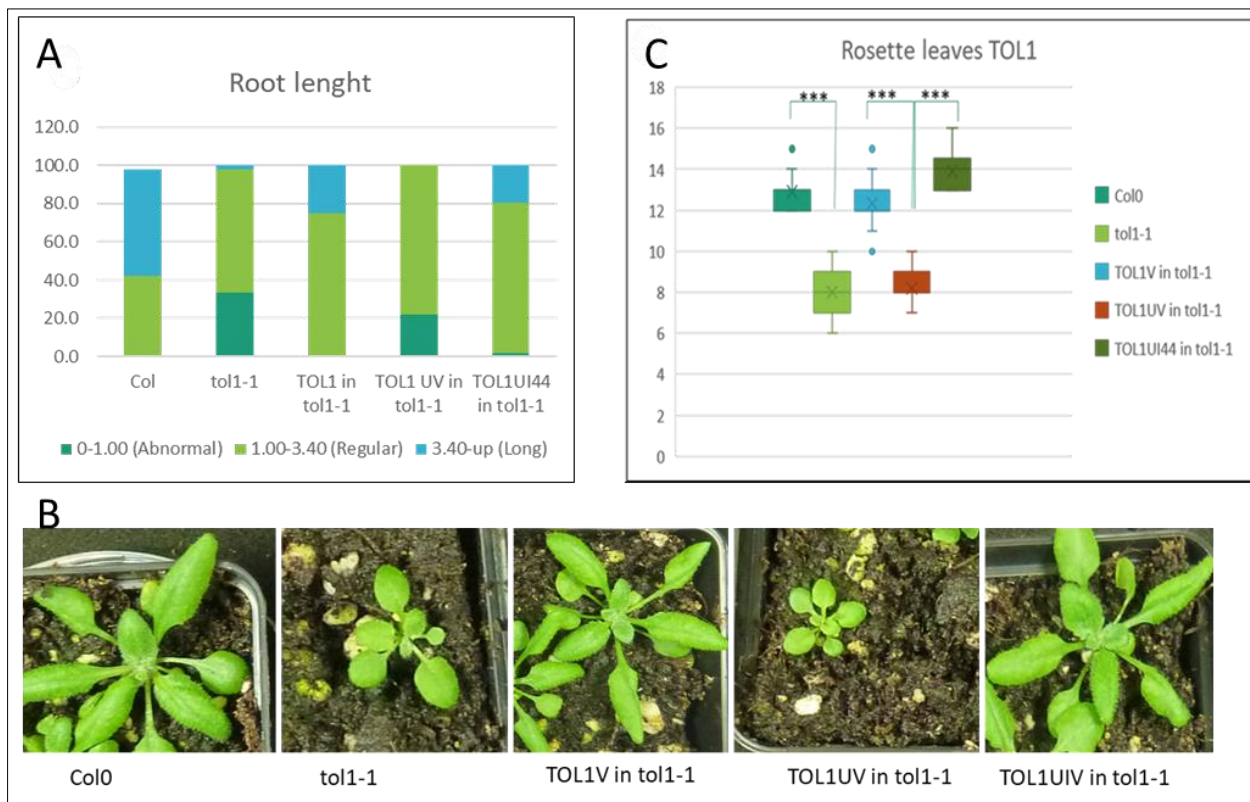


**Figure 27 Monoubiquitination of TOL1 affects with the plant development :** (A) Graphic representation of Col0, *tol1-1*, TOL1:Venus in *tol1-1*, TOLubq:Venus in *tol1-1* and TOLubq<sup>l44A</sup>:Venus root length of seven days old separated in three categories. 3.4cm is the average of Columbia in the same conditions. (B) Phenotype of 21 Days old plants of Col0, *tol1-1*, TOL1V in *tol1-1*, TOL1ubq in *tol1-1* and TOL1ubq<sup>l44A</sup> in *tol1-1*. (C) Graphic representation of rosette leaves counted after all the plants were flowering at the time point when the stem is 1cm in height.

TOL1V=TOL1:Venus; TOL1UV=TOL1ubq:Venus; TOL1UIV=TOL1ubq<sup>l44A</sup>:Venus

#### 4.7.5 Constitutively ubiquitinated TOL5 alter the distribution and function in plant

I performed similar experiments for *pTOL5:TOL5:Venus* in *tol5-1*, *pTOL5:TOL5:ubq:Venus* in *tol5-1*, *pTOL5:TOL5:ubq<sup>I44A</sup>:Venus* in *tol5-1* (Fig. 28A). Subcellular localization analyzed by CLSM, showed TOL5:Venus in the cytoplasm (Fig. 28B, left panel), with some vesicular punctate as previously shown in section 4.3. Upon adding the ubiquitin chimera to the C-terminal TOL5 (TOL5ubq:Venus), it showed clear reduction of cytoplasmic concentration of TOL5ubq:Venus signal (Fig 28B, left). When adding the I44A mutation in ubiquitin chimera, the protein signal of TOL5ubI44A (Fig. 28B right) was again abundantly concentrated at cytoplasmic fraction, restoring the wild type TOL5:Venus signal concentration, therefore, without vesicular punctate. This difference in concentration showed to be statistically significant between TOL5:Venus and TOL5ubq:Venus reporter line as well as for TOL5ubq<sup>I44A</sup>:Venus (Fig. 28C) when measured the ration between the cytoplasm to PM signal (Cytoplasm/PM).

These differences in localization were also reflected in the subcellular fractionation where abundant concentration of TOL5:Venus signal was found at cytoplasm (Fig. 28D left panels). The TOL5ubq:Venus signal showed a clear alteration of its concentration, which is now less pronounced in the soluble fraction and more abundant in the membrane fraction (Fig. 28D middle panels). TOL5ubq<sup>I44A</sup>:Venus was similar to the TOL5:Venus predominantly in the soluble fraction, restoring the TOL5:Venus wild type signal distribution, demonstrating that localization of TOL5 is affected by constitutive ubiquitination.

Thus, the constitutive ubiquitination of TOL5 (TOL5ubq:Venus) changed the cytoplasmic concentration of the TOL5:Venus, which is no longer abundantly concentrated at cytoplasm. These results could indicate that the posttranslational modification of TOL5 with ubiquitin could alter also the function of the protein, emphasizing the regulatory role of ubiquitination of TOL proteins in plant development, similar to the previously showed model by (Hoeller et al., 2006) where, the monoubiquitinated UBD-containing proteins can adopt a closed, auto-inhibited conformation due to the intramolecular UBD-ubiquitin interaction.

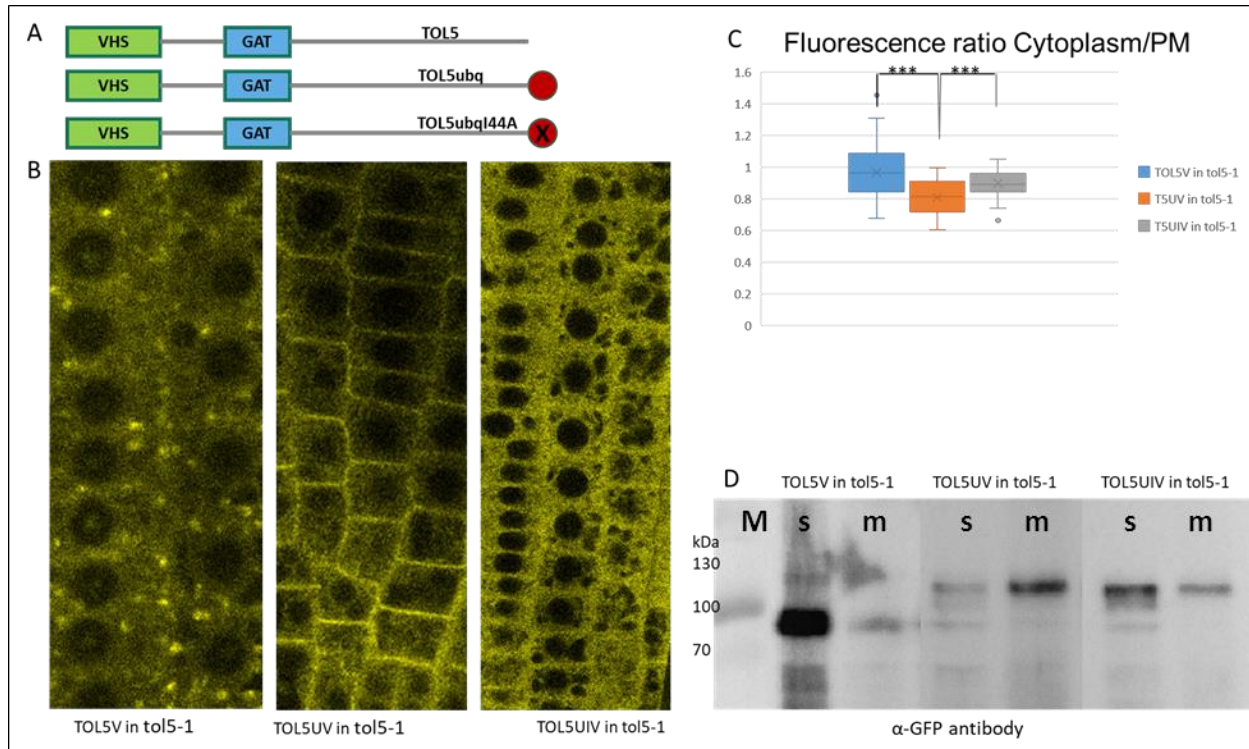


**Figure 28 TOL5ubq:Venus interfere with localization :** (A) Schematic representation of ubiquitin chimera that were used for the described experiments. Red circle represents ubiquitin, red circle with X the mutated ubiquitin I44A. (B) Signal distribution of TOL5p::TOL5:Venus, TOL5p::TOL5:ubiquitin:Venus and TOL5p::TOL5:ubiquitinI44A:Venus in root meristem cells (6 days after germination (DAG)) of *tol5-1* plants. Scale bars = 10 μm (C) Graphic representation for Relative signal intensities of the above mentioned TOL5 ubiquitin chimera at the PM of *tol5-1* root meristem cells after normalization to cytoplasmic signal intensities (n=number of cells analyzed; n=72, n=153 and n=139 respectively; \*\*\* $P \leq 0.001$ , Student's t-test-test). (D) Subcellular localization of TOL5p::TOL5:Venus, TOL5p::TOL5:ubiquitin:Venus and TOL5p::TOL5:ubiquitinI44A:Venus (S=soluble, m=membrane). TOL lysate were separated out of soluble and membrane fraction with long centrifugation and incubated with anti-GFP antibody. TOL5V=TOL5:Venus; TOL5UV=TOL5ubq:Venus; TOL5UIV=TOL5ubq<sup>I44A</sup>:Venus

Furthermore, I also checked the effect off the ubiquitination of TOL5 on the functionality of the protein and its contribution to plant development. I started by measuring the root length, and separated them into the three previously described categories (see 3.10.8). The *tol5-1* single knockout showed some defects in root development with approximately 30% of the roots being exceedingly small. Similar defects but less pronounced at 10%, were also observed in TOL5ubq:Venus in *tol5-1* seedling roots. No defects were observed in seedlings expressing the full length TOL5:Venus or the TOL5ubq<sup>I44A</sup>:Venus in *tol5-1* background, which fully rescue the phenotype or in Col0 seedlings (Fig. 28A).

When counting the rosette leaves, to check the flowering time of different constructs, the single knockout *tol5-1* produces less rosette leaves revealing its earlier flowering time when compared to Col0, or the other lines (Fig. 29B). Statistically, there is no significant



difference between the *TOL5:Venus*, *TOL5ubq:venus* and *TOL5ubq<sup>l44A</sup>:Venus* in *tol5-1* as well as Col0, in the number of rosette leaves, suggesting that, expression of *TOL5ubq:Venus* in *tol5-1* does rescue the *tol5-1* single knockout phenotype. Taken together these results indicates that, the constitutively ubiquitinated *TOL5ubq:Venus* affects the distribution of *TOL5* *in planta* although it does not necessarily affect its function. More detailed analysis will be needed to differentiate between these two different effects.

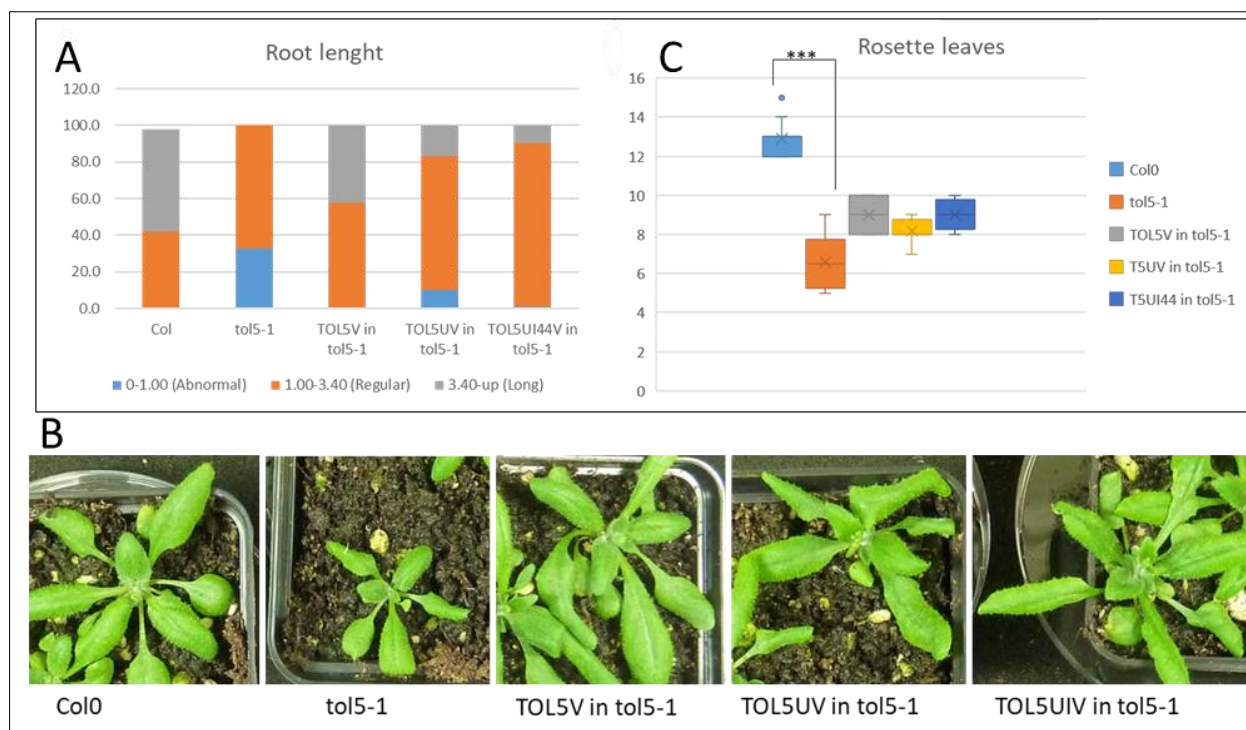


**Figure 29 Monoubiquitination of TOL5 affects with the plant development :** (A) Graphic representation of Col0, *tol5-1*, *TOL5:Venus* in *tol5-1*, *TOLubq:Venus* in *tol5-1* and *TOL5ubq<sup>l44A</sup>:Venus* root length of seven days old separated in three categories. 3.4cm is the average of Columbia in the same conditions. (B) Phenotype of 21 Days old plants of Col0, *tol5-1*, *TOL5:Venus* in *tol5-1*, *TOL5ubq:Venus* in *tol5-1* and *TOL5ubq<sup>l44A</sup>:Venus* in *tol5-1*. (E) Graphic representation of rosette leaves counted after all the plants were flowering showing at the time point when the stem is 1cm in height.

TOL5V=*TOL5:Venus*; TOL5UV=*TOL5ubq:Venus*; TOL5UIV=*TOL5ubq<sup>l44A</sup>:Venus*

## 5 DISCUSSION

### 5.1. The TOL protein family play a role in the degradation of PM proteins between the PM and the cytoplasm

TOL proteins are a family of nine proteins (TOL1-9) described in *Arabidopsis thaliana*, which recognize ubiquitinated cargo at the PM and presumably sort them to the ESCRT machinery to ensure their vacuolar targeting for degradation (Korbei et al., 2013). They contain two conserved UBDs and function as potential alternate to the ESCRT-0 complex in plants in recognition of ubiquitinated cargo destined for degradation (Korbei et al., 2013). Previously, we demonstrated that the TOLs proteins works as a molecular players in the first steps in the degradation of ubiquitinated PM proteins in plants (Korbei et al., 2013). Nevertheless, the detailed mechanism, function and localization of the TOL proteins were still not clear. The results from my PhD showed that, the different members of the TOL proteins are localized differentially *in planta*. TOL6:Venus is clearly localized at PM and in early endosomes, while TOL1:Venus and TOL3:Venus are localized in both the PM and the cytoplasm but mostly in the cytoplasm and TOL5:Venus is localized exclusively in the cytoplasm. Similar results were previously observed for TOL6:mcherry and TOL5:mcherry (Korbei et al., 2013). This difference in localization, where some TOLs are at PM while others are localized in the cytoplasm point towards potentially different functions of the TOLs in the endosomal system of plants. TOL6, which is localized predominantly at the PM, showed its function at the PM, where it aid is the internalization of for example ubiquitinated PIN2, initiating a cascade of events that guide the PIN2 cargo to the vacuole (Korbei et al., 2013). On other side TOL5, which has different localization to TOL6, specifically at cytoplasm, was recently published to have a function on MVB where it co-localizes with BOR1 on its route to the vacuole, when subjected to high concentration of BOR1 (Yoshinari et al., 2018). These differences in functions of the TOL proteins could explain their different localizations observed between different TOL members. Here, I could conclude that, the TOL proteins plays role between the PM and

the MVBs by recognizing, sequestering and sorting ubiquitinated proteins from PM ensuring their targeting to the vacuole for degradation. The differences in localization could either support the idea that the different TOLs target different cargos and therefore localize differently or that the TOLs function in the degradation of ubiquitinated PM proteins, but at different sites in the endomembrane system, potentially handing cargo to one another. TOL proteins could function as a network in the plant endosomal system, where some TOLs localized at PM binding to ubiquitinated PM proteins, internalize them and pass on to the next TOL that is mostly cytoplasmic, potentially on other endosomal structures in the cytosol. This network would allow the TOL protein to pass the ubiquitinated cargo to the rest of the ESCRT machinery at different sites in the endosomal system for their ultimate degradation in the vacuole.

Furthermore, this could explain why so many TOL proteins have to be knocked out to ensure a significant phenotype as in the quintuple mutant *tolQ*, as the TOLs function partially redundantly, at different positions in the endomembrane system. The Venus-tagged reporters for TOL3, TOL5 and TOL6 localize differently in the endomembrane system of plants and the respective genes are knocked out in the quintuple mutant *tolQ*. Therefore, it would also be interesting to check the localization of other TOLs that are part of *tolQ* specifically TOL2, and TOL9, and of course other TOLs family members as well. Nevertheless, this hypothesis would require further assessment using for example endocytosed styryl dye FM4-64, in combinations with different trafficking drugs like wortmannin or BFA to dissect the endosomal pathway in greater detail. Also, reporter constructs, to label the different endosomes, in combination with mutated TOL reporters could be employed to dissect the precise function the TOLs play in the endosomal system of plants.

## 5.2. TOLs bind to phospholipids

Acquirement of membrane identities is promoted by the combinations between the presence of specific lipids and proteins on each membrane (Jean and Kiger, 2012). Phosphoinositides (PIs) are considered as the major determinants of membrane identities. These very low abundant lipids are important players for the recruitment of

peripheral proteins to membranes (Balla, 2013; Heilmann, 2016). Peripheral membrane proteins can be anchored to membranes by different mechanisms like protein-protein and protein-lipid interactions (Cho and Stahelin, 2005). In mammalian and yeast, the VHS and GAT domain are able to interact with phospholipids (Demmel et al., 2008; Wang et al., 2007). My results showed interaction between TOL proteins specifically (TOL6 and TOL2) and phospholipids. The presence of the VHS and GAT domains in the TOL proteins could explain the interaction of the TOLs with phospholipids, but this hypothesis has to be further tested by using for example deletion mutants lacking the VHS and GAT domains in the binding assay. As TOL proteins bind directly with PIs, as well as ubiquitinated cargo, the trafficking of ubiquitinated cargo may be directly regulated by the same PIs that recruit their associated adaptors, like the TOLs, to the appropriate organelle membrane (Dunn et al., 2004).

For both TOL proteins that I tested, exclusive acidic phospholipids were found as binding partners in the PIP strip assay and my results showed the affinity of TOL6 and TOL2 to bind strongly to the phosphatidic acid (PA) and TOL6 also binds weakly to phosphoinositide phosphates (PIPs): PtdIns3P, PtdIns4P and PtdIns5P as well as PtdIns(3,4)P<sub>2</sub>, PtdIns(4,5)P<sub>2</sub>. The phospholipid PA is one of the lipids, which accumulates rapidly in response to different environmental signals like in response to a wide array of abiotic stress stimuli (McLoughlin and Testerink, 2013). PA represent a minor membrane phospholipid, which is formed in several stress conditions (Testerink and Munnik, 2005).

The PM localization of TOL6 might therefore be regulated by its binding to PA in response to certain stress conditions. Since the PM function as boundary layer between extra and intracellular space and the PA play important role in stress response, the TOL proteins can be directly affected by environmental signal that is explained by its binding to PA or to other PM localized PIPs. Thus, TOL proteins could participate in numerous pathways that the PA are involved, like stress response.

With these preliminary results, it would be interesting to use mutated constructs of TOL2 as well as TOL6 to check if the mutated version lost its capacity to bind phospholipids. In addition, of course it would be interesting to test other TOLs as well, which would help to

define the correlation between the PM localization of the TOL proteins with their binding to phospholipids, specifically the PA that is important in stress response.

### **5.3. Mutation of the UBD of TOL6 alter the localization and functionality**

TOL proteins are considered to function as substitutes for ESCRT-0 complex in plants, in the concentration of ubiquitinated PM protein destined for degradation and the loading of the down-stream ESCRT machinery (Dubeaux and Vert, 2017; Gao et al., 2017; Isono and Kalinowska, 2017; Korbei et al., 2013; Sauer and Friml, 2014). TOL proteins are characterized by two  $\alpha$ -helical Ubiquitin binding Domains (UBD), one N-terminal VHS domain, followed by a GAT domain (Korbei et al., 2013). UBD are specialized domains in proteins that recognize ubiquitin molecules and act as ubiquitin receptors (Husnjak and Dikic, 2012). In this thesis, I demonstrated that TOL6 binds strongly to ubiquitin via VHS and GAT domains, as mutation in these two UBD domains, in critical amino acids, abolished the capacity of TOL6 to bind ubiquitin *in vitro*. Mutation of the VHS domain showed no strong alteration in ubiquitin binding, allowing the assumption that either there are additional amino acids involved on the interaction between VHS and ubiquitin in plants or this domain is not as important in plants for ubiquitin binding. Mutation of the GAT domain showed strong alteration in ubiquitin binding of the protein thus giving a high importance to the GAT domain in ubiquitin binding. The mutation in both UBDs, VHS and GAT domains resulted in an ubiquitin binding deficient TOL6, additionally affecting the functionality of the protein in plants.

TOL6 proteins binds to ubiquitinated cargo at the PM and assists in sorting them via the ESCRT machinery to the vacuole for degradation. The UBD deficient version of TOL6 is not able to rescue the *to/Q* phenotype, which the non-mutated version could. Thus, we can speculate that since TOL6 is not able to bind to ubiquitin anymore, the interaction between ubiquitinated PM proteins and ESCRT machinery is abolished, leading to accumulation of the ubiquitinated cargo and therefore the pronounced developmental phenotype. A functional TOL6 needs to be able to bind ubiquitin.

Furthermore, the mutated TOL6 has an altered localization when analyzed *in vivo*. Presumably, the TOL proteins function as a network allowing the interaction between the PM and the ESCRT machinery via its UBD. If there is an alteration of UBD, it can lead to the destabilization of the network and therefore the interaction between PM and ESCRT machinery is abolished. Explaining the altered localization observed for mutated TOL6 *in planta*, which is not anymore at PM but in the cytoplasm. Another version could be that the mutated TOL6 is not able to bind to ubiquitinated cargo at PM anymore, and therefore accumulates in the cytoplasm. In both cases, its functionality would be impaired.

The ubiquitinated proteins triggers the association of ESCRT machinery with membranes, therefore in the absence of ubiquitinated cargos, there is no association between the ESCRT machinery. Thus, the mutated TOL6 that is not able to bind ubiquitinated cargo anymore is also not able to associate with membranes anymore, resulting to complete loss of function observed in mutated TOL6 plant line.

Plants have to respond rapidly and accurately to changes in the environment. PIN protein family are important auxin import facilitators in the PM (Grunewald and Friml, 2010). The abundance of PIN proteins is well controlled by a dynamic response and recycling between PM and endosomes which could culminate with protein degradation (Leitner et al., 2012; Spitzer et al., 2009). PIN2 is a well-known cargo of the ESCRT machinery, which when ubiquitinated is transported to the vacuole for degradation (Leitner et al., 2012; Spitzer et al., 2009). The *tolQ* mutants showed defects on PIN2 and other cargoes degradation and vacuolar delivery with many other PM proteins having the same fate (Korbei et al., 2013). Thus, the mutated TOL6 that is not able to bind to ubiquitinated cargo anymore, presumably also unable to recruit the ESCRT, which leads to defects due to alter protein localization and abundance that culminate with defects in plant development, plant growth, in the non-rescuing mutated TOL6 plant line in *tolQ* as well as to a less severe extend to the *tol6<sup>mTOTAL</sup> :Venus* in *tol6-1* plant line.

#### **5.4. TOL proteins are ubiquitinated and potentially regulated by a mechanism termed coupled monoubiquitination**

Post-translational modifications (PTM) are important for determination of lifetime, localization and activity of proteins (Barbosa et al., 2016; Haglund and Stenmark, 2006). In plants, PTM dynamically regulates many different cellular processes by interfering with the activity, structure complex formation and subcellular localization of target proteins (Guo et al., 2013; Polyn et al., 2015). Ubiquitination serves as a PTM signal triggering endocytosis of PM proteins into the endosomal system and it participates in the regulation of endocytic pathways (Haglund and Dikic, 2005; Haglund and Stenmark, 2006; Hoeller and Dikic, 2010). Ubiquitin also generates interaction network by regulating the interactions between proteins that are important for endocytic machinery organization (Hoeller et al., 2006; Hoeller and Dikic, 2010) as well as affecting the abundance of endocytic sorting machinery components by inducing their proteasomal degradation (Husnjak and Dikic, 2012). Ubiquitin adaptors contain one or more UBD, which binds ubiquitin, furthermore the UBD can attract the ubiquitination machinery allowing for monoubiquitination of proteins containing UBD domain in a process called “coupled monoubiquitination” (Hoeller et al., 2006; Pickart, 2001). Monoubiquitinated adaptor proteins bind in an intramolecular interaction between their ubiquitin and their UBD thereby becoming auto-inhibited (auto-inhibition of endocytic adaptor) (Blanc et al., 2009; Hoeller et al., 2006; Hoeller and Dikic, 2010). Thus, the coupled monoubiquitination works as a negative-feedback control in the molecular machineries, which require transient and consecutive interactions between ubiquitin receptors and their ligands (Haglund and Stenmark, 2006). Furthermore, coupled monoubiquitination prevents binding to the ubiquitinated cargo, as the UBD is already occupied either by intra- or by intermolecular ubiquitin binding (Blanc et al., 2009). The TOL proteins have a crucial function in vacuolar targeting and subsequent degradation of ubiquitinated membrane proteins. TOL proteins contain two well-conserved UBD, the VHS domain at N-terminal followed by a GAT domain (Korbei et al., 2013; Sauer and Friml, 2014).

Here, I was able to show that, the TOL proteins are ubiquitinated *in planta* when I analyzed the immunoprecipitates of TOL1:Venus, TOL3:Venus, TOL5:Venus and TOL6:Venus, as well as the endogenous TOL6. This results are consistent with recent publications that showed ubiquitination of TOL1, TOL2 and TOL3 using mass spectrometric analysis of ubiquitinated proteins and the peptide found for TOL2 showed it is ubiquitinated in the VHS domain (Svozil et al., 2014; Walton et al., 2016).

Interestingly, the ubiquitinated TOL6 was predominantly in the cytosolic fraction and not the membrane fraction. Revealing that, most likely the non-ubiquitinated PM localized TOL6 binds to ubiquitinated cargo at the PM, and sorts it to the endosomal system. This is further supported by the data that the constitutively ubiquitinated TOL6 (TOL6:ubqVenus) does not fully rescue the phenotype and is more cytoplasmic in its localization, while the TOL6:Venus and the TOL6ubqI44A:Venus rescue and are localized at the PM.

Thus, the ubiquitination of TOL6 works as a PTM signal in the regulation of the function of TOL6. The non-ubiquitinated TOL6 fraction is functional and stays at the PM, where it is able to bind to any ubiquitinated cargo from the PM and triggers its transport into endosomal system for degradation. If the TOL6 is ubiquitinated it remains in the cytoplasm and is not able to bind to ubiquitinated cargo anymore due to its UBD that is already occupied. This explains the fact that the cytosolic fraction of TOL6 is ubiquitinated while the membrane fraction not. This was clearly observed when a constitutively functional ubiquitin chimera was added to the C-terminal of TOL6 that changed the localization where the reporter signal was not found at PM anymore, but at cytoplasm. Supporting that, when the TOL6 is monoubiquitinated, it remains at cytoplasm, because it is not able to bind another ubiquitinated cargo anymore. Besides that, it also altered the functionality of the protein, where it could not rescue the *to/Q* phenotype anymore.

Furthermore, ubiquitination of TOL proteins probably functions in the regulation of cargo sorting by controlling the cellular distribution of TOL proteins. This can be explained by the ubiquitination of only the soluble fraction of the TOL6, which demonstrated that, the ubiquitination of the TOLs works as a switch from PM-localized that is not ubiquitinated,



to the cytoplasmic-localized TOL that is ubiquitinated. How this can be fully translated to the other TOLs needs to be further elucidated.

The other TOLs are also ubiquitinated in planta and also show alterations in their localization (for TOL1 and TOL5), when we analyzed the constitutively ubiquitinated TOL reporters. But while TOL1 seems to behave similarly to TOL6, with the constitutively ubiquitinated version being more cytoplasmic than the non-ubiquitinated or the mutated ubiquitin chimera, TOL5 did not. Constitutively ubiquitinated TOL1:Venus revealed its increased concentration in the cytoplasm compared to the wild type TOL1:Venus, and could thus be regulated via a similar coupled monoubiquitination mechanism that works as a negative-feedback control (Haglund and Stenmark, 2006). Thus, the TOL1 monoubiquitination affects the regulatory mechanism by auto-inhibition, avoiding it to bind to ubiquitinated cargo.

TOL5 on the other hand seems to behave differently. Here we see that the constitutively ubiquitinated version is actually more at the PM and less in the cytoplasm where the TOL5:Venus localization is diffuse in the cytoplasm with intracellular punctate potentially also in MVB like structures (Yoshinari et al., 2018). The constitutively ubiquitinated TOL5 (TOL5ubq:Venus) showed an altered localization and is found at very low concentration at cytoplasm, potentially also at the PM. Cellular fractionation experiments revealed that a part of the TOL5:Venus protein concentration is in the membrane fractions, which could be the MVB bound TOL5 fraction (Yoshinari et al., 2018) and the constitutive ubiquitination of TOL5 does not alter the protein concentration in the membrane fraction. Ubiquitinated TOL5 may also generate an interaction network by regulating the interaction between ubiquitinated proteins or other TOLs, potentially at the PM and therefore be localized more at the PM in its ubiquitinated version. However, further detailed assessment will be necessary, including a more detailed analysis of in which endomembrane compartment the endogenous and the constitutively ubiquitinated version of TOL5 resides, before a conclusion of how the ubiquitination affects TOL5 can be drawn.

Also here, the different subcellular localization of different TOLs including the different behavior of TOL1, TOL5 and TOL6 when constitutively ubiquitinated (TOL1ubq:Venus, TOL5 ubq:Venus and TOL6 ubq:Venus) points towards potentially different functions of

the TOL proteins in the endosomal system of plants. Nevertheless, all these scenarios support the idea of a dual role for ubiquitin in endocytic pathways, acting as sorting tag on trafficking cargoes as well as a regulatory signal on UBD-containing proteins.

In figure 30 I summarize the predicted model for the function of TOL6, it recognizes the ubiquitinated PM proteins and sort them to the ESCRT machinery, to ensure vacuolar degradation (Fig. 30 left side). If the UBDs of TOL6 are mutated or the protein is constitutively ubiquitinated, it cannot bind the ubiquitinated cargo at the PM anymore and hand it over to the ESCRT-I machinery and the ubiquitinated cargo is therefore not transported further towards the vacuole for degradation (Fig. 30 right side). Furthermore, the mutated and the constitutively ubiquitinated version of TOL6 are not found at the PM anymore, but are more cytoplasmic (Fig. 30 right side).

That this model applies for all nine TOL proteins is highly unlikely, as they localize differently in planta, with some being more at the PM and others in the cytosol. If a similar model applies to the other TOLs and if the TOLs function consecutively, handing cargo from one TOL to another will still be the topic of further research in this area.

Thus, the work done in this thesis helped to elucidate some of the important question in the early steps of PM protein degradation in plants and therefore adaptation and response to plants to their environment and it will serve as an important corner stone for future studies in this field.

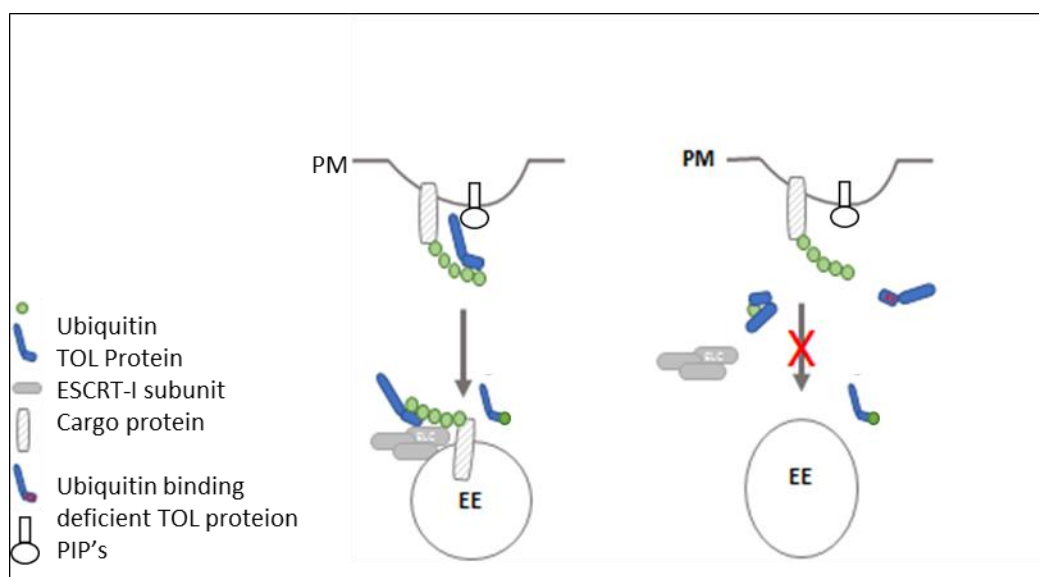


Figure 30  
Working model  
for the function  
of TOL6 proteins  
in the degradation  
of ubiquitinated  
PM proteins:

stress response  
pathway. TOLs  
bind ubiquitin via  
their UBDs and  
are themselves  
ubiquitinated.

Alteration both in its ability to bind ubiquitin as well as its own ubiquitination affects the localization and function of TOLs.

## 6 REFERENCES:

- Albert, B.; Johnson, A. Lewis, J.; Raff, M. Roberts, K.; Walter, P. (2008) *Molecular Biology of the Cell*. Fifth edition. Garland Science.
- Balla, T. (2013). Phosphoinositides: tiny lipids with giant impact on cell regulation. *Physiol Rev* 93, 1019-1137.
- Barbosa, I.C., Shikata, H., Zourelidou, M., Heilmann, M., Heilmann, I., and Schwechheimer, C. (2016). Phospholipid composition and a polybasic motif determine D6 PROTEIN KINASE polar association with the plasma membrane and tropic responses. *Development* 143, 4687-4700.
- Behnia, R., and Munro, S. (2005). Organelle identity and the signposts for membrane traffic. *Nature* 438, 597-604.
- Bertelsen, V., Sak, M.M., Breen, K., Rodland, M.S., Johannessen, L.E., Traub, L.M., Stang, E., and Madhus, I.H. (2011). A chimeric pre-ubiquitinated EGF receptor is constitutively endocytosed in a clathrin-dependent, but kinase-independent manner. *Traffic* 12, 507-520.
- Bilodeau, P.S., Winistorfer, S.C., Allaman, M.M., Surendhran, K., Kearney, W.R., Robertson, A.D., and Piper, R.C. (2004). The GAT domains of clathrin-associated GGA proteins have two ubiquitin binding motifs. *J Biol Chem* 279, 54808-54816.
- Bilodeau, P.S., Winistorfer, S.C., Kearney, W.R., Robertson, A.D., and Piper, R.C. (2003). Vps27-Hse1 and ESCRT-I complexes cooperate to increase efficiency of sorting ubiquitinated proteins at the endosome. *J Cell Biol* 163, 237-243.
- Blanc, C., Charette, S.J., Mattei, S., Aubry, L., Smith, E.W., Cosson, P., and Letourneur, F. (2009). Dictyostelium Tom1 participates to an ancestral ESCRT-0 complex. *Traffic* 10, 161-171.
- Boname, J.M., and Lehner, P.J. (2011). What has the study of the K3 and K5 viral ubiquitin E3 ligases taught us about ubiquitin-mediated receptor regulation? *Viruses* 3, 118-131.
- Bonifacino, J.S. (2004). The GGA proteins: adaptors on the move. *Nat Rev Mol Cell Biol* 5, 23-32.
- Cai, Y., Zhuang, X., Gao, C., Wang, X., and Jiang, L. (2014). The Arabidopsis Endosomal Sorting Complex Required for Transport III Regulates Internal Vesicle Formation of the

- Prevacuolar Compartment and Is Required for Plant Development. *Plant Physiol* 165, 1328-1343.
- Chen, H., and De Camilli, P. (2005). The association of epsin with ubiquitinated cargo along the endocytic pathway is negatively regulated by its interaction with clathrin. *Proc Natl Acad Sci U S A* 102, 2766-2771.
- Cho, W., and Stahelin, R.V. (2005). Membrane-protein interactions in cell signaling and membrane trafficking. *Annu Rev Biophys Biomol Struct* 34, 119-151.
- Chow, C.M., Neto, H., Foucart, C., and Moore, I. (2008). Rab-A2 and Rab-A3 GTPases define a trans-golgi endosomal membrane domain in Arabidopsis that contributes substantially to the cell plate. *Plant Cell* 20, 101-123.
- Clague, M.J., Liu, H., and Urbe, S. (2012). Governance of endocytic trafficking and signaling by reversible ubiquitylation. *Dev Cell* 23, 457-467.
- Clough, S.J., and Bent, A.F. (1998). Floral dip: a simplified method for Agrobacterium-mediated transformation of Arabidopsis thaliana. *Plant J* 16, 735-743.
- Collins, B.M., Watson, P.J., and Owen, D.J. (2003). The structure of the GGA1-GAT domain reveals the molecular basis for ARF binding and membrane association of GGAs. *Dev Cell* 4, 321-332.
- d'Azzo, A., Bongiovanni, A., and Nastasi, T. (2005). E3 ubiquitin ligases as regulators of membrane protein trafficking and degradation. *Traffic* 6, 429-441.
- Deak, M., Kiss, G.B., Koncz, C., and Dudits, D. (1986). Transformation of Medicago by Agrobacterium mediated gene transfer. *Plant Cell Rep* 5, 97-100.
- Dell'Angelica, E.C., Puertollano, R., Mullins, C., Aguilar, R.C., Vargas, J.D., Hartnell, L.M., and Bonifacino, J.S. (2000). GGAs: a family of ADP ribosylation factor-binding proteins related to adaptors and associated with the Golgi complex. *J Cell Biol* 149, 81-94.
- Demmel, L., Gravert, M., Ercan, E., Habermann, B., Muller-Reichert, T., Kukhtina, V., Haucke, V., Baust, T., Sohrmann, M., Kalaidzidis, Y., *et al.* (2008). The clathrin adaptor Gga2p is a phosphatidylinositol 4-phosphate effector at the Golgi exit. *Mol Biol Cell* 19, 1991-2002.
- Dettmer, J., Hong-Hermesdorf, A., Stierhof, Y.D., and Schumacher, K. (2006). Vacuolar H<sup>+</sup>-ATPase activity is required for endocytic and secretory trafficking in Arabidopsis. *Plant Cell* 18, 715-730.

- Dhonukshe, P., Aniento, F., Hwang, I., Robinson, D.G., Mravec, J., Stierhof, Y.D., and Friml, J. (2007). Clathrin-mediated constitutive endocytosis of PIN auxin efflux carriers in *Arabidopsis*. *Curr Biol* 17, 520-527.
- Di Rubbo, S., Irani, N.G., Kim, S.Y., Xu, Z.Y., Gadeyne, A., Dejonghe, W., Vanhoutte, I., Persiau, G., Eeckhout, D., Simon, S., *et al.* (2013). The clathrin adaptor complex AP-2 mediates endocytosis of brassinosteroid insensitive1 in *Arabidopsis*. *Plant Cell* 25, 2986-2997.
- Dikic, I., Wakatsuki, S., and Walters, K.J. (2009). Ubiquitin-binding domains - from structures to functions. *Nat Rev Mol Cell Biol* 10, 659-671.
- Dubeaux, G., and Vert, G. (2017). Zooming into plant ubiquitin-mediated endocytosis. *Curr Opin Plant Biol* 40, 56-62.
- Dunn, R., Klos, D.A., Adler, A.S., and Hicke, L. (2004). The C2 domain of the Rsp5 ubiquitin ligase binds membrane phosphoinositides and directs ubiquitination of endosomal cargo. *J Cell Biol* 165, 135-144.
- Fan, L., Hao, H., Xue, Y., Zhang, L., Song, K., Ding, Z., Botella, M.A., Wang, H., and Lin, J. (2013). Dynamic analysis of *Arabidopsis* AP2 sigma subunit reveals a key role in clathrin-mediated endocytosis and plant development. *Development* 140, 3826-3837.
- Fingerhut, A., von Figura, K., and Honing, S. (2001). Binding of AP2 to sorting signals is modulated by AP2 phosphorylation. *J Biol Chem* 276, 5476-5482.
- Finley, D., Sadis, S., Monia, B.P., Boucher, P., Ecker, D.J., Crooke, S.T., and Chau, V. (1994). Inhibition of proteolysis and cell cycle progression in a multiubiquitination-deficient yeast mutant. *Mol Cell Biol* 14, 5501-5509.
- French, A.P., Mills, S., Swarup, R., Bennett, M.J., and Pridmore, T.P. (2008). Colocalization of fluorescent markers in confocal microscope images of plant cells. *Nature protocols* 3, 619-628.
- Fujita, Y., Krause, G., Scheffner, M., Zechner, D., Leddy, H.E., Behrens, J., Sommer, T., and Birchmeier, W. (2002). Hakai, a c-Cbl-like protein, ubiquitinates and induces endocytosis of the E-cadherin complex. *Nat Cell Biol* 4, 222-231.
- Gadeyne, A., Sanchez-Rodriguez, C., Vanneste, S., Di Rubbo, S., Zauber, H., Vanneste, K., Van Leene, J., De Winne, N., Eeckhout, D., Persiau, G., *et al.* (2014). The TPLATE adaptor complex drives clathrin-mediated endocytosis in plants. *Cell* 156, 691-704.

- Galan, J.M., and Haguenauer-Tsapis, R. (1997). Ubiquitin lys63 is involved in ubiquitination of a yeast plasma membrane protein. *EMBO J* 16, 5847-5854.
- Gao, C., Luo, M., Zhao, Q., Yang, R., Cui, Y., Zeng, Y., Xia, J., and Jiang, L. (2014). A unique plant ESCRT component, FREE1, regulates multivesicular body protein sorting and plant growth. *Curr Biol* 24, 2556-2563.
- Gao, C., Zhuang, X., Shen, J., and Jiang, L. (2017). Plant ESCRT Complexes: Moving Beyond Endosomal Sorting. *Trends Plant Sci* 22, 986-998.
- Geldner, N. (2004). The plant endosomal system--its structure and role in signal transduction and plant development. *Planta* 219, 547-560.
- Geldner, N., and Jurgens, G. (2006). Endocytosis in signalling and development. *Curr Opin Plant Biol* 9, 589-594.
- Gendre, D., Oh, J., Boutte, Y., Best, J.G., Samuels, L., Nilsson, R., Uemura, T., Marchant, A., Bennett, M.J., Grebe, M., *et al.* (2011). Conserved Arabidopsis ECHIDNA protein mediates trans-Golgi-network trafficking and cell elongation. *Proc Natl Acad Sci U S A* 108, 8048-8053.
- Grant, S.G., Jessee, J., Bloom, F.R., and Hanahan, D. (1990). Differential plasmid rescue from transgenic mouse DNAs into *Escherichia coli* methylation-restriction mutants. *Proc Natl Acad Sci U S A* 87, 4645-4649.
- Grunewald, W., and Friml, J. (2010). The march of the PINs: developmental plasticity by dynamic polar targeting in plant cells. *EMBO J* 29, 2700-2714.
- Guo, H., Li, L., Aluru, M., Aluru, S., and Yin, Y. (2013). Mechanisms and networks for brassinosteroid regulated gene expression. *Curr Opin Plant Biol* 16, 545-553.
- Haglund, K., and Dikic, I. (2005). Ubiquitylation and cell signaling. *EMBO J* 24, 3353-3359.
- Haglund, K., and Stenmark, H. (2006). Working out coupled monoubiquitination. *Nat Cell Biol* 8, 1218-1219.
- Haughn, G.W., Wessler, S.R., Gemmill, R.M., and Calvo, J.M. (1986). High A + T content conserved in DNA sequences upstream of *leuABCD* in *Escherichia coli* and *Salmonella typhimurium*. *J Bacteriol* 166, 1113-1117.
- Heard, W., Sklenar, J., Tome, D.F., Robatzek, S., and Jones, A.M. (2015). Identification of Regulatory and Cargo Proteins of Endosomal and Secretory Pathways in *Arabidopsis thaliana* by Proteomic Dissection. *Mol Cell Proteomics* 14, 1796-1813.

- Heilmann, I. (2016). Phosphoinositide signaling in plant development. *Development* 143, 2044-2055.
- Henne, W.M., Buchkovich, N.J., and Emr, S.D. (2011). The ESCRT pathway. *Dev Cell* 21, 77-91.
- Henry, A.G., Hislop, J.N., Grove, J., Thorn, K., Marsh, M., and von Zastrow, M. (2012). Regulation of endocytic clathrin dynamics by cargo ubiquitination. *Dev Cell* 23, 519-532.
- Hicke, L., and Dunn, R. (2003). Regulation of membrane protein transport by ubiquitin and ubiquitin-binding proteins. *Annu Rev Cell Dev Biol* 19, 141-172.
- Hoeller, D., Crosetto, N., Blagoev, B., Raiborg, C., Tikkanen, R., Wagner, S., Kowanetz, K., Breitling, R., Mann, M., Stenmark, H., *et al.* (2006). Regulation of ubiquitin-binding proteins by monoubiquitination. *Nat Cell Biol* 8, 163-169.
- Hoeller, D., and Dikic, I. (2010). Regulation of ubiquitin receptors by coupled monoubiquitination. *Subcell Biochem* 54, 31-40.
- Holstein, S.E., and Oliviusson, P. (2005). Sequence analysis of *Arabidopsis thaliana* E/ANTH-domain-containing proteins: membrane tethers of the clathrin-dependent vesicle budding machinery. *Protoplasma* 226, 13-21.
- Hong, Y.H., Ahn, H.C., Lim, J., Kim, H.M., Ji, H.Y., Lee, S., Kim, J.H., Park, E.Y., Song, H.K., and Lee, B.J. (2009). Identification of a novel ubiquitin binding site of STAM1 VHS domain by NMR spectroscopy. *FEBS Lett* 583, 287-292.
- Honing, S., Ricotta, D., Krauss, M., Spate, K., Spolaore, B., Motley, A., Robinson, M., Robinson, C., Haucke, V., and Owen, D.J. (2005). Phosphatidylinositol-(4,5)-biphosphate regulates sorting signal recognition by the clathrin-associated adaptor complex AP2. *Mol Cell* 18, 519-531.
- Houle, D., Govindaraju, D.R., and Omholt, S. (2010). Phenomics: the next challenge. *Nat Rev Genet* 11, 855-866.
- Huang, F., Goh, L.K., and Sorkin, A. (2007). EGF receptor ubiquitination is not necessary for its internalization. *Proc Natl Acad Sci U S A* 104, 16904-16909.
- Huang, F., Kirkpatrick, D., Jiang, X., Gygi, S., and Sorkin, A. (2006). Differential regulation of EGF receptor internalization and degradation by multiubiquitination within the kinase domain. *Mol Cell* 21, 737-748.

- Huang, F., Zeng, X., Kim, W., Balasubramani, M., Fortian, A., Gygi, S.P., Yates, N.A., and Sorkin, A. (2013). Lysine 63-linked polyubiquitination is required for EGF receptor degradation. *Proc Natl Acad Sci U S A* *110*, 15722-15727.
- Huotari, J., and Helenius, A. (2011). Endosome maturation. *EMBO J* *30*, 3481-3500.
- Huotari, J., Meyer-Schaller, N., Hubner, M., Stauffer, S., Katheder, N., Horvath, P., Mancini, R., Helenius, A., and Peter, M. (2012). Cullin-3 regulates late endosome maturation. *Proc Natl Acad Sci U S A* *109*, 823-828.
- Hurley, J.H. (2010). The ESCRT complexes. *Critical reviews in biochemistry and molecular biology* *45*, 463-487.
- Hurley, J.H., Lee, S., and Prag, G. (2006). Ubiquitin-binding domains. *Biochem J* *399*, 361-372.
- Husnjak, K., and Dikic, I. (2012). Ubiquitin-binding proteins: decoders of ubiquitin-mediated cellular functions. *Annu Rev Biochem* *81*, 291-322.
- Ikeda, F., and Dikic, I. (2008). Atypical ubiquitin chains: new molecular signals. 'Protein Modifications: Beyond the Usual Suspects' review series. *EMBO Rep* *9*, 536-542.
- Isono, E., and Kalinowska, K. (2017). ESCRT-dependent degradation of ubiquitylated plasma membrane proteins in plants. *Curr Opin Plant Biol* *40*, 49-55.
- Jean, S., and Kiger, A.A. (2012). Coordination between RAB GTPase and phosphoinositide regulation and functions. *Nat Rev Mol Cell Biol* *13*, 463-470.
- Kalinowska, K., Nagel, M.K., Goodman, K., Cuyas, L., Anzenberger, F., Alkofer, A., Paz-Ares, J., Braun, P., Rubio, V., Otegui, M.S., *et al.* (2015). Arabidopsis ALIX is required for the endosomal localization of the deubiquitinating enzyme AMSH3. *Proc Natl Acad Sci U S A* *112*, E5543-5551.
- Kang, B.H., Nielsen, E., Preuss, M.L., Mastronarde, D., and Staehelin, L.A. (2011). Electron tomography of RabA4b- and PI-4Kbeta1-labeled trans Golgi network compartments in Arabidopsis. *Traffic* *12*, 313-329.
- Kang, Y.L., Yochem, J., Bell, L., Sorensen, E.B., Chen, L., and Conner, S.D. (2013). *Caenorhabditis elegans* reveals a FxNPxY-independent low-density lipoprotein receptor internalization mechanism mediated by epsin1. *Mol Biol Cell* *24*, 308-318.
- Katzmann, D.J., Stefan, C.J., Babst, M., and Emr, S.D. (2003). Vps27 recruits ESCRT machinery to endosomes during MVB sorting. *J Cell Biol* *162*, 413-423.



- Kim, H.T., Kim, K.P., Lledias, F., Kisselev, A.F., Scaglione, K.M., Skowrya, D., Gygi, S.P., and Goldberg, A.L. (2007). Certain pairs of ubiquitin-conjugating enzymes (E2s) and ubiquitin-protein ligases (E3s) synthesize nondegradable forked ubiquitin chains containing all possible isopeptide linkages. *J Biol Chem* 282, 17375-17386.
- Kim, S.Y., Xu, Z.Y., Song, K., Kim, D.H., Kang, H., Reichardt, I., Sohn, E.J., Friml, J., Juergens, G., and Hwang, I. (2013). Adaptor protein complex 2-mediated endocytosis is crucial for male reproductive organ development in Arabidopsis. *Plant Cell* 25, 2970-2985.
- Klapisz, E., Sorokina, I., Lemeer, S., Pijnenburg, M., Verkleij, A.J., and van Bergen en Henegouwen, P.M. (2002). A ubiquitin-interacting motif (UIM) is essential for Eps15 and Eps15R ubiquitination. *J Biol Chem* 277, 30746-30753.
- Kleine-Vehn, J., and Friml, J. (2008). Polar targeting and endocytic recycling in auxin-dependent plant development. *Annu Rev Cell Dev Biol* 24, 447-473.
- Kolb, C., Nagel, M.K., Kalinowska, K., Hagmann, J., Ichikawa, M., Anzenberger, F., Alkofer, A., Sato, M.H., Braun, P., and Isono, E. (2015). FYVE1 is essential for vacuole biogenesis and intracellular trafficking in Arabidopsis. *Plant Physiol* 167, 1361-1373.
- Komander, D., and Rape, M. (2012). The ubiquitin code. *Annu Rev Biochem* 81, 203-229.
- Korbei, B., Moulinier-Anzola, J., De-Araujo, L., Lucyshyn, D., Retzer, K., Khan, M.A., and Luschnig, C. (2013). Arabidopsis TOL proteins act as gatekeepers for vacuolar sorting of PIN2 plasma membrane protein. *Curr Biol* 23, 2500-2505.
- Laemmli, U.K. (1970). Cleavage of structural proteins during the assembly of the head of bacteriophage T4. *Nature* 227, 680-685.
- Lam, S.K., Siu, C.L., Hillmer, S., Jang, S., An, G., Robinson, D.G., and Jiang, L. (2007). Rice SCAMP1 defines clathrin-coated, trans-golgi-located tubular-vesicular structures as an early endosome in tobacco BY-2 cells. *Plant Cell* 19, 296-319.
- Lange, A., Hoeller, D., Wienk, H., Marcillat, O., Lancelin, J.M., and Walker, O. (2011). NMR reveals a different mode of binding of the Stam2 VHS domain to ubiquitin and diubiquitin. *Biochemistry* 50, 48-62.
- Leitner, J., and Luschnig, C. (2014). Ubiquitylation-mediated control of polar auxin transport: analysis of Arabidopsis PIN2 auxin transport protein. *Methods Mol Biol* 1209, 233-249.
- Leitner, J., Retzer, K., Korbei, B., and Luschnig, C. (2012). Dynamics in PIN2 auxin carrier ubiquitylation in gravity-responding Arabidopsis roots. *Plant Signal Behav* 7, 1271-1273.

- Lohi, O., Poussu, A., Mao, Y., Quiocho, F., and Lehto, V.P. (2002). VHS domain -- a longshoreman of vesicle lines. *FEBS Lett* 513, 19-23.
- Long, D., and Bruschweiler, R. (2011). In silico elucidation of the recognition dynamics of ubiquitin. *PLoS Comput Biol* 7, e1002035.
- Mao, Y., Nickitenko, A., Duan, X., Lloyd, T.E., Wu, M.N., Bellen, H., and Quiocho, F.A. (2000). Crystal structure of the VHS and FYVE tandem domains of Hrs, a protein involved in membrane trafficking and signal transduction. *Cell* 100, 447-456.
- Mayers, J.R., Wang, L., Pramanik, J., Johnson, A., Sarkeshik, A., Wang, Y., Saengsawang, W., Yates, J.R., 3rd, and Audhya, A. (2013). Regulation of ubiquitin-dependent cargo sorting by multiple endocytic adaptors at the plasma membrane. *Proc Natl Acad Sci U S A* 110, 11857-11862.
- McLoughlin, F., and Testerink, C. (2013). Phosphatidic acid, a versatile water-stress signal in roots. *Front Plant Sci* 4, 525.
- McMahon, H.T., and Boucrot, E. (2011). Molecular mechanism and physiological functions of clathrin-mediated endocytosis. *Nat Rev Mol Cell Biol* 12, 517-533.
- Mizuno, E., Kawahata, K., Kato, M., Kitamura, N., and Komada, M. (2003). STAM proteins bind ubiquitinated proteins on the early endosome via the VHS domain and ubiquitin-interacting motif. *Mol Biol Cell* 14, 3675-3689.
- Moller-Steinbach, Y., Alexandre, C., and Hennig, L. (2010). Flowering time control. *Methods Mol Biol* 655, 229-237.
- Nagel, M.K., Kalinowska, K., Vogel, K., Reynolds, G.D., Wu, Z., Anzenberger, F., Ichikawa, M., Tsutsumi, C., Sato, M.H., Kuster, B., *et al.* (2017). Arabidopsis SH3P2 is an ubiquitin-binding protein that functions together with ESCRT-I and the deubiquitylating enzyme AMSH3. *Proc Natl Acad Sci U S A* 114, E7197-E7204.
- Noack, L.C., and Jaillais, Y. (2017). Precision targeting by phosphoinositides: how PIs direct endomembrane trafficking in plants. *Current Opinion in Plant Biology* 40, 22-33.
- Otegui, M.S., Mastronarde, D.N., Kang, B.H., Bednarek, S.Y., and Staehelin, L.A. (2001). Three-dimensional analysis of syncytial-type cell plates during endosperm cellularization visualized by high resolution electron tomography. *Plant Cell* 13, 2033-2051.
- Otegui, M.S., and Spitzer, C. (2008). Endosomal functions in plants. *Traffic* 9, 1589-1598.
- Paczkowski, J.E., Richardson, B.C., and Fromme, J.C. (2015). Cargo adaptors: structures illuminate mechanisms regulating vesicle biogenesis. *Trends Cell Biol* 25, 408-416.

- Paez Valencia, J., Goodman, K., and Otegui, M.S. (2016). Endocytosis and Endosomal Trafficking in Plants. *Annu Rev Plant Biol* 67, 309-335.
- Peters, J.H., and de Groot, B.L. (2012). Ubiquitin dynamics in complexes reveal molecular recognition mechanisms beyond induced fit and conformational selection. *PLoS Comput Biol* 8, e1002704.
- Pickart, C.M. (2001). Mechanisms underlying ubiquitination. *Annu Rev Biochem* 70, 503-533.
- Piper, R.C., Dikic, I., and Lukacs, G.L. (2014). Ubiquitin-dependent sorting in endocytosis. *Cold Spring Harb Perspect Biol* 6.
- Platre, M.P., and Jaillais, Y. (2016). Guidelines for the Use of Protein Domains in Acidic Phospholipid Imaging. *Methods Mol Biol* 1376, 175-194.
- Polyn, S., Willems, A., and De Veylder, L. (2015). Cell cycle entry, maintenance, and exit during plant development. *Curr Opin Plant Biol* 23, 1-7.
- Posor, Y., Eichhorn-Grunig, M., and Haucke, V. (2015). Phosphoinositides in endocytosis. *Biochim Biophys Acta* 1851, 794-804.
- Prag, G., Lee, S., Mattera, R., Arighi, C.N., Beach, B.M., Bonifacino, J.S., and Hurley, J.H. (2005). Structural mechanism for ubiquitinated-cargo recognition by the Golgi-localized, gamma-ear-containing, ADP-ribosylation-factor-binding proteins. *Proc Natl Acad Sci U S A* 102, 2334-2339.
- Prag, G., Watson, H., Kim, Y.C., Beach, B.M., Ghirlando, R., Hummer, G., Bonifacino, J.S., and Hurley, J.H. (2007). The Vps27/Hse1 complex is a GAT domain-based scaffold for ubiquitin-dependent sorting. *Dev Cell* 12, 973-986.
- Puertollano, R. (2005). Interactions of TOM1L1 with the multivesicular body sorting machinery. *J Biol Chem* 280, 9258-9264.
- Puertollano, R., and Bonifacino, J.S. (2004). Interactions of GGA3 with the ubiquitin sorting machinery. *Nat Cell Biol* 6, 244-251.
- Raiborg, C., Bache, K.G., Gillooly, D.J., Madshus, I.H., Stang, E., and Stenmark, H. (2002). Hrs sorts ubiquitinated proteins into clathrin-coated microdomains of early endosomes. *Nat Cell Biol* 4, 394-398.
- Raiborg, C., Rusten, T.E., and Stenmark, H. (2003). Protein sorting into multivesicular endosomes. *Curr Opin Cell Biol* 15, 446-455.

- Raiborg, C., and Stenmark, H. (2009). The ESCRT machinery in endosomal sorting of ubiquitylated membrane proteins. *Nature* 458, 445-452.
- Rapoport, I., Miyazaki, M., Boll, W., Duckworth, B., Cantley, L.C., Shoelson, S., and Kirchhausen, T. (1997). Regulatory interactions in the recognition of endocytic sorting signals by AP-2 complexes. *EMBO J* 16, 2240-2250.
- Richardson, L.G., and Mullen, R.T. (2011). Meta-analysis of the expression profiles of the Arabidopsis ESCRT machinery. *Plant Signal Behav* 6, 1897-1903.
- Richter, S., Voss, U., and Jurgens, G. (2009). Post-Golgi traffic in plants. *Traffic* 10, 819-828.
- Robinson, D.G., and Pimpl, P. (2013). Receptor-mediated transport of vacuolar proteins: a critical analysis and a new model. *Protoplasma*.
- Sato, Y., Yoshikawa, A., Mimura, H., Yamashita, M., Yamagata, A., and Fukai, S. (2009). Structural basis for specific recognition of Lys 63-linked polyubiquitin chains by tandem UIMs of RAP80. *EMBO J* 28, 2461-2468.
- Sauer, M., and Friml, J. (2014). Plant biology: gatekeepers of the road to protein perdition. *Curr Biol* 24, R27-29.
- Scheuring, D., Viotti, C., Kruger, F., Kunzl, F., Sturm, S., Bubeck, J., Hillmer, S., Frigerio, L., Robinson, D.G., Pimpl, P., *et al.* (2011). Multivesicular bodies mature from the trans-Golgi network/early endosome in Arabidopsis. *Plant Cell* 23, 3463-3481.
- Sen, A., Madhivanan, K., Mukherjee, D., and Aguilar, R.C. (2012). The epsin protein family: coordinators of endocytosis and signaling. *Biomol Concepts* 3, 117-126.
- Shewan, A., Eastburn, D.J., and Mostov, K. (2011). Phosphoinositides in cell architecture. *Cold Spring Harb Perspect Biol* 3, a004796.
- Shiba, Y., Katoh, Y., Shiba, T., Yoshino, K., Takatsu, H., Kobayashi, H., Shin, H.W., Wakatsuki, S., and Nakayama, K. (2004). GAT (GGA and Tom1) domain responsible for ubiquitin binding and ubiquitination. *J Biol Chem* 279, 7105-7111.
- Shields, S.B., and Piper, R.C. (2011). How ubiquitin functions with ESCRTs. *Traffic* 12, 1306-1317.
- Sigismund, S., Polo, S., and Di Fiore, P.P. (2004). Signaling through monoubiquitination. *Curr Top Microbiol Immunol* 286, 149-185.

- Spitzer, C., Reyes, F.C., Buono, R., Sliwinski, M.K., Haas, T.J., and Otegui, M.S. (2009). The ESCRT-related CHMP1A and B proteins mediate multivesicular body sorting of auxin carriers in Arabidopsis and are required for plant development. *Plant Cell* 21, 749-766.
- Stringer, D.K., and Piper, R.C. (2011). A single ubiquitin is sufficient for cargo protein entry into MVBs in the absence of ESCRT ubiquitination. *J Cell Biol* 192, 229-242.
- Studier, F.W., and Moffatt, B.A. (1986). Use of bacteriophage T7 RNA polymerase to direct selective high-level expression of cloned genes. *J Mol Biol* 189, 113-130.
- Studier, F.W., Rosenberg, A.H., Dunn, J.J., and Dubendorff, J.W. (1990). Use of T7 RNA polymerase to direct expression of cloned genes. *Methods Enzymol* 185, 60-89.
- Svozil, J., Hirsch-Hoffmann, M., Dudler, R., Gruissem, W., and Baerenfaller, K. (2014). Protein abundance changes and ubiquitylation targets identified after inhibition of the proteasome with syringolin A. *Mol Cell Proteomics* 13, 1523-1536.
- Telfer, A., Bollman, K.M., and Poethig, R.S. (1997). Phase change and the regulation of trichome distribution in Arabidopsis thaliana. *Development* 124, 645-654.
- Tenno, T., Fujiwara, K., Tochio, H., Iwai, K., Morita, E.H., Hayashi, H., Murata, S., Hiroaki, H., Sato, M., Tanaka, K., *et al.* (2004). Structural basis for distinct roles of Lys63- and Lys48-linked polyubiquitin chains. *Genes Cells* 9, 865-875.
- Terrell, J., Shih, S., Dunn, R., and Hicke, L. (1998). A function for monoubiquitination in the internalization of a G protein-coupled receptor. *Mol Cell* 1, 193-202.
- Testerink, C., and Munnik, T. (2005). Phosphatidic acid: a multifunctional stress signaling lipid in plants. *Trends Plant Sci* 10, 368-375.
- Urbe, S. (2005). Ubiquitin and endocytic protein sorting. *Essays Biochem* 41, 81-98.
- Varadan, R., Assfalg, M., Haririnia, A., Raasi, S., Pickart, C., and Fushman, D. (2004). Solution conformation of Lys63-linked di-ubiquitin chain provides clues to functional diversity of polyubiquitin signaling. *J Biol Chem* 279, 7055-7063.
- Viotti, C., Bubeck, J., Stierhof, Y.D., Krebs, M., Langhans, M., van den Berg, W., van Dongen, W., Richter, S., Geldner, N., Takano, J., *et al.* (2010). Endocytic and secretory traffic in Arabidopsis merge in the trans-Golgi network/early endosome, an independent and highly dynamic organelle. *Plant Cell* 22, 1344-1357.
- Walter, A., Liebisch, F., and Hund, A. (2015). Plant phenotyping: from bean weighing to image analysis. *Plant Methods* 11, 14.

- Walton, A., Stes, E., Cybulski, N., Van Bel, M., Inigo, S., Durand, A.N., Timmerman, E., Heyman, J., Pauwels, L., De Veylder, L., *et al.* (2016). It's Time for Some "Site"-Seeing: Novel Tools to Monitor the Ubiquitin Landscape in *Arabidopsis thaliana*. *Plant Cell* 28, 6-16.
- Wang, J., Sun, H.Q., Macia, E., Kirchhausen, T., Watson, H., Bonifacino, J.S., and Yin, H.L. (2007). PI4P promotes the recruitment of the GGA adaptor proteins to the trans-Golgi network and regulates their recognition of the ubiquitin sorting signal. *Mol Biol Cell* 18, 2646-2655.
- Wang, T., Liu, N.S., Seet, L.F., and Hong, W. (2010). The emerging role of VHS domain-containing Tom1, Tom1L1 and Tom1L2 in membrane trafficking. *Traffic* 11, 1119-1128.
- Winter, V., and Hauser, M.T. (2006). Exploring the ESCRTing machinery in eukaryotes. *Trends Plant Sci* 11, 115-123.
- Wlodarski, T., and Zagrovic, B. (2009). Conformational selection and induced fit mechanism underlie specificity in noncovalent interactions with ubiquitin. *Proc Natl Acad Sci U S A* 106, 19346-19351.
- Woelk, T., Oldrini, B., Maspero, E., Confalonieri, S., Cavallaro, E., Di Fiore, P.P., and Polo, S. (2006). Molecular mechanisms of coupled monoubiquitination. *Nat Cell Biol* 8, 1246-1254.
- Yoshinari, A., Korbei, B., and Takano, J. (2018). TOL proteins mediate vacuolar sorting of the borate transporter BOR1 in *Arabidopsis thaliana*. *Soil Sci Plant Nutr* 64, 598-605.
- Zhang, Y., Persson, S., Hirst, J., Robinson, M.S., van Damme, D., and Sanchez-Rodriguez, C. (2015). Change your TPLATE, change your fate: plant CME and beyond. *Trends Plant Sci* 20, 41-48.
- Zouhar, J., and Sauer, M. (2014). Helping hands for budding prospects: ENTH/ANTH/VHS accessory proteins in endocytosis, vacuolar transport, and secretion. *Plant Cell* 26, 4232-4244.

## 7 INDEX OF FIGURES

Figure 1 Secretory and endocytic pathway:.....	3
Figure 2 Endocytic pathway :.....	4
Figure 3 General overview of endocytic and endosomal trafficking :.....	6
Figure 4 Clathrin mediated endocytosis : .....	8
Figure 5 Recognition and degradation of ubiquitylated PM-proteins by ESCRT and ESCRT-interacting proteins :.....	14
Figure 6 In silico analysis of the domains of proteins with VHS and GAT domains in <i>Arabidopsis thaliana</i> and <i>Homo sapiens</i> : .....	16
Figure 7 Protein structure of VHS and GAT domain :.....	18
Figure 8 Schematic diagram for cloning strategy : .....	34
Figure 9 Western blot of plant lysates with anti-TOL6 serum : .....	81
Figure 10 TOL proteins expression: expression of transgenic TOL proteins in a single knockout plant lines .....	84
Figure 11 Subcellular Localization of TOL proteins in planta : .....	86
Figure 12 In vitro lipid binding assay.....	88
Figure 13 VHS and GAT domains sequence alignment : .....	90
Figure 14 VHS, GAT domain structure and schematic TOL6 mutations: .....	91
Figure 15 Typical TOL6 in vitro binding assays :.....	93
Figure 16 Signal distribution of TOL6 and mutated TOL6 :.....	95
Figure 17 Rescue of <i>A.thaliana</i> tolQ : .....	97
Figure 18 Mutation of TOL UBD affects the plant development : .....	99
Figure 19 Coupled Monoubiquitination : .....	101
Figure 20 Immunoprecipitation (IP) of TOL6 :.....	103
Figure 21 Ubiquitination of other TOL family members: .....	105
Figure 22 Helical ubiquitin-binding domain structures : .....	106
Figure 23 TOL6ubq:Venus interfere with the localization : .....	109
Figure 24 Monoubiquitinated TOL6 has diminished functionality in planta : .....	111
Figure 25 Monoubiquitination of TOL6 affects with the plant development :.....	113
Figure 26 TOL1ubq:Venus interfere with the localization : .....	115
Figure 27 Monoubiquitination of TOL1 affects with the plant development : ;.....	116

Figure 28 TOL5ubq:Venus interfere with localization : .....	118
Figure 29 Monoubiquitination of TOL5 affects with the plant development : .....	119
Figure 30 Working model for the function of TOL proteins in the degradation of ubiquitinated PM proteins: .....	127



## 8 INDEX OF TABLES

Table 1 Primer sequences list .....	24
Table 2 Plant lines generated and used during this study .....	34
Table 3 Antibodies .....	35
Table 4 Preparation of 20µl reaction mix .....	39
Table 5 Reaction mix for colony PCR .....	39
Table 6 PCR amplification program designed for the primers .....	40
Table 7 Preparation of 50µl reaction mix for site direct mutagenesis .....	41
Table 8 PCR amplification programme designed for the DNA for T/A cloning approaches .....	42
Table 9 PCR mixture .....	42
Table 10 PCR amplification program designed for standard PCR.....	43
Table 11 Preparation of the different antibiotic used in this study.....	46
Table 12 Preparation of the antibiotics solution for selection.....	51
Table 13 Preparation of separation gel.....	60
Table 14 Preparation staking gel: .....	61
Table 15 Preparation 15 mL of the separating gel solution used for Total membrane protein extraction .....	61
Table 16 Preparation 6 mL of the separating gel solution used for Total membrane protein extraction .....	62
Table 17 Preparation 50mL IP buffer.....	77

## 9 ABREVIATIONS

% v/v	Volume-volume percentage
% w/v	Weight-volume percentage
2,4-D	2,4-dichlorophenoxyacetic acid
Amp	Ampicillin
APS	Ammonium persulfate
bp	Base pairs
BSA	Bovine serum albumin
°C	Degree Celsius
CCV	Clathrin coated vesicle
cDNA	Complementary DNA
CK2	Casein kinase 2
CLSM	Confocal laser scanning microscope
CME	Clathrin mediated endocytosis
Col-0	Columbia ecotype 0
DAG	Days after germination
dH <sub>2</sub> O	Distilled water
DMF	Dimethylformamid
DMSO	Dimethyl sulfoxide
DNA	Deoxyribonucleic acid
dNTPs	Deoxynucleotide triphosphates
DTE	1,4 Dithioerythrit
DUB	Deubiquitinating enzyme
DUIM	Double sided ubiquitin interacting motif
E.coli	Escherichia coli
EDTA	Ethylenediaminetetraacetic acid
EE	Early endosome
EGTA	Ethylene glycol tetraacetic acid
EMS	Ethylmethansulfonate
ESCRT	Endosomal sorting complex required for transport
ER	Endoplasmatic Reticulum
EtBr	Ethidium bromide
<i>E. coli</i>	<i>Escherichia coli</i>
EDTA	Ethylene diamine tetraacetic acid
FREE1	FYVE domain protein required for endosomal sorting 1
FYVE	Fab1, YOTB, Vac1 and EEA1
g	Gram
GAT	GGA and Tom
gDNA	Genomic DNA
Gent	Gentamycin
GFP	Green fluorescent protein
GGA	Golgi-localized, gamma-ear containing, ADP-ribosylation factor binding
GST	Glutathione-S-transferase
GTP	Guanosine triphosphate

## ABBREVIATIONS

GUS	β-glucuronidase
HRP	Horseradish peroxidase
Hrs	Hepatocyte growth factor regulated tyrosine kinase substrate
ILVs	Intraluminal vesicles
IPTG	Isopropyl beta-D-1-thiogalactopyranoside
Kan	Kanamycin
kb	Kilo base pairs
kDa	Kilo Dalton
kV	Kilo Volt
LB	Lysogeny broth
LE	Late Endosome
l	Liter
LB	Left border
IPTG	Isopropyl-d-thiogalactopyranoside
Kan	Kanamycin
kb	Kilo base pairs
kDa	Kilo Dalton
μl	Microliter
μM	Micromolar
M	Molar
MCS	Multiple cloning site
MES	(2-N-Morpholino)ethanesulfonic acid
mg	Miligram
min	Minute
MIU	Motif interacting with ubiquitin
ml	Milliliter
mm	Millimeter
mM	Millimolar
MS	Murashige-Skoog
MCS	Multiple cloning site
MVB	Multivesicular bodies
nm	Nanometer
OD	Optical density
o/n	overnight
ORF	Open reading frame
PAGE	Polyacrylamide gel electrophoresis
PCR	Polymerase chain reaction
PI-3P	Phosphatidylinositol-3-phosphate
PM	Plasma membrane
PMP	Plasma membrane protein
PMSF	Phenylmethylsulfonylfluoride
PNS	Plant nutrient sucrose
PP2Cs	Group-A 2C protein phosphatases
RIPA	Radio immunoprecipitation assay
PVDF	Polyvinylidene fluoride
RB	right border
Rif	Rifampicin

## 10 APENDIX

Publications related to this PhD project:

### 1. Expression of Arabidopsis TOL genes.

Moulinier-Anzola J, **De-Araujo L**, Korbei B.

Plant Signal Behav. 2014; e28667. doi: 10.4161/psb.28667

#### ABSTRACT

A strict control of abundance and localization of plasma membrane proteins is essential for plants to be able to respond quickly and accurately to a changing environment. The proteins responsible for the initial recognition and concentration of ubiquitinated plasma membrane proteins destined for degradation, are well characterized in mammals and yeast, yet no clear orthologs were found in plants. Recently, we have identified a family of proteins in higher plants, which function in vacuolar targeting and subsequent degradation of ubiquitinated plasma membrane proteins termed TOM1-like (TOL) proteins.

### 2. Immunoprecipitation of Membrane Proteins from Arabidopsis thaliana Root Tissue.

Waidmann S, **De-Araujo L**, Kleine-Vehn J, Korbei B.

Methods Mol Biol. 2018; 1761:209-220. doi: 10.1007/978-1-4939-7747-5\_16.

#### ABSTRACT

Here, we present different methods for immunoprecipitating membrane proteins of *Arabidopsis thaliana* root material. We describe two extraction methods for the precipitation either for an integral membrane protein of the endoplasmic reticulum (ER) or a peripheral membrane protein partially localized at the plasma membrane, where we precipitate the protein out of the total membrane as well as total cytosolic fractions.

### 3. Function and regulation of TOLs: ubiquitin receptors in the endosomal system of plants

Jeanette Moulinier-Anzola\*, **Lucinda De-Araújo\***, Max Schwihla, Christina Artner, Lisa Jörg and Barbara Korbei. **(SUBMITTED)**

(\* Both authors have equal contribution)

#### **Abstract**

Ubiquitination is decisive in numerous aspects of plant development and in adaptation to changing environmental conditions. To understand the significance and the variety of roles played by this modification, the function of ubiquitin receptors, which translate the ubiquitin signature into a cellular response, needs to be elucidated. Attachment of K63-linked ubiquitin chains is essential for the proper sorting of endocytosed plasma membrane (PM) proteins to the vacuole for subsequent degradation. In this study, we show that TOL (TOM1-like) proteins function uniquely in plants as multivalent ubiquitin receptors in the first steps of ubiquitinated cargo delivery to the vacuole via the conserved Endosomal Sorting Complex Required for Transport (ESCRT) pathway. TOL6, which resides at the PM and in early endosomes, interacts with components of the ESCRT machinery and binds to K63-ubiquitinated cargo, via two tandemly arranged conserved ubiquitin binding domains. Mutation of these domains results not only in loss of ubiquitin binding but also altered localization and abolishes TOL6 ubiquitin receptor activity. Function and localization of TOL6 is regulated by coupled mono-ubiquitination, whereby TOL6 ubiquitination modulates the efficiency in the degradation of PM-localized cargos, potentially assisting in the fine-tuning of the delicate interplay between protein recycling and downregulation. We have thus analyzed in depth and for the first time in plants, the function and regulation of a ubiquitin receptor involved in vacuolar degradation of PM proteins.

## CURRICULUM VITAE

### ***Personal Details:***

Last name: De-Araujo

First name: Lucinda Alculete Lopes

Day and place of birth: 15th of August 1978, Quelimane - Mozambique

Nationality: Mozambican

Children's: Evelyn (born 2007) and Lucio (born 2013)

Home Address: Erdbergstrasse 95/15-16; 1030, Vienna, Austria

Laboratory address: Institute for Applied Genetics and Cell Biology

University of Natural Resources and Applied Life Sciences

Muthgasse 18, 1190 Vienna, Austria

Telephone: +4366766595125 (mobile). +43-1-47654-94174/5 (office)

E-mail: lucinda.alculete-lopes-de-araujo-feitio@boku.ac.at or lalculete@yahoo.com

2014 - 2019: Doctoral thesis at the University of Natural Resources and

Life Sciences within the Department of Applied Genetics and Cell Biology in the group of Mag. Dr. Barbara Korbei group under supervision of Univ.Prof. Dipl.-Ing. Dr.rer.nat. Eva Stöger. Title: Gatekeepers of Vacuolar Sorting Of Plasma Membrane Protein in Plants - Functional Analysis of TOL Proteins.

### ***Education:***

01/2015 - 12/2017: Recipient of a Doctoral Fellowship Programme of Austrian Academy of Science (26 project "DOC ÖAW"). Title: Gatekeepers of Vacuolar Plasma Membrane Protein Sorting in Plants". Department of Applied Genetics and Cell Biology, University of Natural Resources and Applied Life Sciences, Vienna, Austria.

2011-2013: Master degree at Department of Applied Genetics and Cell Biology and Eduardo Mondlane University-Mozambique with title "Mutational analysis of the Ubiquitin binding Capacity of the VHS domain in *Arabidopsis thaliana*".

## DECLARATION

I hereby declare that, the present work reports about original research and I confirm that the dissertation was written in accordance with the terms and conditions of good scientific practice. I confirm that I wrote the dissertation on my own, without using any other than the declared sources, references and tools and did not use any impermissible tools. All passages included from other works in verbatim or in content, have been identified as such. The content of the presented dissertation has not been used as a whole for another scientific work or publication so far. If own publications have been included partially, they have been identified as such

---

Lucinda De-Araujo (Candidate)